Effect of (il)luminance and age on color perception

Spieringhs, R.M.

Award date:
2019

Technische Universiteit
Eindhoven
University of Technology

Department of Industrial Engineering and Innovation Sciences
Human Technology Interaction Research Group
in commission of the Signify Research Group

Effect of (il)luminance and age on color perception

Master Thesis

Rik Marco Spieringhs
Student number: 0823938

Supervisors:
Dr.ir. R.H. Cuijpers
Dr. M. Lucassen
Dr. J.L. Souman
Dr. K. Teunissen
Dr. I.M.L.C. Vogels
Dr. K.C.H.J. Smolders

First version

Eindhoven, August 2019

Abstract

In lighting research, researchers often create (or simulate) controlled visual environments, in which researchers can manipulate one factor at a time. In daily life, however, the visual environment is less controlled and much more complex, both spatially and spectrally. Current color spaces have aimed to best predict the chromatic discrimination of colored targets at variant visual environments. The color discrimination at photopic vision has been extensively studied. However, often used color spaces were less representative of the chromatic discrimination at lower light levels. Previous research about color discrimination has shown that the color rendition, luminance, the spectral power distribution, and age are important factors for chromatic discrimination. Furthermore, previous research reported tritan like effects caused by weak S-cone mediated hue signals at mesopic light levels. Based on the previous studies about chromatic discrimination, showing that luminance and the spectral power distribution of the light source influenced the chromatic discrimination, we were interested in the influence of luminance at the standard illuminant C, on the chromatic discrimination for mesopic and photopic light levels. Additionally, we were interested in how to further explain and model this large S-cone mediated variation in cap order found at the mesopic light levels.

An experiment was carried out to investigate the differences in chromatic discrimination for different light levels and age groups. Five different illuminance levels, two different age groups and the color cap ordering of the four different trays of the FM-100 hue color vision test were included. The calculated error score of the FM100-Hue test was an indication of the chromatic discrimination under illuminant C.

The results of the experiment confirmed that there were significant differences in chromatic discrimination between light levels, especially at the lower light levels. Besides the main effect of light level, there was a significant interaction effect on the error score between the light level and the age group. The post hoc analysis of the interaction effect showed that the younger age group on average had a lower error score at the lowest light level than the older age group.

An attempt to model the chromatic discrimination at mesopic light levels was made. Threshold detection ellipses were estimated for two detection coefficients and predicted the data for a root mean squared error of less than 0.08. An inequality was observed in the detection functions which indicated the inaccuracy of the human visual system to discriminate colors along the tritan axis at mesopic light levels.

Preface

In my bachelors graduation project my enthusiasm for doing perceptual research was sparked and I had a great motivation of continuing this enthusiasm into my master education. The masters study was very informative and helped me understand which perceptual attributes are important in measuring and modeling the human psychophysics. During my masters study I also had the amazing opportunity to do several different studies on the human perception of light. One of these studies was at the Munsell Color Science Laboratory (MCSL), Rochester Institute of Technology (RIT) in the USA. The study was about the time course of chromatic adaptation under dynamic lighting. Additionally, I learned a lot about the history of color science, the principles of color science and the computational vision science with many thanks to Roy Berns and Susan Farnand for allowing me to attend their lectures and assignments. My deepest gratitude goes to my supervisor at RIT for his friendly yet professional guidance, Michael Murdoch. Also my deepest gratitude goes to everyone at MCSL for the warm welcome and thanks for providing me an experience that I will never forget.

This research project was conducted in commission of the Signify research group and I would like to thank my current supervisors at Signify, Marcel Lucassen, Jan Souman and Kees Teunissen for their amazing guidance and for allowing me to conduct my graduation project at their renowned facility.

Second to last I would like to thank the Eindhoven University of Technology and my first supervisor Raymond Cuijpers for his educative guidance and his helpful feedback on the research project. Also I am thankful for Xiangzhen Kong for his support and feedback.

Last but foremost I would like to thank my family, friends and girlfriend in supporting me throughout the graduation project.

Contents

List of Figures

List of Tables

Chapter 1

Introduction

Have not the small Particles of Bodies certain Powers, Virtues or Forces, by which they act at a distance, not only upon the Rays of Light for reflecting, refracting and reflecting them, but also upon one another for producing a great part of the Phenomena of Nature? Sir Isaac Newton, 1718

The human visual system is a very complex and interesting sensory system being able to adapt to all sorts of lighting conditions while they change over time [2] [3]. These changing illumination conditions can have profound effects on perceived object colors in that space [4][5]. Differences in the illumination of indoor lighting not only affect color appearance but can also greatly impact the performance of cognitive tasks, interpersonal behavior, and psychological functioning [6][7]. Light and colors are very important in the sense that they can impact the visibility of the environment, direct or tune attention, increase self-awareness, and affect peoples affective state.

Light Emitting Diodes (LEDs) made lighting applications more reliable, efficient, enduring, cost-effective and is providing a wide range of reproducible colors with relatively high accuracy [8]. LEDs surpassed the efficiency of Hg-discharge based fluorescent as well as the historic incandescent lamps and is being used more frequently in everyday appliances [9]. LEDs typically are also relatively small and are used in most computer displays nowadays. The most interesting and probably most important part of LEDs for psychophysics is its ability to provide this dynamic wide range of colored lighting.

With the invention and growth of LEDs, the understanding of the perception of (dynamic) lighting became much more important, making it necessary to understand and account for all the characteristics of the human visual system. The light that reaches the human retinae depends on the visual environment that transmits, reflects, absorbs and/or emits the light. The human visual system, therefore, can be very complex to model and research. Psychophysics has made an effort to accurately predict visual sensitivity and visual discrimination.

In the past, visual sensitivities and visual discrimination of object colors were researched by many in highly controlled laboratory environments for uniform targets often using only a few observers. Nowadays, advancements in artificial lighting made it possible to easier control the light spectrum and display different colors. These advancements made it possible to further investigate and model the visual system.

The visual system is involved in many complex tasks and is an extensively studied concept. However, less was known about the chromatic adaptation, color fidelity, and chromatic discrimination. A short literature study was carried out about the color fidelity and chromatic discrimination which is shown in appendix .1. The rest of this study mainly focuses on chromatic discrimination.

In the mid 19^{th} century, Brown, in his study about describing the sensitivity to the discrimination of colors for different luminance levels (1951), found that the sensitivity to color differences is mostly constant above a luminance of 3.4 cd/m^2 [10]. Brown, however, used only a 2 degree field size (i.e. the angular size of the light stimuli) and had only 2 observers. A later study by Wyszecki and Fielder about the color matching ellipses (1971), found inconsistencies in data among and between observers and found field size effects on the color matching ellipses [11]. Another study by Yeh, Pokorny, and Smith about the chromatic discrimination of illuminated surfaces with variation in chromaticity and luminance (1993) suggests a model for chromatic discrimination thresholds to be mediated by the S-cone axis and the L/M-cone axis [12].

In the early twenty-first century, a study by Pridmore and Melgosa about the effect of sample luminance on color discrimination ellipses (2005), indicated a decrease in axis dimensions and ellipse area with a higher luminance for all the data of the studies that were investigated [13]. They describe the luminance dependency including other dependencies such as the surround and adaptation state to be important for color discrimination. These dependencies were also confirmed by Jennings and Barbur (2010) [14].

These studies mentioned above indicate that the (il)luminance and chromaticity of the light source affect the discrimination of illuminated surfaces. However, a specific (il)luminance and chromaticity can be constructed in many different ways, by different spectral power distributions. Most of these studies use slightly different setups and light sources, therefore, they have slightly different spectral power distributions and reflectances. This would imply slightly different color-rendering differences of the stimuli. For uniform neutral (low-chroma) surfaces, this would perhaps be less noticeable. However, when using more complex objects with different chromatic surfaces these differences are noticeable [15]. Also, other studies have indicated that the spectral power distribution is an important factor in chromatic discrimination [16][17].

Previous research has shown that luminance influences chromatic discrimination, espe-

cially for luminance levels less than 20 cd/m^2 (e.g. Yebra, Garcia, Nieves, and Romero, (2001) [18]; Pridmore and Melgosa, (2005) [13]). Furthermore, Knoblauch et al. in 1987, reported significant age and illuminance effects in the Farnsworth-Munsell 100-hue test under an illuminant of 6600 Kelvin [19]. This study reported tritan like effects caused by weak S-cone mediated hue signals at mesopic light levels explained by a two cycle sine wave model. These studies, however, did not measure chromatic discrimination under the standard illuminant C and the results are normally reported in FM-100 hue test scores. We are, therefore, interested in the effect of illuminance on chromatic discrimination for mesopic and photopic light levels, with fixed spectral distribution (illuminant C). Additionally, we are interested in how to further explain and model this large S-cone mediated variation in cap order found at the mesopic light levels.

Furthermore, previous research has shown that age is another factor that influences chromatic discrimination, especially for people older than 39 or younger than 18 [20]. Based on this study, we are also interested in the influence of age on chromatic discrimination for mesopic and photopic light levels. Mesopic vision believed to extend from 0.001 to about 10 cd/m^2, is between photopic and scotopic vision, and is supported by both rods and cones (previously explained in the introduction) [21][22]. Photopic vision is believed to extend from several cd/m^2 or higher [23] where foveal cones support the vision.

To add to the existing literature on the effect of luminance on chromatic discrimination under illuminant C, this study was established. This study aims to produce guidelines to determine at which light levels the current available colorimetric models can accurately predict chromatic discrimination, and when not. This knowledge is relevant in situations where the illumination can change from bright to dim light levels. This study also aims to investigate the difference in chromatic discrimination between age groups at different light levels. This knowledge is relevant for the personal customization of the illumination.

Therefore, the main research question is: *'How is our ability to discriminate object colors affected by our age and by the illumination level?'*. Based on the research by Yebra, Garcia, Nieves, and Romero (2001) that luminance has a large effect on the area of color discrimination ellipses, the main hypothesis of this study states *'there is a significant positive effect of illuminance on chromatic discrimination'*. Additionally based on research by Kinnear and Sahraie (2002) that age affects the performance on the color discrimination test Farnsworth-Munsell 100 hue test, the second hypothesis of this study states *'there is a significant negative effect of age on chromatic discrimination'*.

To investigate differences in chromatic discrimination for different light levels and age groups, an experiment was conducted. In this experiment, the chromatic discrimination was measured for different age groups and light levels under illuminant C.

Chapter 2

Theoretical Background

2.1 Human Visual System

In this section different physiological characteristics of the human visual system are discussed. First the structure of the human eye is explained, followed by the different photoreceptors in the human eye, additionally the post receptor pathways are described with the distinctive trichromacy and opponency for the cone photoreceptors.

2.1.1 The Human Eye

The human eye has a particular structure, where the light enters through the cornea and the pupil. The pupil is part of the mechanism that controls the amount of light entering the eye. The diameter of the pupil is controlled by the iris via expanding and contracting muscles. After the pupil and iris, the light propagates through the eye lens, which can change its shape allowing for the focus of incoming light onto the retina. Henceforth, the light reaches the interior of the human eye, where the light is absorbed by the photoreceptors in the retina. The retina contains three different types of photoreceptors, namely the rods, cones and ganglion cells [24].

As shown in figure 2.1, the light first reaches the ganglion cell layer and thereafter the rods and cones. The rods and cones transmit information to the ganglion cells via the second order bipolar cells.

2.1.2 The Photoreceptors

The human eye roughly contains 120 million rod cells. The rods are photoreceptors that are sensitive to lower light levels and can respond to even a single photon of light. They are, however, distinctively different from the cones, which are more sensitive to higher light levels and are mostly responsible for color vision. The human eye roughly contains 7 million cone cells, which are highly concentrated in the fovea [24]. The concentration of the photoreceptor is, however, dependent on the geometry of the eye that changes by muscle activation pushing photoreceptors closer together or spreading them apart. The human

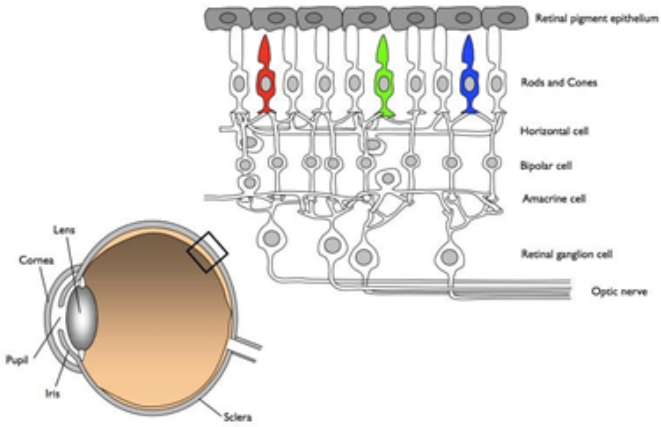

Figure 2.1: Schematic cross section of the human eye and its cell layer. Source: lecture slides of lecture 2 of the course 0HM200 Psychology of Light and Time.

visual system is dependent on the photon absorption by photopigment in the photoreceptors. The photon absorption probability is determined by the spectral sensitivity of such photoreceptor at a given frequency of the photon. There is one class of rods and three different classes of cones all having different spectral sensitivities, see figures 2.2 and 2.3.

From a physiological viewpoint, the eye contains three types of cone receptors. The three types of cone receptors are differently sensitive to the visible region of the electromagnetic spectrum, often referred to as the L, M, and S cones. The L cones are mainly sensitive to the longer wavelengths (with peak sensitivity at 575nm), the M cones to the middle wavelengths (peak at 535nm) and the S cones to the shorter wavelengths (peak at 440nm) [25]. These L, M, and S cones mainly contribute to the human visual perception at medium and high light levels. At the lower light levels (dim light) the achromatic photoreceptors, rod cells, are utilized instead. The three types of cones mainly allow for color vision at the medium and high light levels, whereas at the lower light levels color vision is mostly diminished.

Another retinal photoreceptor that was suggested already in the early 1900s, but in the later 1900s further researched is the intrinsically photosensitive ganglion cell (ipRGC). The ipRGCs do not directly attribute to the visual pathway, however, they do play an important part in the (acute) melatonin suppression. The ipRGCs, therefore, are important in the effects of light on our circadian rhythm (internal clock). The photopigment of the ipRGCs, a light sensitive protein, called melanopsin has a peak sensitivity at 480nm [26].

2.1.3 Scotopic

The rods and cones are distinctively different in their visual functioning, where the rods are more sensitive to lower luminance levels and the cones more sensitive to higher luminance levels [27]. At the lower luminance levels the cones are mostly saturated and the rods mostly

allow for vision, these lower luminance levels are characterized as the scotopic (night time) vision regime. The CIE, the international commision that regulates standardization in light and color, determined two spectral efficiency functions, V(λ) for the photopic vision regime and V'(λ) for the scotopic vision regime, see figure 2.2. The V(λ) is called the luminous efficiency curve, which represents the sensitivity in respect to the perceived brightness for different wavelengths.

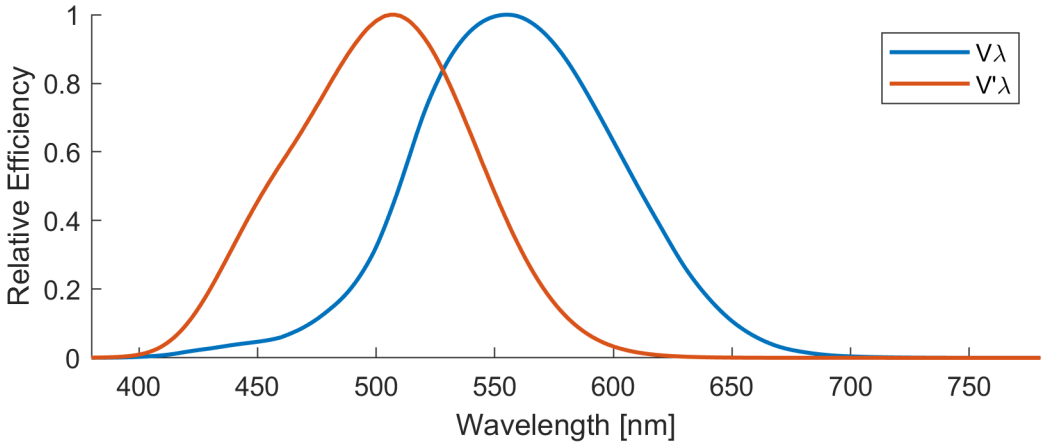

Figure 2.2: The $V_M(\lambda)$ 1988 luminous efficiency function for photopic vision and the V'(λ) luminous efficiency function for scotopic vision.

2.1.4 Photopic

In the higher luminance levels the rods are mostly saturated and the cones mostly allow for vision, these higher luminance levels are characterized as the photopic (daytime) vision regime. The photopic vision is believed to extend from several cd/m^2 to higher [23] where foveal cones support the vision.

2.1.5 Mesopic

In between the lower and higher luminance levels both the cones and rods function, which is characterized as the mesopic vision regime. The mesopic vision, believed to extend from 0.001 to about 10 cd/m2, is in between the photopic and scotopic vision and is supported by both rods and cones [21][22]. Mesopic light levels are often encountered in emergency and street lighting.

2.1.6 Postreceptor pathway

Once a photon is absorbed by the photoreceptors, cones and/or rods, there is a chance of a photoreceptor response. An absorption of a photon does not guarantee such photoreceptor

response and could also be dispatched as heat [28]. When a photon does result in an actual photoreceptor response, wavelength dependent variants of rhodopsin allow for a change in the receptor membrane potential.

2.1.7 Trichromacy

Trichromacy is the result of the human visual system having three distinct cone types. Trichromacy allows the human visual system to see a large variation in color. With the combination of the three different cones (L, M and S) with different sensitivities at different wavelengths it is necessary to at least have two different cone types to distinguish colors. With at least two different cone types the brain can distinguish between different signals of the receptors and recognize different colors and intensities of the light.

2.1.8 Opponency

The L, M and S cone cells have an interesting characteristic where neighbouring and different cone cells can inhibit each other by their spatial connectivity in the retina. This phenomenon can therefore cause positive input from the individual receptors to lead to both negative and positive outputs in their communal signal to the brain. Henceforth, retinal ganglion cells, cells in the lateral geniculate nucleus and in the visual cortex are identified to have color opponency, see figure 2.3. Meaning that no bluish yellow or reddish green can be observed. The opponency in red and green is believed to be caused by the inhibitory response in the post-receptoral pathways of the L and M cone cells (L-M). The opponency in blue and yellow is believed to be caused by an excitatory response in the post-receptoral pathways between the L and M cone cells, combined to an inhibitory response of the S cone cells (S - (L+M)). There is also a third combination, related to light and dark opponency and the luminous efficiency function, resulting from the excitatory response in the post-receptoral pathways of the L and M cone cells (L+M).

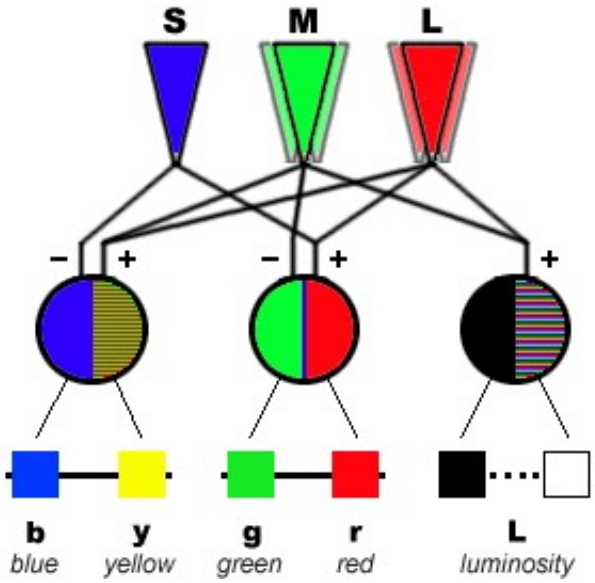

Figure 2.3: L-, M- and S-cone responses retrieved from https://www.handprint.com/HP/WCL/color2.html

2.2 Physical Properties of Light

In this section the physical properties of light are explained. These properties are used to describe the interaction of a light source with objects in the visual scene and the visual system (eye and brain). First the visible spectrum is defined. Second the descriptive radiometric and photometric quantities of light are explained. Third the transmission, absorption and reflectance are explained.

2.2.1 Wavelengths

When light is described as a wave the range of frequencies of the electromagnetic radiation can be determined. Often the physical electromagnetic spectrum is expressed in wavelengths which can be calculated by dividing the speed of light by the frequency of the electromagnetic radiation. The total physical electromagnetic spectrum is distinctively different than the visible electromagnetic spectrum. The human eye can only perceive light in the range of about 398-750 nm [29], between infrared and ultraviolet, while the total electromagnetic spectrum covers a broad range from pm to Mm, see figure 2.4.

2.2.2 Radiometric

Visible light is usually expressed in either Radiometric or Photometric quantities. When light is expressed in Radiometric quantities four different descriptions are used. As a radiometric quantity for the total energy that is emitted by the light source radiant flux is used. The radiant flux is a measure of the joules per second, commonly known as

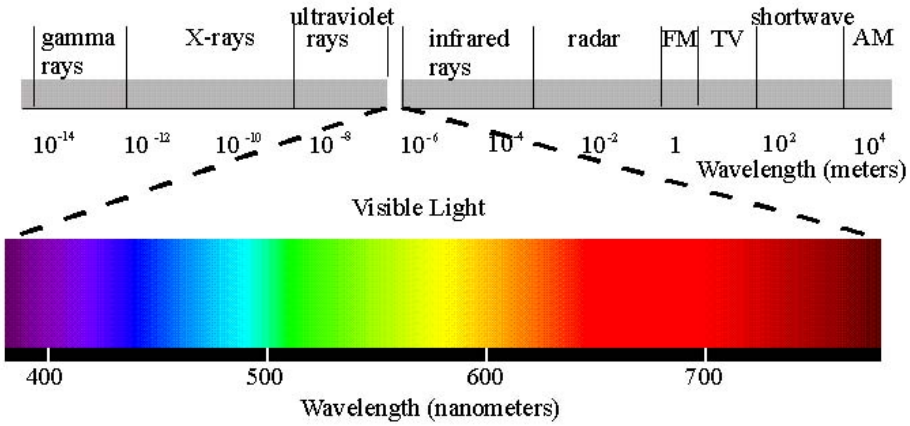

Figure 2.4: Visible and physical electromagnetic spectrum retrieved from `http://solar-center.stanford.edu/SID/activities/GreenSun.html`

watts. When the energy that is received at a surface is measured, the radiometric quantity irradiance is used in watts per squared meters. For the energy that is measured directly from a point source from a certain solid angle, the radiometric quantity radian intensity is described in watts per steradian. The radiometric quantity for the energy from an extended source is described as the radiance in watts per squared meter and per steradian.

2.2.3 Photometric

The photometric quantities are basically similar to the radiometric quantities when the radiometric quantities are weighted for the human eye. The radiometric quantities are weighted by the previously explained luminous efficiency functions. So, the total energy emitted from the light source is described in photometric quantities as the measure of the perceived power of the light in luminous flux as lumen (lm). The measure of total luminous flux as the incident on a surface per unit area is described by the illuminance in lux (lm/m^2). The measure of the power emitted by a light source in a direction per unit solid angle then is described as the luminous intensity in candela (lm/sr). The photometric quantity for the energy from an extended source as the measure of luminous intensity per unit area of light going into a certain direction is described by the luminance in candela per square meter (cd/m^2).

2.2.4 Transmission

The receiving light at the specific location in a space that is illuminated by a light source can either be transmitted, absorbed or reflected. The light that is transmitted is basically the light that passes through a material. The (total) transmittance of a material depends on the amount of absorption, reflection, scattering and refraction of the light that passes through the material.

2.2.5 Absorption

The absorption of a material is essentially the amount of light that is converted into heat or lost when the light hits and passes through a certain material.

2.2.6 Reflectance

The reflectance of a material is essentially the amount of light that is reflected and/or refracted at a certain angle. Depending on the surface and the smoothness of this surface the angle of the surface reflected light is determined. Often surfaces are described as glossy, semi-glossy or matte.

2.3 Colorimetry

In this section the numerical approach to represent colors is described. First, the color matching functions are described for the different standard observers, and finally some color spaces are discussed.

2.3.1 Color Matching

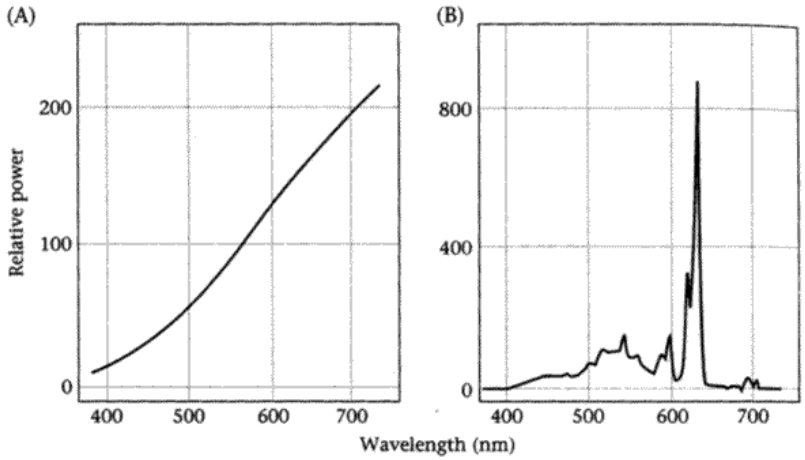

Figure 2.5: The relative power distribution of a tungsten light bulb on the left and a color matched TV display on the right (retrieved from Wandell, 1997 [1])

In the late 1920's William David Wright published a study about the trichromatic coefficients of the spectral colors [30]. In this study the quantitative links between the physical electromagnetic spectrum and color perceived by human observers was defined. Furthermore, in the early 1930's Guild published his research about the color matching functions which were derived independently of the study of Wright [31]. These independently performed studies, by Wright and Guild, resulted in the CIE 1931 RGB color space determined

by the International Commission on Illumination (CIE) in 1931. The color space maps the scope of all possible physical light spectra to an objective description of these colors, based on color matching experiments [32]. Figure 2.5 shows an example of a television display that is color matched to a Tungstun light bulb, both having different spectral power distributions. Color matching functions are fundamental for the reproduction of images by just red, green and blue lights and for the color specification. Color matching functions were derived by observers color matching two halves of a split field of view. One half was a fixed light source controlled by the researcher and unknown to the participants. The other half was controlled by the participants which was illuminated by three primaries red (700 nm), green (546.1 nm) and blue (435.8 nm). The participants could adjust the intensities of these three primaries such that it matched the unknown light source on the other half. The responses were recorded and repeated for different unknown light sources. The color matching functions represent the chromatic response of an average observer. But since they were derived from a particular color matching experiment, they were dependent on the specific light primaries used in those experiments. At the time, the individual cone sensitivities were unknown, and color matching functions allowed the specification of light and color. Currently, color matching functions are still of central importance in lighting industry.

2.3.2 Cone Fundamentals

In 2000 and 2006 Stockman and Sharpe published their research on the cone fundamentals [33][34]. In their research they managed to derive the individual L- and M-cone sensitivities by using heterochromatic flicker photometry and by isolating the S-cone responses for dichromats. The S-cone responses were then derived by blue cone monochromatic observers. The L-, M- and S-cone sensitivities are shown in figure 2.6.

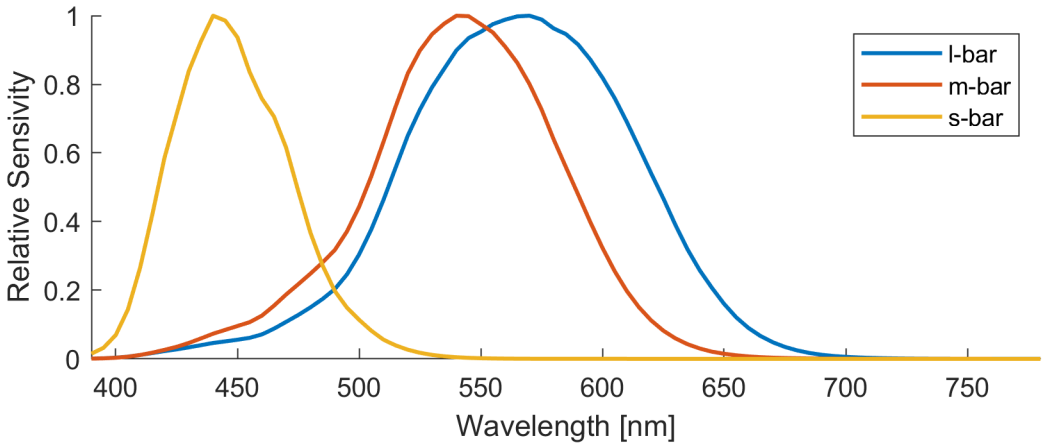

Figure 2.6: Cone fundamentals (CIE 170-1:2006, prepared by Mark Fairchild) for an average observer of 20 years old for a 2-degree field size.

2.3.3 Standard Observers

2.3.3.1 2-degree observer

Since the introduction of the CIE 1931 standard observer 2-degree color matching functions, many researchers have performed similar research to determine the accuracy of the color matching functions of that time. In deriving the CIE 1931 color matching functions the CIE 1924 V(λ) was used. In 1951 Judd proposed a slightly modified version of the CIE 1931 2-degree color matching functions which was based on the knowledge that the CIE 1924 V(λ) underestimated the sensitivities at lower wavelenghts (below 460nm) [35]. In 1978 Vos further modified these functions and proposed the $V_M(\lambda)$ luminosity function [36]. Furthermore, in 1955 Stiles and Burch proposed their own 2-degree color matching functions [37] and in 2006, another set of 2-degree color matching functions was derived from the CIE (2006) 2-degree L-, M- and S-cone fundamentals.

2.3.3.2 10-degree observer

Originally the CIE 1931 color matching data was based on data obtained by a color matching experiment for a 2-degree visual field size. Stiles and Burch, and Speranskaya in 1959 both proposed 10-degree color matching functions which were used to create the CIE 1964 standard observer [38][39]. The CIE 1964 standard observer was mostly dominated by the data obtained by Stiles and Burch, whereas the data of both studies were weighted and the data from Speranskaya was given less weight.

2.3.4 Chromaticity coordinates

2.3.4.1 Two dimensional color spaces

The RGB color space is conceptualized by three different primary lights (red, green and blue), but can also be conceptualized by imaginary primary lights that cannot be produced with any light spectrum, which is the case for the 1931 CIE XYZ and 1976 CIE USC color spaces. In line with color perception, most color spaces are 3 dimensional, having a lightness component and two chromaticity components (covering hue and saturation). When the lightness component is kept constant, color can be described in a 2D chromaticity diagram, such as the CIE x,y, and CIE u'v' chromaticity diagrams.

2.3.4.2 Three dimensional color spaces

The approach to model the chromaticity and lightness independently and then combining them resulted in three-dimensional spaces such as the CIELAB and CIELUV.

2.3.4.3 Color Temperature

When a black body is thermally heated it emits electromagnetic radiation. An example of a close approximation of such black body radiator is the sun. The color of this black

body can be described by its chromaticity coordinates (e.g. x,y or u'v') or by its color temperature. The color temperature (CT), used to describe the color of the black body radiator, is the technical term used for the tone of white light, varying from cool (high CT) to warm (low CT) white. In the chromaticity space the black body radiators of different temperatures are located on the black body or planckian locus. When the chromaticity coordinates of the white light source do not align with the black body locus the correlated color temperature (CCT) is used. The CCT is determined by the iso- temperature lines around the black-body locus, whose perceived colors match most closely to a color on the black body locus. The visibility difference between CCTs has been extensively researched where usually in establishing the visibility thresholds the just noticeable CCT differences are used [40][41].

2.3.4.4 Color space uniformity

In 1942 Macadam introduced the Macadam ellipses where the ellipses indicate the just noticeable difference for different chromaticity coordinates in the CIE 1931 xy chromaticity space [42]. These ellipses were used to indicate the perceptual uniformity of the color space, where the size of the ellipses in the CIE 1931 xy chromaticity space were largely unequal. Since the introduction of the Macadam ellipses there has been a widespread search for the most uniform color space, a space in which equal distances correspond to equal perceptual differences, irrespective of the position in color space. Since the introduction of the CIE 1931 XYZ color matching functions researchers have been busy trying to make a color space most uniform.

2.3.4.5 Multi dimensional color models

Some color models account for the color appearance which are called color appearance models (CAM). These models normally account for other factors influencing the perception of a color in a certain environment, such as adaptation, background, surrounding and size of the stimulus. In 2002 the CIE introduced the CIECAM02 color appearance model that accounts for these factors and uses the chromatic adaptation transform CIECAT02 [43]. The model calculates chromaticity channels based on the correlates for red-green and blue-yellow. Additionally, the model also provides estimates for the correlate of chroma, colorfulness, saturation, lightness, brighness, hue (angle) and the achromatic response.

2.4 Visual Adaptation

In the daily environment we are exposed to a wide variety of illumination, both by daylight and artificial lighting. The human perception of the world is, therefore, not absolute. The perceived color of objects in the environment depend on various aspects, such as the surrounding colors and the illumination, and the adaptation state of the human visual system. To compensate for a change in the illumination the human visual system is able to adjust its sensitivity or perception. The adaptation state of the human visual system

depends on the type of change in illumination. At the higher light levels cones mainly contribute to vision, whereas at the lower light levels the rods mainly contribute to vision. The ability of the eye to adapt to a certain illumination, therefore, depends on the characteristics of the photoreceptor that attributes to vision at that moment [44]. In this section three types of adaptation are explained, namely, dark adaptation, light adaptation and chromatic adaptation.

2.4.1 Dark Adaptation

When the illumination changes from a very intense light to a dim light the sensitivity of the visual system also changes. The recovery of visual sensitivity to this dim light after being exposed to the very intense light is often referred to as dark adaptation. Dark adaptation has been research by several scientists and is a generally well known phenomenon [45][46]. The time course of dark adaptation was determined by psychophysical experiments that used the absolute intensity threshold as a measure for the sensitivity of the eye [47]. The time course of dark adaptation consisted of two components, a fast and a slow component, that both could be described by a decreasing exponential function [48]. The fast component had a time constant of approximately 5-10 minutes and was believed to be related to a neural adaptation process. The slow component, however, had a time constant of approximately 40-50 minutes and was associated to the rhodopsin concentration in the eye [49].

2.4.2 Light Adaptation

When the illumination changes from a dim light to a intense light the sensitivity of the visual system changes very rapidly. The recovery of the visual sensitivity to this intense light after being exposed to the dim light is referred to as light adaptation. During the exposure to the intense light the human eye is unable to instantly reduce the pupil size. Due to this inability to reduce the pupil size instantly large amounts of photopigments are being broken down instantaneously, and as a result, rod bleaching occurs. This initial over excitement of the photoreceptors is believed to cause glare and depending on the intensity of the amount of exposed light, cone mediated vision is restored very rapidly. The time course of light adaptation was determined by increment thresholds and described as a very rapid exponential gain change. This exponential gain change had a time constant of approximately 10-15 seconds [50].

2.4.3 Chromatic Adaptation

When the illumination changes from color the sensitivities of the three types of cones (L, M and S) and the related opponent channels (S-(L+M), L-M and L+M) change. Some studies have researched the time course of adaptation from daylight to incandescent lighting. Hunt and Jameson et al. both discovered that the adaptation state was complete

after approximately 5 minutes and already 80-90% after 1 minute. The first study that investigated the time course of chromatic adaptation was by Fairchild and Reniff where they found two mechanisms of adaptation [3]. The two mechanisms consisted of an extremely rapid component and a slower component, that both could be described by a exponential function. The extremely rapid component had a time constant of approximately a few seconds and the slower component had a time constant of approximately a minute. Another study that investigate the time course of chromatic adaptation was by Rinner and Gegenfurtner [2] where they found a slow, fast and extremely rapid component. The slow component had a half life of approximately 20 seconds. The fast component had a half life of approximately 40-70 milliseconds and the extremely rapid component had a half life faster than 10 milliseconds. The fast and slow component of both studies were explained by photoreceptor adaptation, whereas the extremely rapid component from the Rinner and Gegenfurtner study was believed to be based on multiplicative spatial interactions in neural processing stages.

2.5 Psychophysical methods

In this section different methods for psychometric scaling are discussed. The advantages and limitations of each method are described, and the purpose of each method is explained. The description of the methods is based on the book by Engeldrum that explain these methods in more detail for image quality scaling [51]. Participant judgment and human perception can be difficult to objectively measure. Most participants want to satisfy the researcher and normally would provide desirable information. Participants also often do not realize when they perceived a stimulus or where their exact threshold lie. To most objectively measure the human perception, several methods in history were used to determine the threshold and differences for the human visual system. First the method of limits is discussed, second the method of adjustment, and the method of constant stimuli.

2.5.1 Method of limits

The method of limits is very efficient method to determine a certain threshold value where a stimulus is barely or not perceivable. In the method of limits, the stimulus value is increased or decreased until the observer reports that the stimulus is barely or not perceivable. Other adaptive techniques to automate the threshold determination for the method of limits which are often used are the Parameter Estimation by Sequential Testing (PEST) proposed by Taylor and Creelman in 1967 [52] or the QUEST procedure that was introduced by Watson and Pelli in 1983 [53].

2.5.2 Method of adjustment

The method of adjustment is a very intuitive task in which the observer can adjust a randomly selected stimulus himself by adjusting a knob or by pressing different keys to

find a threshold value. The task is very simple and requires an actual input of the observer keeping him busy and most likely keeping him more immune to fatigue.

2.5.3 Method of constant stimuli

The method of constant stimuli is a rather different from the method of limits and method of adjustment. It allows for a psychometric curve to be fitted to data that is obtained. The method of constant stimuli can be more accurate in finding the actual threshold value, however, selecting the range of stimuli that is needed can be difficult. For a psychometric curve to be fitted a researcher would need a stimulus set which is never perceived, and a stimulus set which is always perceived. The remaining sets of stimuli should be in between these two sets to find the threshold value. The absolute threshold as a point on this psychometric curve is determined by the psychometric model that is used. For the method of constant stimuli many different adaptations or variations are possible such as the staircase procedure or the paired comparison task.

Chapter 3

Method

To investigate differences in chromatic discrimination for different age groups and different light levels, an experiment was conducted. In the experiment participants performed the FM-100 Hue color vision test under different light levels. In this section the experimental procedure is described. First the overall setup, software, color characterization and the general stimuli are explained and thereafter the experiment is explained in more detail.

3.1 Experimental Setup

The experiment took place in a dark room in the Signify Research Heinrich Rudolf Hertz Laboratory (HTC building 7). Two light boxes, with Thouslite LED cubes mounted on top were placed on a table. The light boxes were each 80x80x45 cm (HxLxD) and the LED cubes were 30x30 cm. The bottom of the light box was fully covered with black paper. The rest of the light box was covered in neutral white paint. A small dark screen, covering the top part of the light box, was placed in front of the light box. The dark small screen prevented the participants from seeing the LED cube directly. The LED cube consisted of 11 different LEDs and were mounted in the top of the box behind a diffuse glass plate. They broadcasted spectra by combining different LEDs. To reduce the light intensity two polarization filters were placed on top of each in front of the diffuse glass plate. One polarization filter was fixed into position and the other filter could be rotated. Additional to the selected light spectras, four trays of the FM-100 hue test caps were used. Each of the four trays were placed in the center of the light box in an orderly sequence. The entire-setup is displayed in figure 3.1.

Figure 3.1: Experiment setup.

3.2 Software

Several Matlab programs were developed. First, a program was created to control the LED cube illumination system and to control the JETI Specbos 1201 spectroradiometer, used for colorimetric characterization. Second, a program was made to create a LUT model and to calculate the accuracy and uniformity of the illumination in the light box. Next, all color rendering was done via Matlab to minimize interferences between software packages and to display the most accurate color. Finally, a graphical user interface (GUI) was created to show the different combinations of the LEDs in the LED cube for different chosen spectral power distributions. This GUI was used to best approximate illuminant C.

3.3 Colorimetric characterization

In the colorimetric characterization of the LED cube the spectroradiometer was horizontally placed at bottom and in the middle of the light box with an attached 90-degree diffusor. The diffusor was used to allow in axis irradiance measurements. The opening of the diffusor was aimed directly at the light emitting LED cubes. The spectroradiometer had a relative luminance accuracy of 2 % at a luminance of 100 cd/m^2 for standard illuminant A. Furthermore, it had a color accuracy of +- 0.002 in CIE 1931 x, y at illuminant A and a spectral range of 350-1000 nm with a wavelength accuracy of 0.5 nm, according to their online brochure retrieved at March 2019. Before the measurement the JETI was configured to a wavelength range of 360 to 830 nm, and to report the average of five repeated measurements. Also, between each consecutive measurement the JETI would pause for five seconds to most accurately measure the stimulus. This pause was necessary to provide enough time for the light setting to change. The 11 LED's inside the LED cube were individually controlled (10 bits per channel) by a Matlab script. The stimuli used for the characterization consisted of combinations of the 11 LEDs. The stimuli consisted of eleven ramps with their digital counts from 8 to 1023 in increments of 4 for each primary

individually, LED1 (8:4:1023, 0, 0, 0, 0, 0, 0, 0, 0, 0, 0), LED2 (0, 8:4:1023, 0, 0, 0, 0, 0, 0, 0, 0, 0), LED3 (0, 0, 8:4:1023, 0, 0, 0, 0, 0, 0, 0, 0), etc, see figure 3.2. Furthermore, the stimuli consisted of a gray ramp, where the digital count for each channel was the same, also from 8 to 1023 in increments of 4 (8:4:1023, 8:4:1023, 8:4:1023, 8:4:1023, 8:4:1023, 8:4:1023, 8:4:1023, 8:4:1023, 8:4:1023, 8:4:1023, 8:4:1023). The maximum digital count of 1023 was also measured for each individual LED and also for the gray ramp where all the LEDs were simultaneously set at their maximum digital count. Before measuring each ramp, the LED or LEDs that were going to be used were turned to their maximum digital counts for five minutes. This provided enough time for the LED or LEDs to warm-up and be mostly consistent throughout the measurement period. During the measurements all other lights inside the room were turned off.

The uniformity of the light box was measured at nine different positions. Four positions were chosen at the edges of the box 7 cm from both sides, one position was chosen at the middle and the other four were chosen at 10 cm from the center in the 0, 90, 180 and 270 degree direction. For each of these nine positions the gray ramp was measured and compared to the measurements that were done previously in the middle position directly under the LED cube. There were large color differences at the other locations compared to the middle. The chromatic color differences were reasonable small, whereas the lightness differences were substantially high. The color differences were slightly different over their lower digital counts but remained somewhat constant above 50 digital counts. Furthermore, the CIEDE2000 differences between the measured at the middle of the light box and the measured at all other positions were determined. With those nine CIEDE2000 differences, where the middle position had a value of zero, an ellipsoid was fitted, as shown in figure 3.3.

The ellipsoid in figure 3.3 was mathematically determined using linear least squares and had the form of equation 3.1.

$$\begin{aligned} -1.01x^2 - 3.90y^2 + 7.91dE^2 - 0.0282xy \\ +0.159xdE + 0.229ydE + 0.415x + 1.43y + 104dE = 0 \end{aligned} \tag{3.1}$$

Besides the uniformity measurements with the JETI, an LMK luminance camera was used to create colorimetric images of the LED cube. The LMK camera was used to easier and more accurately observe the non-uniformity of the light box, see figure 3.4.

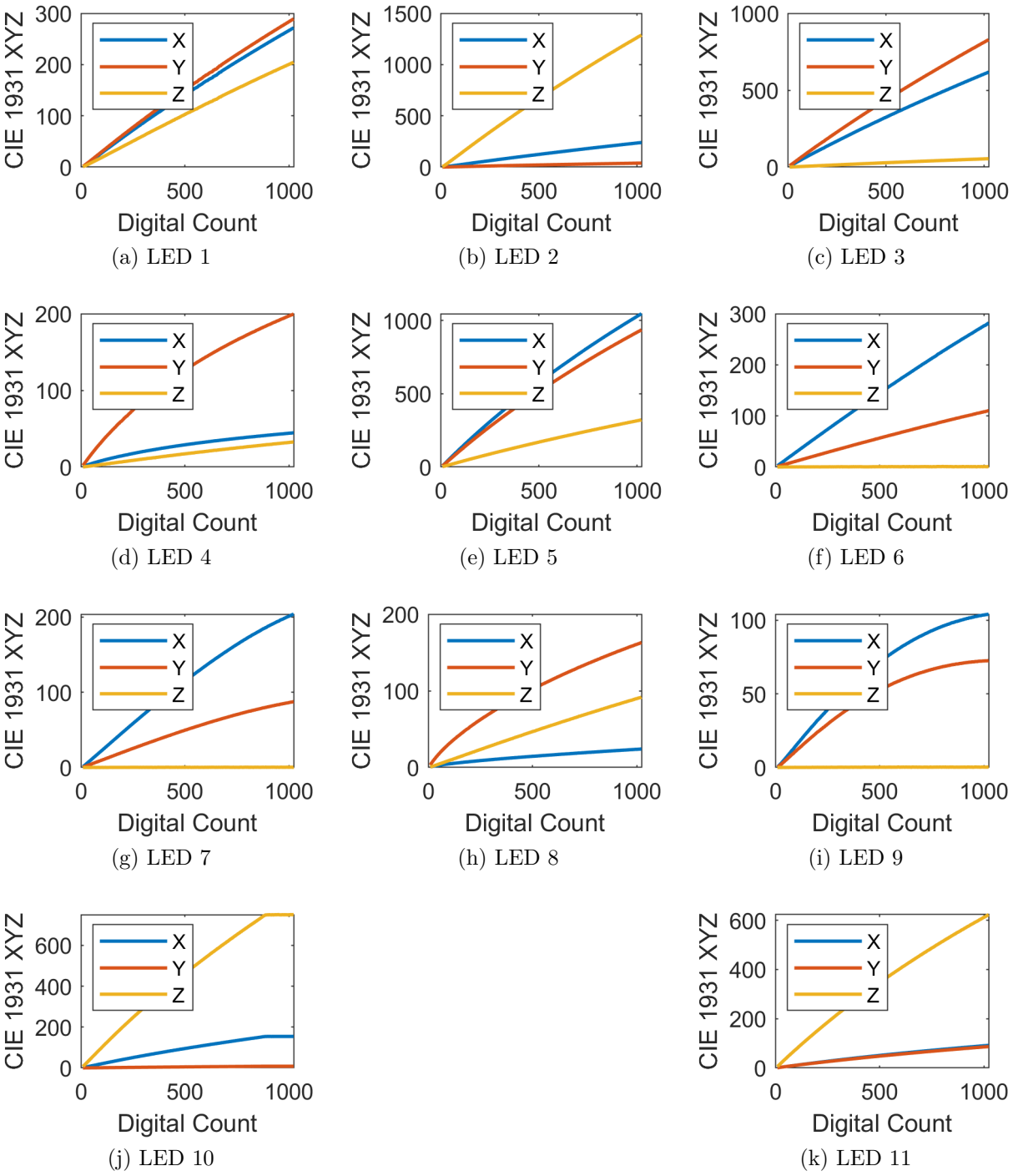

(a) LED 1 (b) LED 2 (c) LED 3

(d) LED 4 (e) LED 5 (f) LED 6

(g) LED 7 (h) LED 8 (i) LED 9

(j) LED 10 (k) LED 11

Figure 3.2: The digital count ramp measured for each LED in their CIE 1931 XYZ chromaticity coordinates.

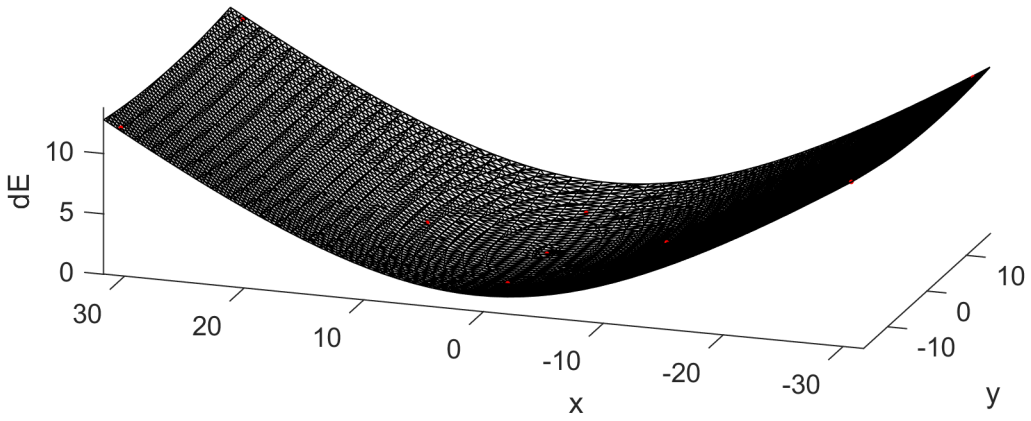

Figure 3.3: Fitted ellipsoid to the measured nine positions at the bottom plane of the light box. The x-axis indicates the depth of the light box whereas the y-axis indicates the length inside the light box.

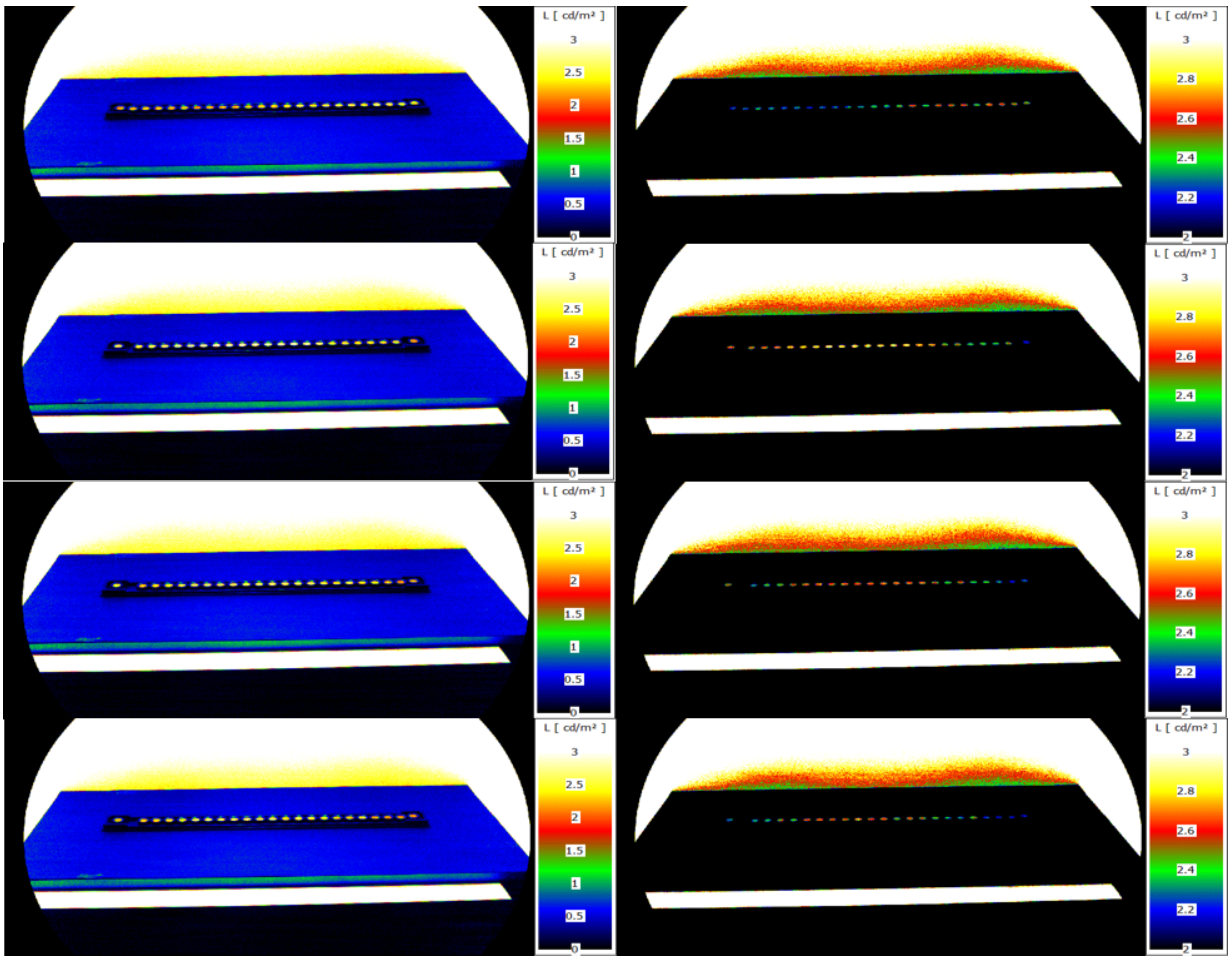

Figure 3.4: LMK luminance images for tray 1, tray 2, tray 3 and tray 4, from top to bottom. The left-hand figures range between 0 and 3 cd/m2 and the right-hand figures between 2 and 3 cd/m2.

3.4 Experimental Methodology

3.4.1 Experimental design

The experimental design of this experiment was a full factorial within subject design with illuminance (5 levels: 307, 34.9, 17.9, 5.6 and 0.7 lux) and age (2 age groups: 18-30 and 45-60) as the independent variables and the FM100-Hue test results as the dependent variable.

3.4.2 Participants

The recruitment of participants was done within Signify Research (i.e. employees and interns) and the TU/e student population. Participants could participate in the experiment when they could speak English or Dutch, were in the age range 18-30 or 45-60 years, were color normal and not oversensitive to light. There were 24 participants, 12 participants for the younger group, 5 females and 7 males, and 12 participants for the older group, 4 females and 8 males. The participants in the younger group were aged from 18 to 29 years old, with an average age of 23.8. years (SD = 3.0). The participants in the older group were aged from 46 to 59 years old, with an average age of 52.9. years (SD = 4.2).

3.4.3 Stimuli

3.4.3.1 Illumination

The FM100 Hue test was designed by Farnsworth under illuminant C in the photopic vision regime at 25-foot candles (269 lux) or more. For the standard observer without any color deficiencies, the FM100 Hue test should be accurately performed without any large displacements in cap order. The illumination condition for our experiment, therefore, was chosen to best represent illuminant C. This illumination was then decreased in light intensity to investigate at which point the FM100 hue color caps would be displaced and which color caps would be most affected. The CIE 1931 XYZ chromaticity coordinates of the illumination were determined by equation 3.2, 3.3 and 3.4 for the CIE 1931 color matching functions. The CIE 1931 XYZ chromaticity coordinates were then transformed to the CIE 1976 UCS chromaticity coordinates for the u' and v', see equations 3.9 and 3.10.

$$X = \int_{\lambda} I(\lambda)\bar{x}_2(\lambda)d\lambda \tag{3.2}$$

$$Y = \int_{\lambda} I(\lambda)\bar{y}_2(\lambda)d\lambda \tag{3.3}$$

$$Z = \int_{\lambda} I(\lambda)\bar{z}_2(\lambda)d\lambda \tag{3.4}$$

Illuminant C in this study was approximated by combining the 11 LEDs such that the spectral power distribution and the uv coordinates were most similar to those of illuminant

C. A colorimetric model using the nonlinear solver fmincon in Matlab was used to determine the digital counts from a look up table which minimized the differences in spectral power distribution and uv coordinates. The look up table consisted of the interpolated values of the color characterization files. The spectral distribution of the approximated illuminant C, from now on referred to as C_a and the actual reported illuminant C are shown in figure 3.5. Illuminant C_a was spectrally less flat than illuminant C, especially around 480nm.

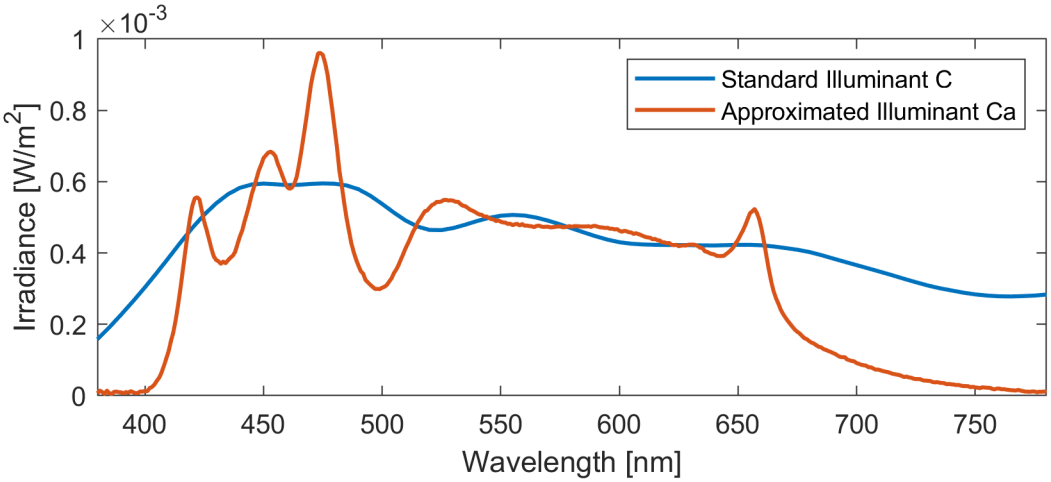

Figure 3.5: The illuminance weighted spectral distribution of the standard illuminant C and the measured approximation C_a with the LED cubes.

All 85 color caps of the FM100-Hue test were presented under illuminant C_a. The actual position of the 85 color caps in CIE 1976 UCS diagram for this illuminant are shown in figure 3.6. Noticeable in this figure is that all color caps together do not form a perfect circle and the center of all the color caps does not align with the actual position of the illuminant. This might be explained by imperfections in the cap production and the fact that the color caps were not originally designed to be circular in this color space.

In the experiment the 85 color caps were presented under different light levels. To find optimal light levels to measure the effect of reduced illuminance on color discrimination, polarization filters were applied to the illuminant C_a. The polarization filters were necessary because the resolution of the LED cubes didnt allow to go lower in digital counts while keeping the accuracy of reproducing illuminant C_a. In the experiment, two polarization filters were placed on the LED cubes where the first polarization filter was fixed, and the second polarization filter could be rotated. The LED cube and the first polarization filter were a 30x30 cm square. The second polarization filter was, therefore, made circular to allow for an easier rotation which is shown in figure 3.7. Because the second polarization filter was made circular, the corners of the square were filled with black paper.

The transmission of the combined two polarization filters in the aligned position, 0 degrees rotation of the second polarization filter, were measured and shown in figure 3.8. Almost zero spectral irradiance was measured below 400 and above 760 nm which would explain the noise in transmission above and below these wavelengths. Furthermore, between

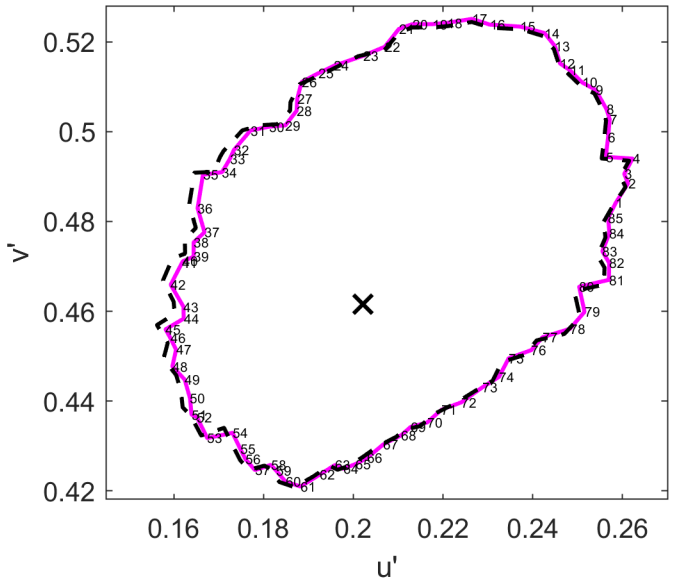

Figure 3.6: The chromaticity coordinates of the color caps aligned for its correct order for the approximated illuminant C_a as the solid magenta line and for the standard illuminant C as the dotted black line in the CIE 1976 UCS diagram. The chromaticity coordinates of the approximated and standard illuminant C are indicated with a black cross.

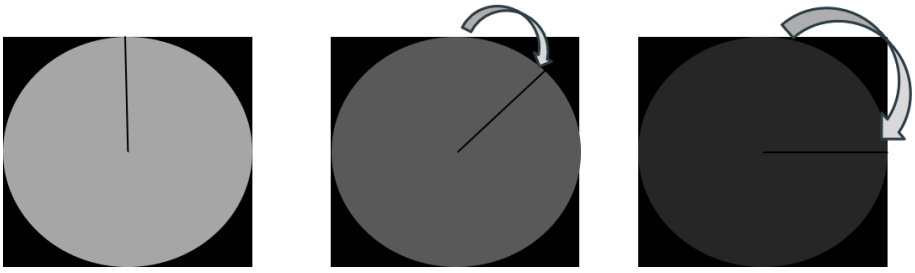

Figure 3.7: Graphical representation of the two polarization filters, where the second polarization filter is rotated 0 degrees in the left figure, 45 degrees in the middle figure and 90 degrees rotated in the right figure.

400 and 460 nm the transmission was less than 0.4. This was corrected by increasing LED 2 and 10 which had peaked distributions in irradiance at those wavelenghts. The correction by which these LEDs were increased was calculated by taking the ratio between the desired transmission ratio of 0.4 and the actual transmission that was measured at those wavelengths.

The spectral power distribution of the illuminant C_a after increasing the two LEDs and at different rotations of the second polarization filter were re-measured and compared against the original spectral power distribution of illuminant C_a without the filters corrected for its lightness to be similar to the measured spectra, see figure 3.9. The re-measured

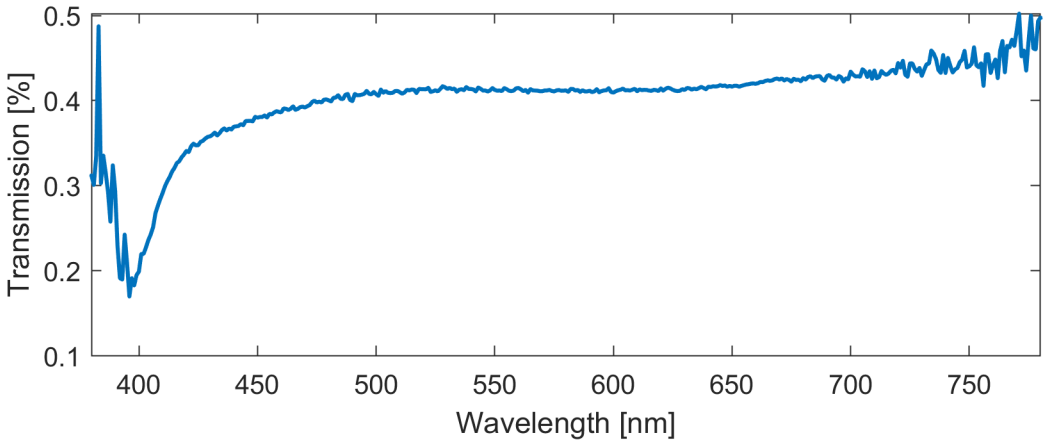

Figure 3.8: Percentage of transmission of the two polarizaton filters when the second polarization filter is aligned with the first.

spectra were very similar to the original illuminant C_a as also indicated by the Global Lighting Association calculation tool for CIE 13.3-1995 with associated CRI-based colour rendition properties 2018, shown in appendices .1.3, .1.3, .1.3, .1.3, .1.3 and .1.3.

After the spectra were re-measured and compared for their spectral power distribution their chromaticity coordinates were also compared to the chromaticity coordinates of illuminant C. As shown in figure 3.10 the approximated spectral power distribution for the different rotation of the second polarization filter were very accurate, where only the chromaticity coordinates of the lowest possible spectral irradiance, with the rotation of the second polarization filter perpendicular to the first fixed polarization filter, showed minor differences. These differences, however, could be explained by the inaccuracy of the JETI measurement device at these very low light levels.

Additionally, to checking the spectral power distribution at each angular position of the second polarization filter, the normalized luminance factor reduction was measured at nine different angles, see figure 3.11. The figure shows that the luminance reduction was correlated linearly with the rotation angle.

These measurement tests show that the polarization filters behaved relatively consistent in their transmission factor and transmission spectra. The eventual rotation angles that were used in the experiment were determined by a pilot study, which used five independent measures for two participants. The selection criteria of the stimuli were based on finding a stimulus where participants were making almost no displacements in the FM100-Hue test and finding a stimulus that would almost represent a random placement of the color caps. The four luminance levels that were found to be most useful for this criteria, based on a pilot involving three participants, were 10, 5, 1.5 and 0.2 cd/m^2 (for a white reference patch with a reflection of 87.2 %). In illuminance this was 34.9, 17.9, 5.6, 0.7 lux. Besides the four chosen luminances the test was also performed under illuminance C at 85 cd/m^2 (307 lux) as a reference to how people would perform the FM100-Hue test under the preferred

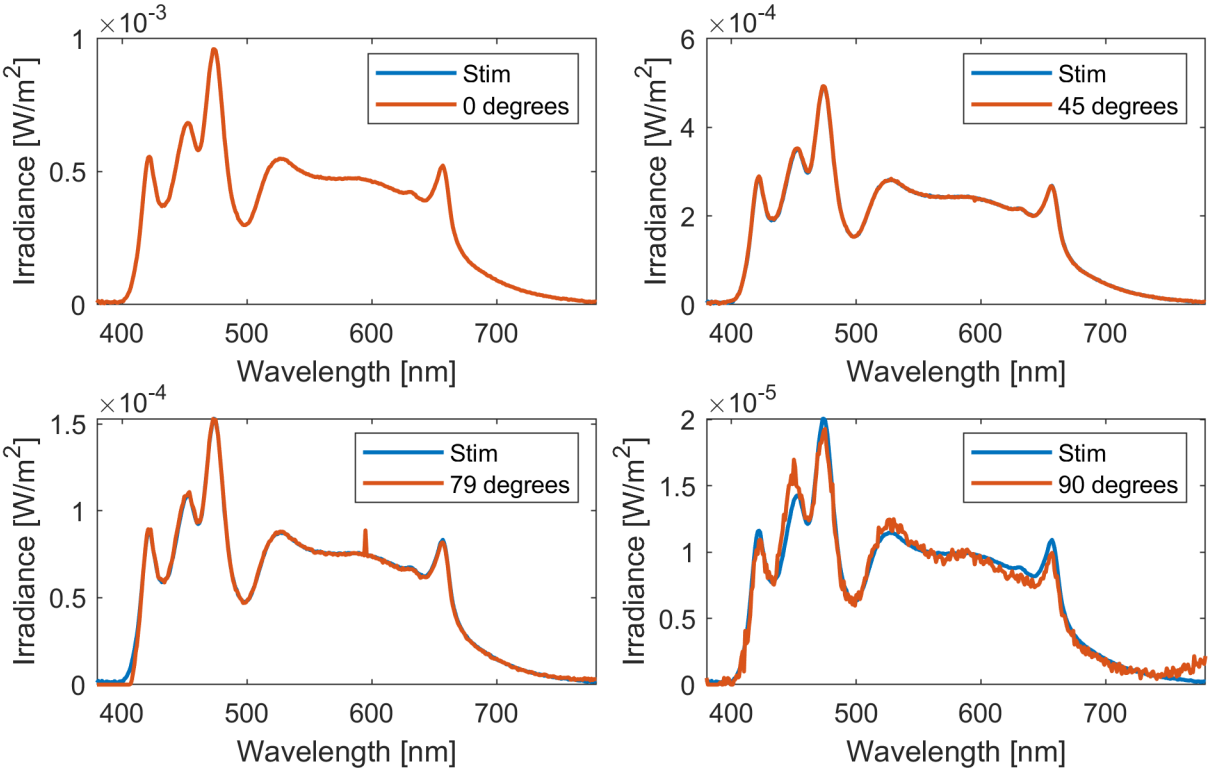

Figure 3.9: The weighted irradiance of the approximated stimulus and the measured irradiance at different rotations of the second polarization filter.

light level as reported by Farnsworth (>269 lux).

3.4.3.2 Hue test

The objects used in the experiment were uniform matte color caps taken from the FM100-hue test. The FM-100 hue test kit contains four trays with different fixed anchor caps, first tray containing 22 color caps and the remaining three containing 21 color caps. In total the FM-100 hue test kit only contains 85 color caps instead of the 100 color caps that is was originally designed for. Farnsworth decided to remove 15 caps because 100 color caps seemed to difficult for participants to reliably perform. In each tray the color caps are presented in order of chromaticity with two fixed anchor caps at each end of the tray. The boxes were chosen by Farnsworth based on the L- and M- cone excitation (red-green axis) and the S-cone excitation (tritan axis). Both axes are believed to correspond to the midget cells and small-bistratified ganglion cells involved in color vision (Knight et al., 1998). The color caps were determined for the standard illuminant C, which was proposed by Farnsworth to be similar to daylight. Furthermore, the color caps supposedly were also isoluminant under illuminant C, however, for different illuminants the luminance differences between the caps are slightly noticeable. The color caps of the FM100-hue

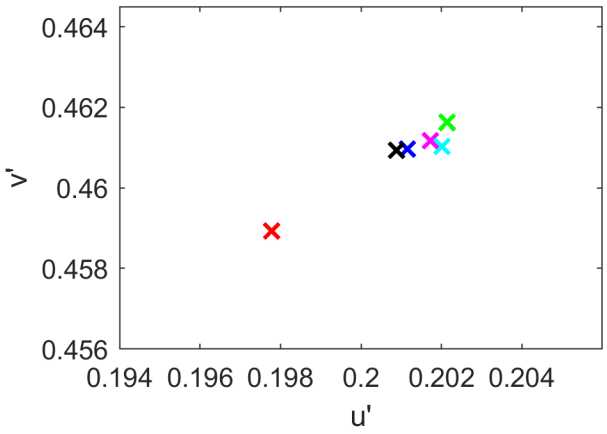

Figure 3.10: The chromaticity coordinates of the spectral power distributions of standard illuminant C and the approximated illuminant C_a by the LED cube system at the different rotations. Black cross indicates the standard illuminant C, all other crosses the illuminant C_a at different light levels. Blue indicates 307 lux, green 34.9 lux, cyan 17.9 lux, magenta 5.6 lux and red 0.7 lux.

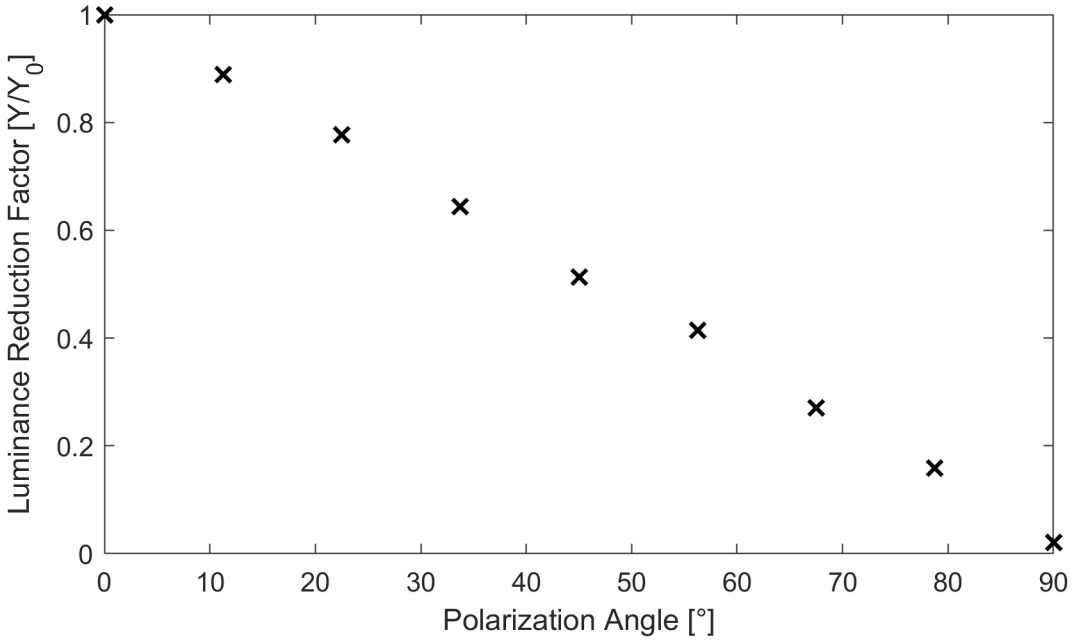

Figure 3.11: The luminance reduction factor at different polarization angles.

test are distributed fairly equal at the standard illuminant C and represent typical hue angle differences. The color of the caps originates from the Munsell book of colors and these book colors originate from the fundamental five principal hues, Yellow, Green, Red,

Purple and Blue as well as the five intermediate colors of the principal hues. Newer, more widely used, models that supplement the Munsell book of colors are the CIELAB and CIECAM02 color systems. The FM100-hue color caps are, therefore, relevant in determining whether color spaces such as CIELAB and CIECAM02 describe the differences in chromatic discrimination under different illuminations, surroundings, adaptations and backgrounds. A picture of the FM100-Hue color caps is shown in figure 3.12.

Figure 3.12: The FM100-hue test with tray 1, tray 2, tray 3 and tray 4 from top to bottom.

The color caps reflectance spectra R(λ) were used to calculate the chromaticity coordinates of each cap for a chosen illumination I(λ) by using the equations 3.5, 3.6, 3.7 and 3.8 for the CIE 1931 $\overline{x}$, $\overline{y}$ and $\overline{z}$ color matching functions.

$$X = \frac{K}{N}\int_{\lambda} R(\lambda)I(\lambda)\bar{x}_2(\lambda)d\lambda \tag{3.5}$$

$$Y = \frac{K}{N}\int_{\lambda} R(\lambda)I(\lambda)\bar{y}_2(\lambda)d\lambda \tag{3.6}$$

$$Z = \frac{K}{N}\int_{\lambda} R(\lambda)I(\lambda)\bar{z}_2(\lambda)d\lambda \tag{3.7}$$

where

$$N = \int_{\lambda} I(\lambda)\bar{y}_2(\lambda)d\lambda \tag{3.8}$$

$$u' = \frac{4X}{X + 15Y + 3Z} \tag{3.9}$$

$$v' = \frac{9Y}{X + 15Y + 3Z} \tag{3.10}$$

The CIE 1931 XYZ chromaticity coordinates were then transformed to the CIE 1976 UCS chromaticity coordinates for the u' and v', see equations 3.9 and 3.10. The reflectance spectra of the color caps were available between 380 and 730 nm at 10 nm interval. The reflectance spectra of the color caps were linear extrapolated beyond 730 nm to 780 nm. Between the 380 and 780 nm the reflection spectra were then interpolated to smaller steps of 1 nm, see figure 3.13.

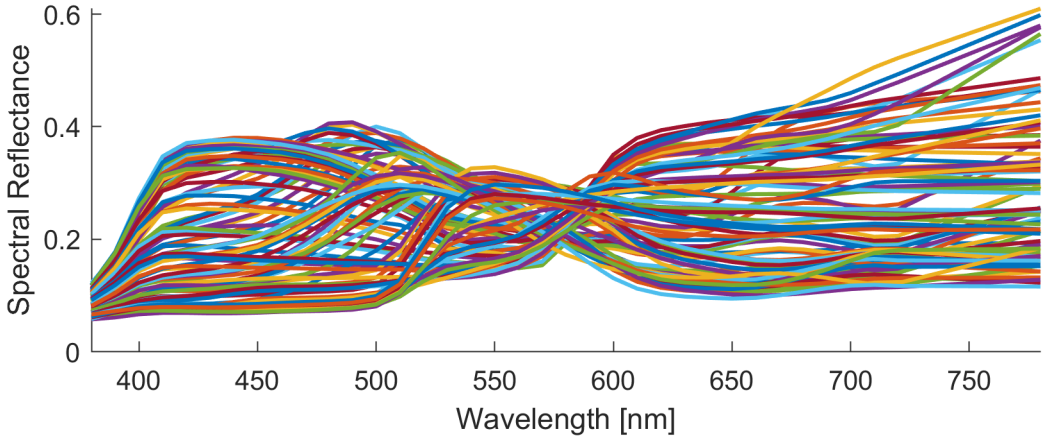

Figure 3.13: The extrapolated and interpolated reflectance spectra of all color caps.

3.4.4 Procedure

Before the start of the experiment, participants received an introduction to the procedure and possible risks and harms were explained. After this introduction, participants gave their written consent and were screened for color vision deficiencies. They performed the Ishihara color vision test in the left light box under illuminant C with an illuminance of 307 lux. The Ishihara color vision test score was then stored for later comparison with the FM100 Hue test results. After performing the Ishihara test, a few practice trials with the FM100 Hue test followed to get participant familier with the procedure. When the participants successfully finished the practice trials, the actual experiment started.

The experiment consisted of five different trials (ca 15-20 min per trial) in which the approximated illuminant C_a was shown at different illuminance levels (i.e. a fixed illuminance per trial). The first trial was performed in the left light box without the polarization filters at 307 lux. The remaining four trials were performed in the right light box using different polarization angles. For each remaining trial the second polarization filter angle was

changed such that the illuminance was 34.9, 17.9, 5.6, or 0.7 lux. The order of the remaining four trials was counterbalanced [1] between participants using a Latin-square design. For each trial the FM100-Hue test was performed as a measure of chromatic discrimination. In the FM100-Hue test, all four trays were used and presented in a sequential random order. In the experiment no time limit was issued, but the participants were instructed to preferably not to take too long time with the cap ordering. Before starting a trial, each of the four trays had its color caps shuffled randomly, such that the correct order of the caps could not be retraced. Also, before each trial, a pre-adaptation period started which lasted for five minutes to have the participant adapted to the illuminant of that trial. During this pre-adaptation period participants were instructed to look around at the white walls of the light box. The procedure of the experiment is shown in figure 3.14.

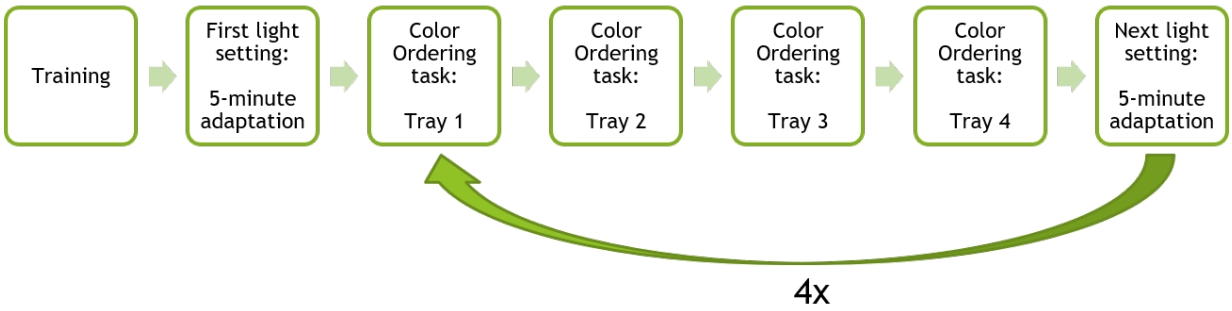

Figure 3.14: Experimental procedure

A trial started with placing the first tray of the FM100-Hue test in the middle of the light box at an illumination angle of 90 degrees and an observation angle of 60 degrees. The color caps were placed in front of the tray except for the two fixed anchor caps, see figure 3.15.

The participant's task was to rearrange the randomly shuffled color caps and place them back on the tray such that the color cap ordering was chromatically consistently changing between the two anchor caps, see figure 3.16.

[1] The order of the trials of first two participants were not correctly counterbalanced. Because of the lack of time and number of participants their data was used for the analysis.

Figure 3.15: Picture of the shuffled color caps.

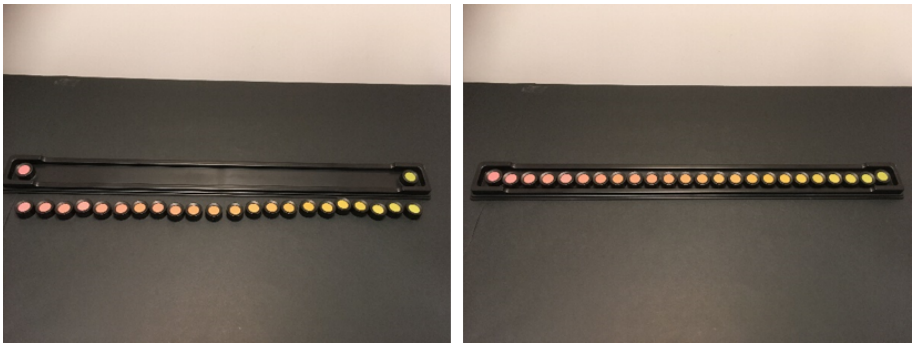

Figure 3.16: Picture of the order color caps in front (left) and on the tray (right).

When the participant was confident about the color cap ordering the participant notified the experimenter and the tray was substituted with the next tray inside the light box. After the four trays were confidently ordered by the participant, the color cap ordering of each tray was recorded by taking a photograph and the total time spend on the trial was recorded by a Matlab script. After recording the response and time, the polarization angle was changed such that it matched the illuminance of the next trial and an adaptation period of five minutes would start. During the adaptation period the color caps of each tray of the FM100-Hue test was again shuffled.

3.5 Analysis

3.5.1 Standard cap order

Each of the color caps of the FM100-Hue test has a specific number printed on its back, see figure 3.17. This number then allowed the standard cap order defined by Farnsworth to be retraced. Since the FM100-Hue test was originally designed under illuminant C, the

standard cap order as indicated on the back of the caps depended on how well the illuminant represented illuminant C. Also, any transposition of color caps could be retraced by finding color caps that did not fit the standard cap order on that tray between the two colored anchor caps. In the experiment participants had to place the color caps on each tray for each light level. The participants were instructed to place the caps based on their colors such that the caps form a regular color series between the two anchor caps. The positioned color caps by the participants were then recorded by looking at the numbers printed on the back. Expected was that when the illuminant was similar to illuminant C and was above 270 lux the standard cap order would be similar to the order of the participants.

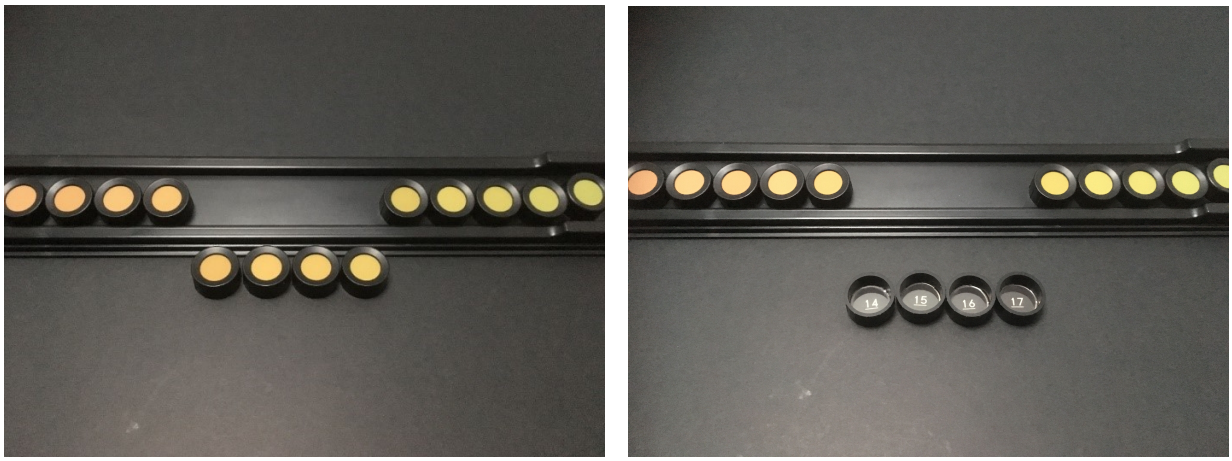

(a) Color caps in their normal position.

(b) Color caps turned around reveiling their numbers on the back.

Figure 3.17: Pictures of the positioned color caps on the tray.

3.5.2 Standard FM-100 Hue test score

The standard FM100-Hue test score was determined for each color cap. The FM100-Hue test score was based on the sum of differences of neighboring color cap numbers. The smallest difference between adjacent color caps was 1 and the largest difference was 22 for the tray with 24 color caps and 21 for the trays with 23 color caps. For the calculation of the standard FM-100 Hue test score, in the first tray (color cap numbers 85 and 1 to 21) the color cap number 85 was recoded as 0 and the anchor point 84 on the first tray was recoded as -1. In the other trays the original color cap number was used to determine the difference between neighbouring color caps. See figure 3.18 for an example of how the FM-100 Hue test score was determined.

The standard FM-100 Hue test score was determined for each light level, color cap and participant. The score was calculated by taking the absolute difference between neighbouring color caps see equation 3.11. In these equations i indicates the counter for the four

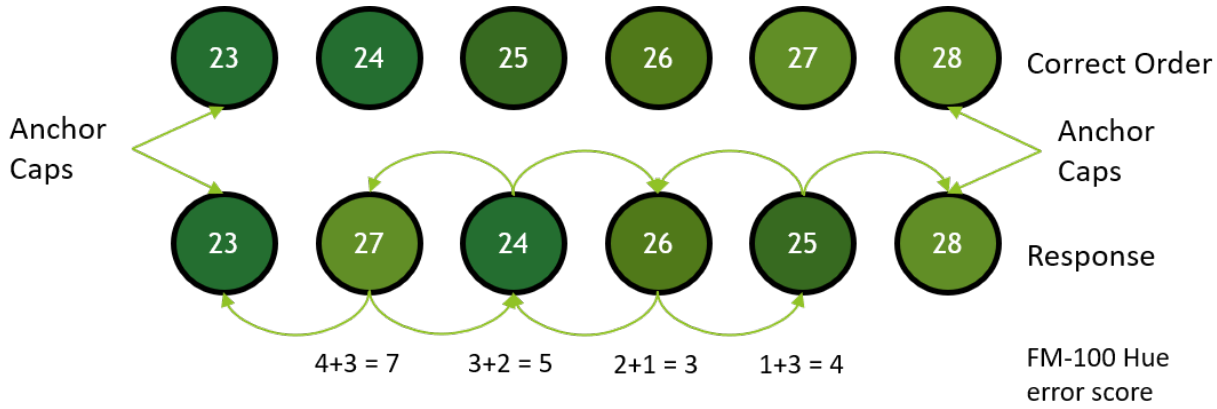

Figure 3.18: An example, for a series of imaginary color cap numbers, of how the FM-100 Hue test score was determined.

trays, $FMCE_j$ the cap error of the j^{th} cap, C_j the cap number of the j^{th} cap, n the number of move able caps in the tray, $1FMES$ the summed error score for tray 1, $2FMES$ the summed error score for tray 2, $3FMES$ the summed error score for tray 3, $4FMES$ the summed error score for tray 4 and $TFMES$ the total error score.

$$TFMES = \sum_{i=1}^{4} FMES_i = \sum_{i=1}^{4} \sum_{j=1}^{n+2} FMCE_j \tag{3.11}$$

where $FMCE_j$ is determined by equation 3.12.

$$FMCE_j = |C_j - C_{j-1}| + |C_j - C_{j+1}| \tag{3.12}$$

3.5.3 Order based on Hue angle

For the analysis of the ordering of the color caps by their hue angles, the CIE 1976 UCS and CIECAM02UCS chromaticity coordinates were determined. The obtained u and v, a and b values then determined their position in that color space. Additionally, the hue angles of the color caps to the corresponding illuminant were determined in both color spaces. Both color spaces had slightly different hue angles.

The color cap ordering was analyzed by their hue angles. The hue angles of the 85 color caps were determined in the CIE 1976 UCS and CIECAM02UCS color spaces. Also, the hue angles were determined for each light level, so the small differences between the weighted spectral power distribution of the intended approximated illuminant C_a and the spectral power distribution at that light level were accounted for. The cap ordering determined by Farnsworth for illuminant C originated from the Munsell book of colors and was confirmed by the order in hue angle in the CIE 1931 xyY color space. The uniformity of the CIE 1931 xyY color space has now been refuted by many researchers, therefore, this cap ordering

was compared to the hue angles in more recent color spaces such as the CIE 1976 UCS and CIECAM02UCS. In calculating the CIECAM02 chromaticity coordinates and hue angles, the relative luminance of the background was set at 7% of the luminance of the light setting for a 87.2 % white reflectance patch, the adapting field luminance was set at 20% of the luminance of the light setting for a 87.2 % white reflectance patch, the impact of the surround set at 0.69 with the corresponding chromatic induction factor and factor of degree of adaptation depended on the adapting field luminance. In both color spaces the predicted cap ordering determined by Farnsworth largely corresponded with the cap ordering determined by the calculated hue angle. The relative luminance of the background was estimated from the LMK measurement, where the background was roughly 7% of the luminance of the light setting. The adapting field luminance was set at 20% of the luminance of the light settings as the average of the total adapting field (gray).

The hue angles between each cap combination varied more in the two updated color spaces than in the CIE 1931 xyY color space. This was somewhat expected because in the updated color spaces different colorimetric equations are used. The CIE 1976 UCS color space could directly be retraced by using a conversion formula between the CIE 1931 xyY chromaticity coordinates and the CIE 1976 UCS chromaticity coordinates, see equations 3.13 and 3.14. The CIECAM02UCS color space, however, was fundamentally different because it accounts for the adapting field luminance, relative tristimulus values of the sample, relative luminance of the background and the degree of adaptation. Based on these additional parameters in the CIECAM02UCS color space expected was that the CIECAM02UCS color space would much better predict the participant color cap order than the CIE 1976 UCS color space.

$$u' = \frac{4x}{-2x + 12y + 3} \tag{3.13}$$

$$v' = \frac{9Y}{-2x + 12Y + 3} \tag{3.14}$$

3.5.4 Modified FM-100 Hue test score

In 2017, Esposito and Houser introduced a modified FM-100 Hue test score based on the hue angles of the color caps in the CIECAM02UCS color space [54]. Furthermore they also proposed a light source error score to test the amount of light source-induced cap transpositions according to the hue angles of the color caps in the CIECAM02UCS color space for the different light source [54]. In this study this modified FM-100 Hue error score and the light source error score were investigated according to their equations 3.15, 3.16, 3.17 and 3.18. To calculate the modified FM-100 Hue error score and the light source error score a MATLAB script was created that used the CIECAM02 model with the relative luminance of the background set at 7% of the luminance of the light setting, the adapting field luminance set at 20% of the luminance of the light setting, the impact of the surround

set at 0.69 with the corresponding chromatic induction factor and the factor of degree of adaptation set at 1.

$$TFMES_{adj} = \sum_{i=1}^{4} FMES_{adj,i} = \sum_{i=1}^{4}((\sum_{j=1}^{n+2} FMPE_j) - ((n+2)2)) \tag{3.15}$$

where $FMPE_j$ is determined by equation 3.16.

$$FMPE_j = |P_j - P_{j-1}| + |P_j - P_{j+1}| \tag{3.16}$$

In equation 3.15 and 3.16 i indicates the counter for the four trays, $FMPE_j$ the place error of the j^{th} cap, P_j the place number of the j^{th} cap, n the number of move able caps in the tray, $1FMES_{adj}$ the summed adjusted error score for tray 1, $2FMES_{adj}$ the summed adjusted error score for tray 2, $3FMES_{adj}$ the summed adjusted error score for tray 3, $4FMES_{adj}$ the summed adjusted error score for tray 4 and $TFMES_{ajd}$ the total adjusted error score.

$$R_d = \sum_{i=1}^{4} R_{d,i} = \sum_{i=1}^{4}((\sum_{j=1}^{n+2} FMCEt_j) - ((n+2)2)) \tag{3.17}$$

where $FMCEt_j$ is determined by equation 3.18.

$$FMCEt_j = |Ct_j - Ct_{j-1}| + |Ct_j - Ct_{j+1}| \tag{3.18}$$

In equation 3.17 and 3.18 i indicates the counter for the four trays, $FMCEt_j$ the cap error of the j^{th} cap

When standard illuminant C was used, the modified FM-100 Hue test score was expected to provide the same results as the standard FM-100 Hue test score. When the illuminant was altered and light source-induced cap transpositions for the order based on the hue angles occurred the modified FM-100 Hue test score differed from the standard FM-100 Hue test score. The place number used to calculate the place error score in the modified FM-100 Hue test score depended on the order based on the hue angles. The place number was determined by cross referencing the numerical cap number with the order based on the hue angles. The modified FM-100 hue test score, therefore, was not expected to induce many or any difference from the standard FM-100 Hue test score in this study.

3.5.5 Confusion distances

Alternatively, to the FM100-Hue test score also the confusion distance was determined for each displaced color cap. A switch model explained by Jiaye Li in her thesis about the visibility and predictability of perceived colour differences (2017) was used to determine the total error of chromatic discrimination for each of these displacements. The confusion distance is the distance between all other caps that were incorrectly ordered by the displacement of a single color cap. Figure 3.19 illustrates how the confusion distance was

determined. The FM100-Hue test does not account for a single color cap to explain the displacement of other color caps, for which the model by Jiaye Li would be more appropriate.

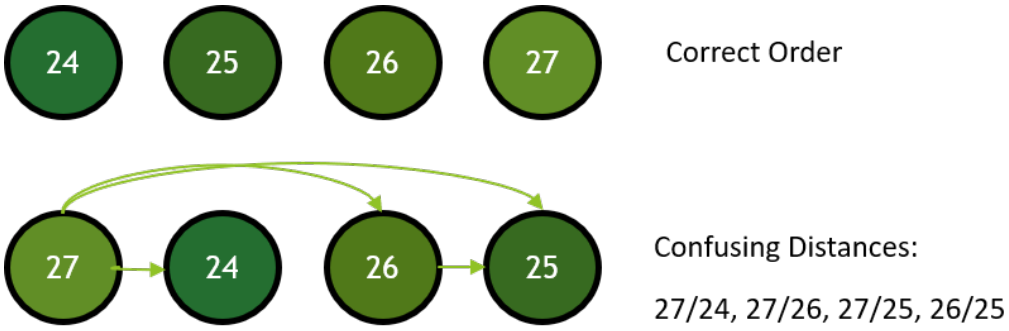

Figure 3.19: The correct order on top and the confusion distances for a certain misplacement of color caps.

A switch matrix then was used to calculate the total error score for the collection of discrimination errors for all the confusion distances. First all possible combinations of confusion distances between each color cap within each tray were determined. Afterwards the color distance in the CIECAM02UCS color space for each of these distances was calculated and stored in a distance matrix. The euclidean color distance was determined by equation 3.19. Second the total error score for the confusion distances of the ordering of the participant was determined by finding the confusion distances and using the switch and distance matrix to determine the total discrimination error score. So, for example the E-CAM02UCS for the confusion distance 27/24 is 6.3, 27/25 is 4.2 and 27/26 is 2.4, and the confusion distance 27/24 was found 3 times between participants, 27/25 4 times and 27/26 5 times, then the total discrimination error score for 27/24 would be 3 and the distance 6.3. Whereas the error score for 27/26 would be 5 and the distance 2.4. This error score determination was different than how Jiaye Li first introduced it, Jiaye Li would also sum the amount of displacements for each repeated measurement and participant, whereas in this study no repetitions per light setting were performed, therefore, only the total error of all the participants were summed. Furthermore, there is also the advanced switch model also introduced Jiaye Li, which accounts for the illuminant in determining the correct order. In this experiment, the correct order was slightly different in both color spaces and did not fully correspond to the order of the numbers specified on the back of the color caps, so and this advanced switch model was also implemented to determine the confusion distances.

$$\Delta E_{i,j} = \sqrt{(a_i - a_j)^2 + b_i - b_j)^2} \tag{3.19}$$

With the number of occurrences of each possible confusing distance an error percentage was calculated by dividing the number of occurrences by the total number of participants. This resulted in an error distribution for the percentage displaced color caps between participants. The error distribution was then plotted against the euclidean chromaticity distance in the CIECAM02UCS ab plane. To this data a psychometric curve was fitted for a negative cumulative Gaussian with boundaries at the 1 and 0 proportion of displacements. The psignifit (v.4) software (see: Schutt, Harmeling, Macke, and Wichmann [55]) was used to fit this psychometric curve for each light level. The fitted psychometric curve was expected to reach a proportion of displacements of 0.5 as the distance in the CIECAM02UCS ab plane between two color caps would get closer to 0 and reach a proportion of 0 as the distance would get larger. The just noticeable difference point (threshold) was indicated at the 50% point where more than half the participants would be displacing two color caps. In this analysis, the Wichmann and Hill method for the Monte Carlo simulation of bootstrap to obtain the confidence intervals around the threshold was also considered. Hill, Kuss et all. [56] and Fründ et al. [57], however, showed that the confidence intervals obtained by bootstrapping for the estimation of psychometric functions were too narrow. Therefore in this study, intervals according to the Bayesian statistics were calculated. Additionally, the Bayesian credible intervals for the posterior distribution based on a standard prior were estimated. These intervals and credible intervals were calculated with the equations defined by Schutt, Harmeling, Macke, and Wichmann in the psignifit (v.4) software [55].

3.5.6 Circular statistics

Additionally, the number of the cap order was also analyzed and compared with the hue angles of the color caps in the specified color spaces. To allow for circularity in the data the data was statistically analyzed with the Circular Statistics Toolbox (Directional Statistics) of Matlab. Allowing for circularity in this data set was important when using the hue angles to determine the ordering of the participant. A measure of association was calculated between the hue angles according to the circular-circular correlation explained by Berens in his paper about a MATLAB Toolbox for Circular Statistics [58]. A measure of association was calculated as an indication of how well the participant data could be explained by other factors. Before the circular-circular correlation could be determined first the hue angles were converted into radians according to equation 3.20. Because the color caps of FM-100 Hue test were originally designed to be uniformly distributed around the Munsell color circle, a ground truth of uniform distances between color caps in hue angles was assumed.

$$\alpha_{radiance} = \frac{2\pi\alpha_{degree}}{360} \tag{3.20}$$

After converting the circular variables to radians a correlation coefficient ρ_{cc} was computed by using equation 3.21 [58][59].

$$\rho_{cc} = \frac{\sum_i sin(\alpha_i - \bar{\alpha})sin(\beta_i - \bar{\beta})}{\sqrt{\sum_i sin^2(\alpha_i - \bar{\alpha})sin^2(\beta_i - \bar{\beta})}} \tag{3.21}$$

where ρ and β are the circular variables in radians with the $\bar{\beta}$ and $\bar{\alpha}$ as the angular mean. For the null hypotheses of no correlation between the two variables the significance can be estimated by computing a p-value for the correlation coefficient ρ_{cc} with the test statistic following a normal distribution shown by equation 3.22.

$$t = \sqrt{f}\rho_{cc} \tag{3.22}$$

where f is determined by equation 3.23.

$$f = N\frac{\sum_i sin^2(\alpha_i - \bar{\alpha})\sum_i sin(\beta_i - \bar{\beta})}{\sum_i sin^2(\alpha_i - \bar{\alpha})sin^2(\beta_i - \bar{\beta})} \tag{3.23}$$

3.5.7 Thurstonian analysis

In the experiment participants compared multiple color caps and create a color series between the two fixed anchor caps. When assuming that in creating the color series participants compared each color cap with one another, a frequency matrix could be created. This assumption, however, was difficult to prove as it was unclear whether participants actually made every visual comparison between each color cap. Nonetheless, a Thurstone scaling on the frequency matrix would provide information on the ordering of the color based on the participants. Besides assuming paired comparisons for the Thurstone scaling also assumed was that the error variances were equal and uncorrelated. Commonly referred to the Thurstone Case V that describes a scale value with an arbitrary unidentified multiplier.

To get scale estimates from the frequency matrix, a Thurstonian analysis as described by P.G. Engeldrum was performed [51]. First, all the responses from each participant for all possible color cap transpositions were added to a single frequency matrix in Matlab. Second, the frequency matrix was divided by the total number of observers (N = 24). Third, the proportion matrix was transformed to a scale difference matrix including the z-scores by using the inverse cumulative distribution function of Matlab. Saturated comparisons were corrected by a -2.96 z-score for the proportion of 0 and 2.96 z-score for the proportion 1. The scale value estimates were determine for the least squares solution by taking the mean of each column of this scale difference matrix. These scale value estimates have an arbitrary constant and average to zero. The 95% confidence intervals were calculated according to the Montag equation [60], see equation 3.24 and 3.25. Capital N indicating the number of participants and the small n indicating the number of stimuli.

$$\sigma = 1.76(n + 3.08)^{-0.613}(N + 2.55)^{-0.491} \tag{3.24}$$

$$CI = \pm 1.96\frac{\sigma}{\sqrt{N}} \tag{3.25}$$

3.5.8 Bipolarity and axis analysis

Another interesting procedure for analyzing the FM-100 Hue test score was proposed by Knoblauch in 1987 [61]. The analysis was based on quantifying the bipolarity and axis of the FM-100 Hue test score. The analysis provided estimates of parameters that characterized the degree of bipolarity, orientation of axis of the bipolarity and the standard overall FM-100 Hue test score. This analysis was based on fitting a sine wave of two cycles per revolution around the standard error diagram. The modulation and amplitude of this two cycle sine wave characterized the degree of bipolarity. The phase angle and the cap positions at the maximum of the sine wave characterized the orientation of axis of the bipolarity. The mean error characterized the standard overall FM-100 Hue test score. The resulting two cycle sine wave had the form of equation 3.26.

$$f(i) = M + Asin(\frac{4\pi(i-1)}{85} + \phi) \tag{3.26}$$

In equation 3.26 i indicates the cap position, M the mean standard FM-100 Hue test score, A the amplitude and ϕ the phase angle.

The mean standard FM-100 Hue test core was computed with equation 3.27. Where e_i was the standard FM-100 Hue cap score associated with position i according to the Kinnear method of plotting [62].

$$M = \sum_{i=1}^{85} \frac{e_i}{85} \tag{3.27}$$

The amplitude was calculated by first determining the amplitude of the sine and cosine units in radians, see equations 3.28 and 3.29. Then the amplitude was determined by equation 3.30.

$$a_s = \sum_{i=1}^{85} \frac{e_i}{42.5} sin(\frac{4\pi(i-1)}{85}) \tag{3.28}$$

$$a_c = \sum_{i=1}^{85} \frac{e_i}{42.5} cos(\frac{4\pi(i-1)}{85}) \tag{3.29}$$

$$A = (a_s^2 + a_c^2)^{1/2} \tag{3.30}$$

From the amplitude of the sine and cosine units the phase angle was determined by equation 3.31.

$$\phi = \begin{cases} tan^{-1}(a_c/a_s) & \text{if } a_s > 0; \\ \pi + tan^{-1}(a_c/a_s) & \text{if } a_s < 0. \end{cases} \tag{3.31}$$

The maxima of equation 3.26 indicate the cap positions through which the axis of the two cycle sine wave passes. The maxima were determined by equations 3.32 and 3.33.

$$\alpha_1 = \frac{85}{4\pi}(\pi/2 - \phi) + 1 \tag{3.32}$$

$$\alpha_2 = \frac{85}{4\pi}(5\pi/2 - \phi) + 1 \tag{3.33}$$

The modulation of the two cycle sign wave was computed as the ratio between the sine wave amplitude and the mean standard FM-100 Hue test score see equation 3.34.

$$\beta = \frac{A}{M} \tag{3.34}$$

Furthermore, Kenneth Knoblauch provided equations for calculating the standard errors (SE) for each parameter estimate which was derived from large sample methods [63], see equations 3.35, 3.36 and 3.37.

$$SE(A) = (\frac{MSE}{42.5})^{1/2} \tag{3.35}$$

where MSE is $\sum_{i=1}^{85}(f[i] - e_i)^2/82$

$$SE(\alpha_1) = SE(\alpha_2) = \frac{85SE(A)}{4\pi A} \tag{3.36}$$

$$SE(\beta) = 0.707SE(A)(\beta^2 + 2)^{1/2}/M \tag{3.37}$$

Chapter 4

Results

In the experiment, the cap ordering was measured for 20 conditions (4 trays x 5 illuminance levels). The four trays were from the FM-100 Hue test kit and the illuminance levels were 307, 34.9, 17.9, 5.6 and 0.7 lux.

4.1 Standard cap order

The standard cap order determined by Farnsworth was for tray 1: [85 1:21], tray 2: [22:42], tray 3: [43:63] and for tray 4: [64:84]. At every position in the trays for each light level the participant had to place a color cap. Each color cap had a specific number printed on its back such that the sequence of the these numbers ordered by the participant could be stored inside a Matlab file. The order based on the participants was then compared to the the standard cap order by calculating the standard FM-100 Hue test score. The amount of times a color cap was placed by participants at a position on the tray was plotted for the lowest light level in figure 4.1 for the younger age group, and figure 4.2 for the older age group. The figures show that displacements were more likely to occur with neighbouring color caps than with color caps that further apart in the standard order. The figures also show that the younger age group were generally less likely to displace a color cap than the older age group.

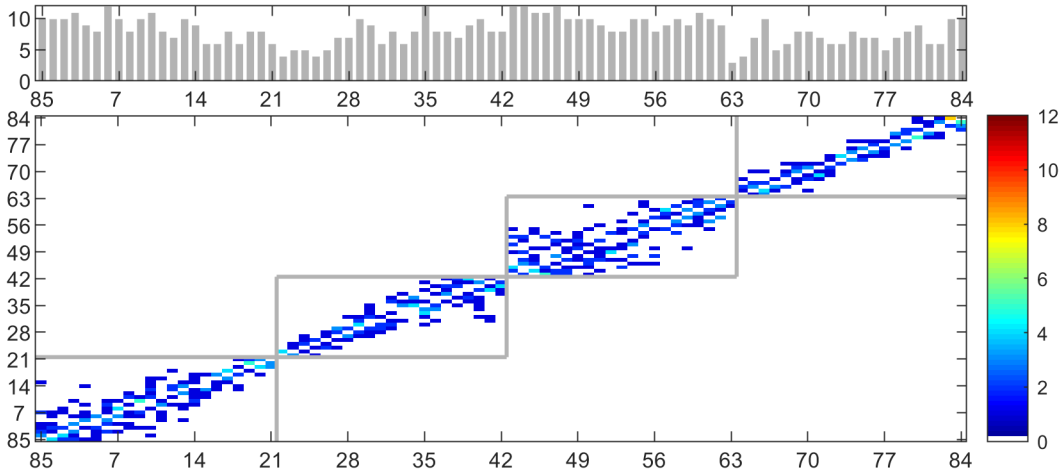

Figure 4.1: Displacement matrix showing the number of times a color cap (x-axis) was misplaced at another color cap position (y-axis) for the lowest light level and the younger age group. The top bar graph indicates the sum of the transpositions for each color cap.

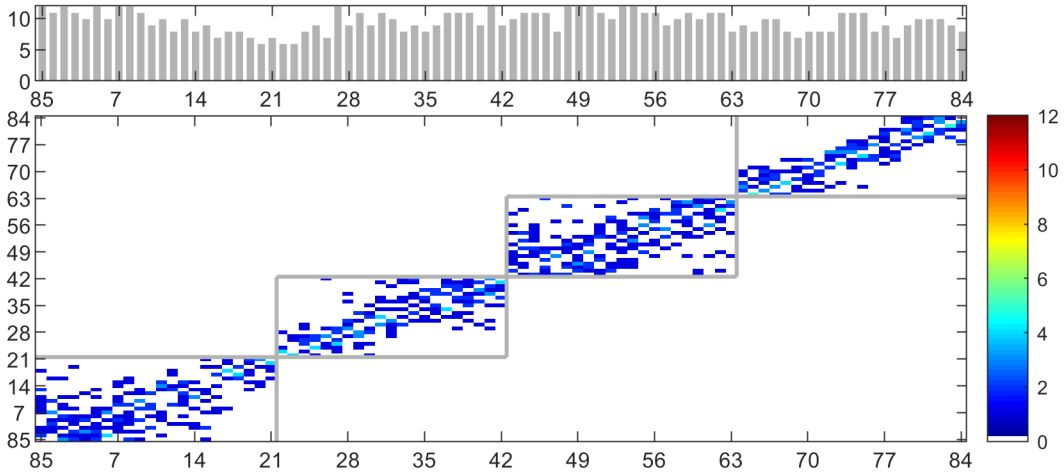

Figure 4.2: Same as Figure 4.1, now for the older age group.

4.2 Standard FM-100 Hue test score

The average FM-100 Hue test score for each color cap over all the participants was determined and plotted to investigate at which color cap and at which tray participants made the most displacements see figure 4.3. The figure indicates an increase in bipolarity for the average FM-100 Hue test score by a decrease in illuminance. The average FM-100 Hue test score increases in tray 1 and tray 3 for a decrease in illuminance.

The total FM-100 Hue test score was then used for the hypothesis testing by a repeated measures ANOVA. The main hypothesis was *'there is a significant positive effect*

of illuminance on chromatic discrimination' and the second hypothesis was *'there is a significant negative effect of age on chromatic discrimination'*. Prior to further analysis, the assumption of normal distribution and equal variances of the data were checked. The Shapiro-Wilk W test for normal data and Skewness/Kurtosis tests for Normality were used to test these assumptions. For the FM-100 Hue test score for each light setting and each tray, Shapiro-Wilk W test ($p < 0.05$) was rejected for the trays 3 and 4 of light settings 34.9 and 307 lux in the younger age group. Skewness/Kurtosis test ($p < 0.05$) was rejected for the trays 3 and 4 of light settings 34.9 and 307 lux in the younger age group. One transformation of the FM-100 Hue test scores seemed to slightly improve the normality for these trays and light settings which was the log transform. The problem of normality rises from most of the younger participants scoring perfectly on the FM100 hue test at higher light levels with the minimal error score possible. This age group therefore had a very peaked distribution of error scores for which normality was rejected.

A repeated measures ANOVA was performed to look at any statistical relationship between the total FM-100 Hue test score and age, tray number and illuminance level. The dependent variable was Logarithmic FM-100 Hue error score, the independent variables were: AgeGroup (between-subjects), Tray (within-subjects) and Light level (within-subjects). Also two-way interaction effects were included. The repeated measures ANOVA revealed significant main effects for Tray ($F_{66,3} = 54.71; p < .0001; \eta^2 = .71$) and Light ($F_{88,4} = 272.02; p < .0001; \eta^2 = .93$), as well as a significant interaction between Light and AgeGroup ($F_{88,4} = 8.39; p < .0001; \eta^2 = .39$) and between Light and Tray ($F_{264,12} = 15.79; p < .0001; \eta^2 = .42$). Furthermore, the between-subjects term was significant ($F_{22,1} = 6.66; p < .05; \eta^2 = .23$), indicating differences in FM-100 Hue test scores between participants.

To better understand the interaction effect of Light and AgeGroup, the post-hoc pairwise predicted margins of the FM-100 Hue error score were plotted for each Light and AgeGroup level in figure 4.4. The illuminance in the figure was plotted on a 10-log scale. An increasing trend in the predicted FM-100 Hue error score for a decreasing illuminance level was observed. Generally, participants needed a higher illuminance to perform better on the FM-100 Hue test especially for the older participants group. The coefficient of determination (goodness of fit: R^2) of the two-term exponential fit for the younger age group was 0.73 and for the older age group 0.85.

To better understand the interaction effect of Light and Tray, the post-hoc pairwise predicted margins of the FM-100 Hue error score were plotted for each Light and Tray number in figure 4.5. The illuminance in the figure was plotted on a 10-log scale. A increasing trend in the predicted FM-100 Hue error score for a decreasing illuminance level was observed. Generally, participants needed a higher illuminance to perform better on the FM-100 Hue test especially at tray number 1 and 3. The goodness of fit for tray 1 was

0.66, tray 2 0.70, tray 3 0.72 and tray 4 0.69.

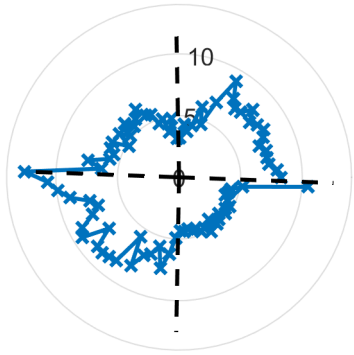

(a) 0.7 lux

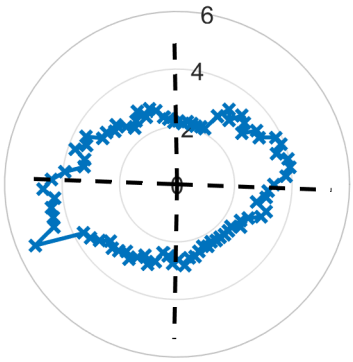

(b) 5.6 lux

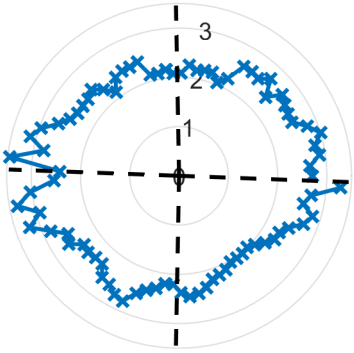

(c) 17.9 lux

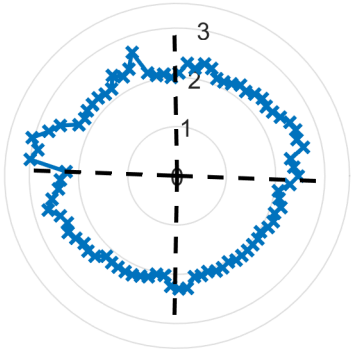

(d) 34.9 lux

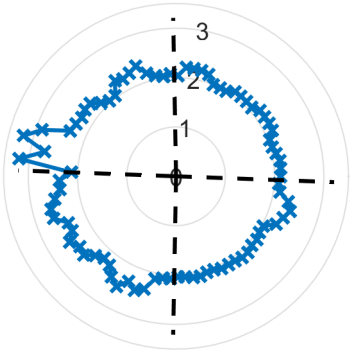

(e) 307 lux

Figure 4.3: The distributions were plotted according to the Farnsworth method, where the radius indicates the average FM-100 Hue test score and the angle indicates the cap number. The dashed lines indicate the different trays counting from 1 to 4 counterclockwise.

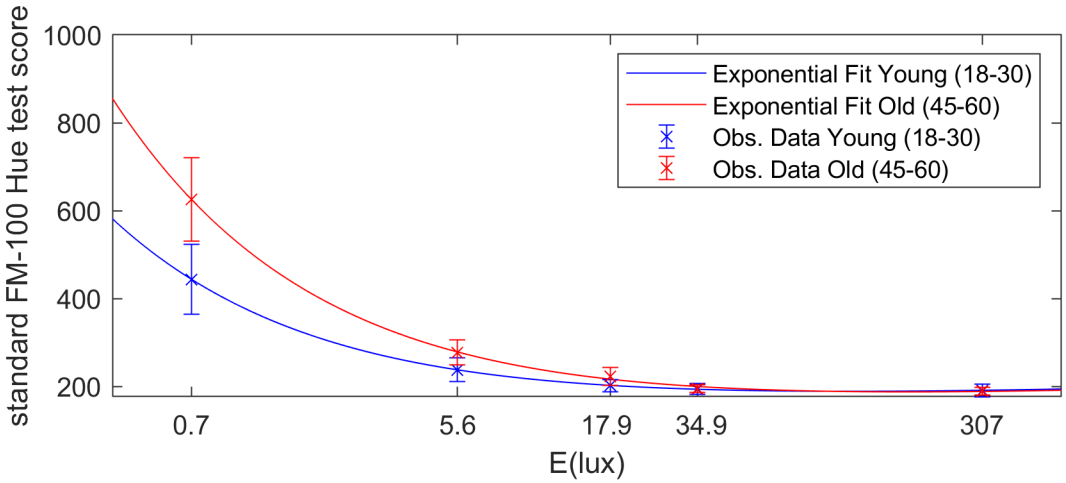

Figure 4.4: Interaction effect of light level and age group on the FM-100 Hue error score plotted with their 95% confidence intervals and two-term exponential fit.

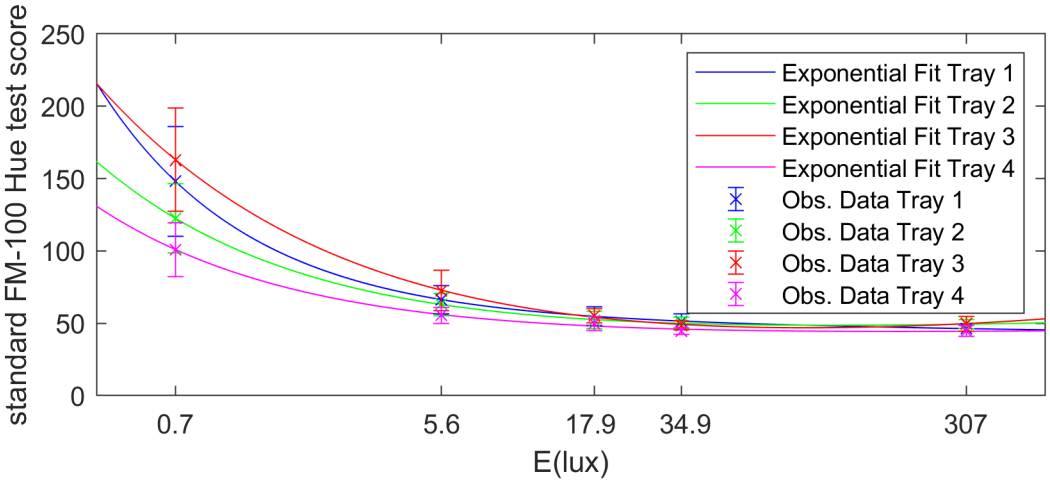

Figure 4.5: Interaction effect of light level and tray number on the FM-100 Hue error score plotted with their 95% confidence intervals and two-term exponential fit.

4.3 Order based on Hue angle

After having determined a hue angle for each color cap at each light level, the standard cap order, order based on the hue angle and the order based on the participant were compared in radian hue angles. This comparison was similar to the comparison of the standard cap order and the order based on the participant in their number sequence retrieved by the number printed on the back. In the standard FM-100 Hue test score the angular distance between color caps had no consequence on the error score whatsoever. However, by comparing these orders in hue angles the actual angular distance was taken into account. An example of the hue angle for each color cap number was shown in figure 4.6.

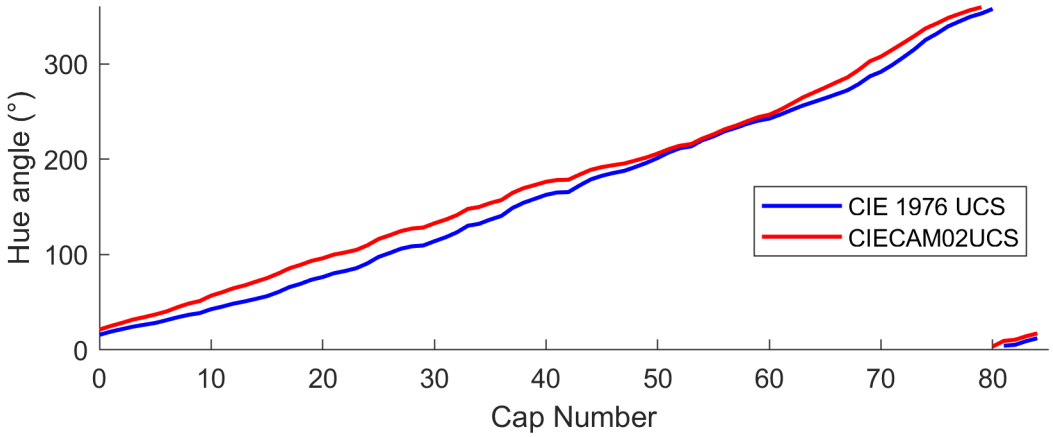

Figure 4.6: Hue angles of both CIE 1976 UCS and CIECAM02UCS plotted for each color cap. Color cap 85 is coded as cap number 0.

The cap order based on the participant and cap order based on the hue angle were examined for each color space. The cap order based on the hue angle in each color space was similar to the predicted order determined by Farnsworth. The predicted order according the Farnsworth was for tray one [85 1-21], for tray two [22-42], for tray three [43-63] and for tray four [64-84]. Figure 4.7 shows the cap number for the order based on the hue angle for each light level. The other lines not shown in the legend in this figure indicate the cap order of the participants. At lower light levels more variation in the cap order of the participants was observed than at higher light levels. Ideally the lines in figure 30 would follow a linear relationship which would be the predicted order determined by Farnsworth.

The average FM-100 Hue test score for each color cap over all the participants was determined and plotted to investigate at which color cap and at which tray participants made the most transpositions of color caps. The color cap test scores were first shown for their CIE 1976 UCS hue angles to have a more accurate indication of how closely they were in the CIE 1976 UCS color space, see figure 4.8. Second the color cap test scores were shown for their CIECAM02UCS hue angles, see figure 4.9.

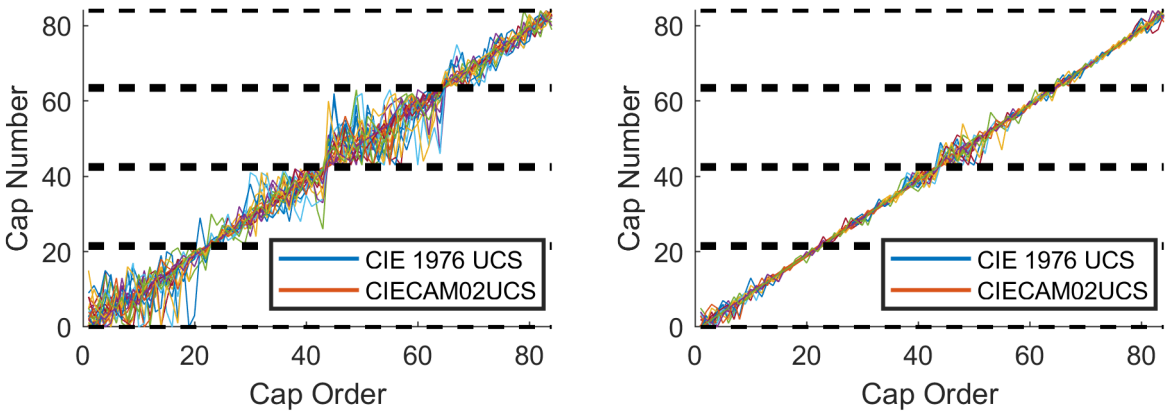

(a) 0.7 lux

(b) 5.6 lux

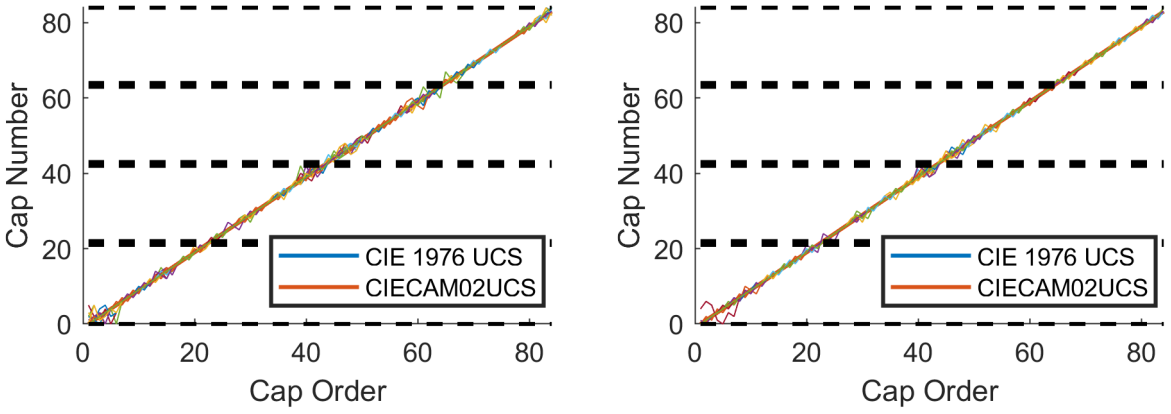

(c) 17.9 lux

(d) 34.9 lux

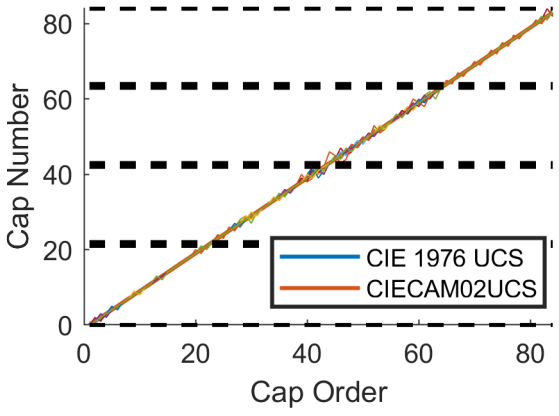

(e) 307 lux

Figure 4.7: The cap number by the order based on the hue angle for both the responses and the two color spaces (blue and orange). Color cap 85 is coded as cap number 0. The black dashed line indicates the anchor caps.

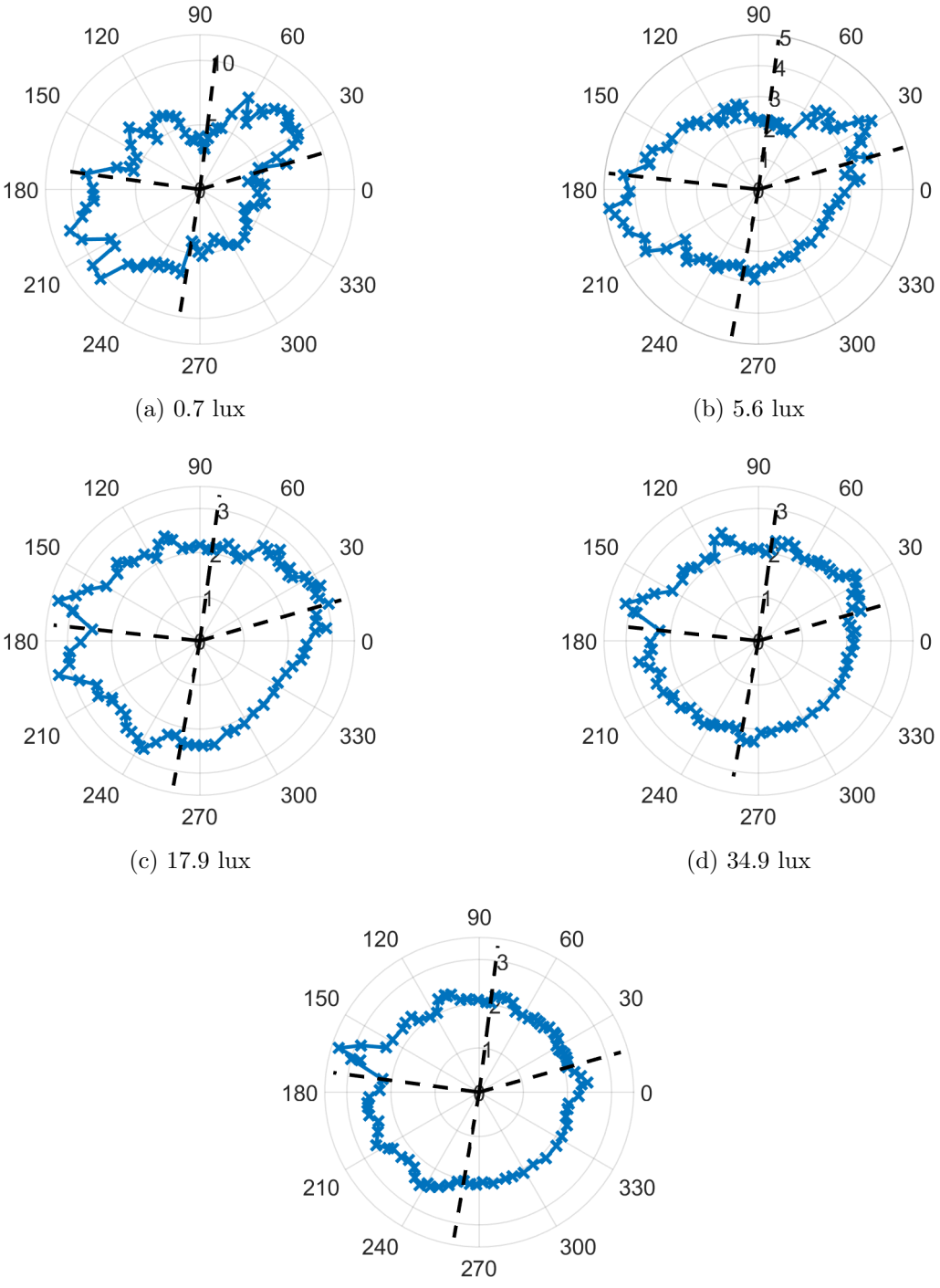

(a) 0.7 lux

(b) 5.6 lux

(c) 17.9 lux

(d) 34.9 lux

(e) 307 lux

Figure 4.8: Polarplot of the hue angles in the CIE 1976 UCS color space, where the radius indicates the average FM-100 Hue test score. The dashed lines indicate the different trays counting from 1 to 4 counterclockwise.

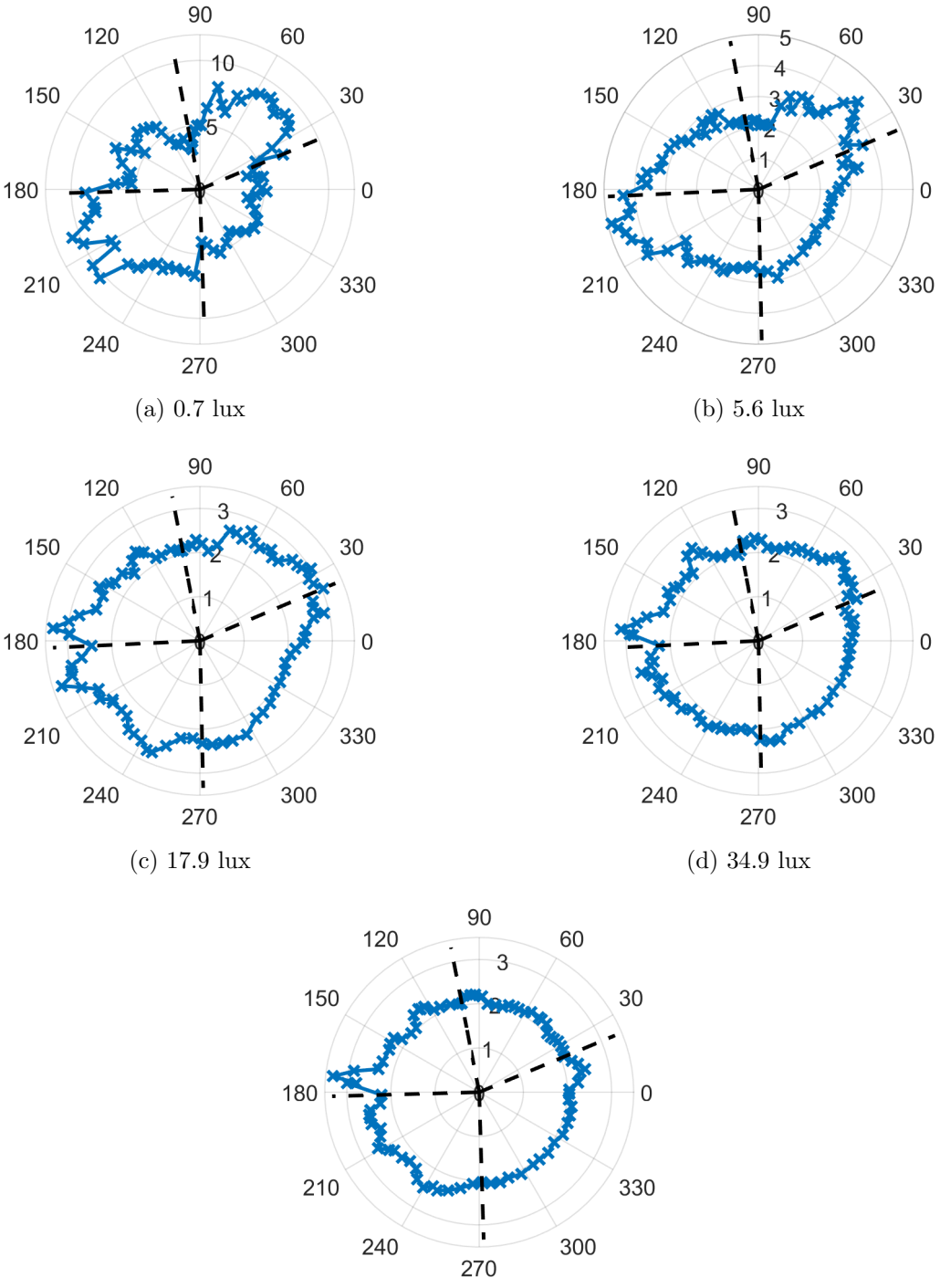

(a) 0.7 lux

(b) 5.6 lux

(c) 17.9 lux

(d) 34.9 lux

(e) 307 lux

Figure 4.9: Polarplot of the hue angles in the CIECAM02UCS color space, where the radius indicates the average FM-100 Hue test score. The dashed lines indicate the different trays counting from 1 to 4 counterclockwise.

4.4 Modified FM-100 Hue test score

Before calculating the modified FM-100 Hue test score, the light source error score as explained by Espositio and Houser was calculated. This light source error score was a source-specific error score for the light source-induced cap transpositions [54]. As expected the calculated total light source error score was zero. This was expected because in this study a close representation of illuminant C was used. The modified FM-100 Hue error score, therefore, was almost identical to the original FM-100 Hue error score except for the correction of minus 2 which did not seem a necessary step to include for the analysis.

4.5 Confusing distances

4.5.1 Error distribution

The problem with the FM-100 Hue test score was that the predicted ordering of the color caps according to Farnsworth were slightly different depending on the spectral power distribution of the light source and the color space that were used. So when participants would correctly order the color caps according to the hue angles in either the CIE 1976 UCS or CIECAM02UCS color space it could still show errors on the FM-100 Hue test score because this was determined for the standard illiminant C and originated from the Munsell book of colors. Because in this study the approximated illuminant C_a was similar to the standard illuminant C, the spectral power distribution of the illuminant C_a did not result in any transposition of color caps compared to the standard cap order. Nonetheless, the switch and distance matrix introduced by Jiaye Li was used to convert every confusing distance to an error score based on the amount of occurrences of such confusing distance between the participants. The distance was based on the euclidean distance in the CIECAM02UCS color space between the two color caps that were displaced. The error score for each possible displacement for each light level is shown in figure 4.10. The figure shows that when the light level is decreased the amount of displacements increases.

4.5.2 Threshold estimation

The thresholds were estimated by fitting a psychometric curve as described in section 3.5.5. The threshold estimation is shown in figure 4.11 which shows that at every light level no just noticeable difference could be accurately be predicted. The fitted negative cumulative Gaussian line would never reach the 0.5 inside the data region, only outside the data region in the extrapolated region at the 17.9, 45.9 and 307 lux a negative threshold was estimated. A negative threshold, however, would be impossible because the euclidean distance between the color caps could not be negative. Therefore, the thresholds were not used in modelling the large S-cone mediated variation in cap ordering at mesopic light levels.

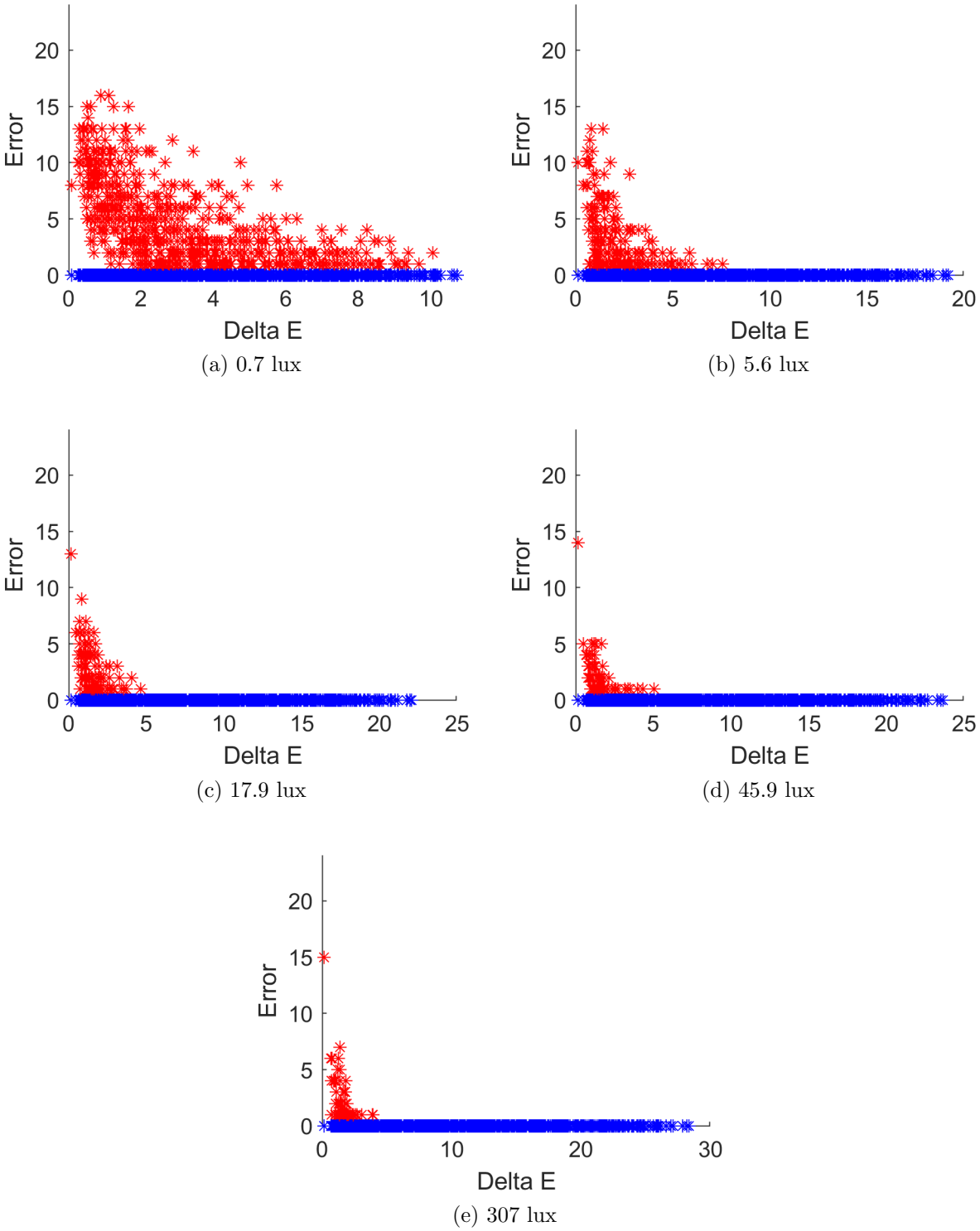

(a) 0.7 lux

(b) 5.6 lux

(c) 17.9 lux

(d) 45.9 lux

(e) 307 lux

Figure 4.10: The number of occurrences of a displacement for the euclidean distance in the CIECAM02UCS color space plotted for each illuminance condition.

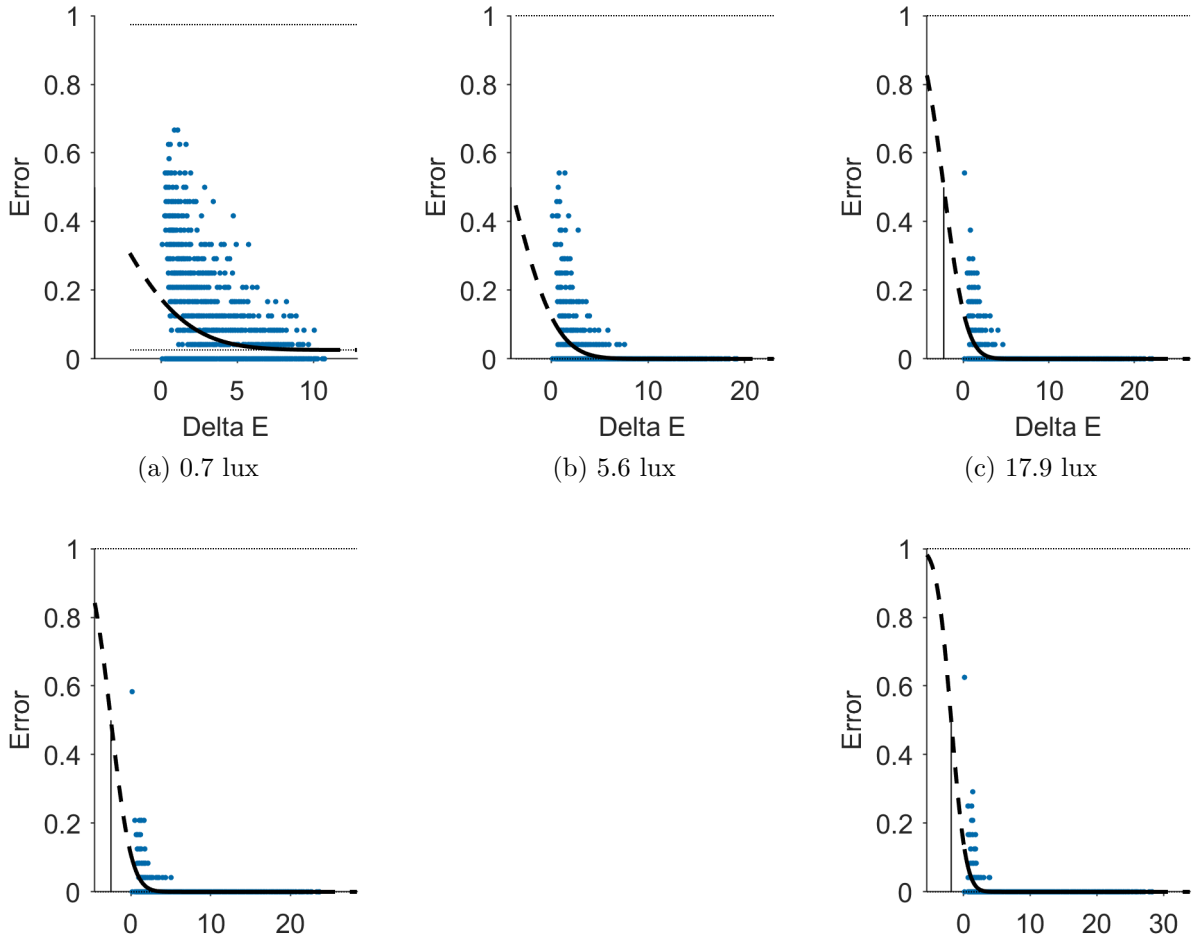

(a) 0.7 lux (b) 5.6 lux (c) 17.9 lux

(d) 45.9 lux (e) 307 lux

Figure 4.11: Threshold estimation for the different light levels for the error percentage against the euclidean distance in the CIECAM02UCS a, b plane.

4.6 Circular statistics

Because the FM100-Hue error test score does not account for the chromatic distances between the color caps circular statistics was used as described in section 3.5.6. Any transposition of color caps by the participants in opposition to the standard cap order resulted in a correlation coefficient between the two orders based on their hue angles. Correlation coefficient was the most appropriate form to calculate the fit between color cap sequences, because the correlation coefficient indicated how well the responses of the participant at each light setting were predicted by the standard cap order or the order based on hue angles retrieved from the color spaces. The hue angles were calculated for each order in two often used color spaces, namely the CIECAM02UCS and CIE1976 UCS color spaces. These two color spaces were chosen because they fundamentally differed from each other and to investigate the difference in their prediction of the participant responses. They were fundamentally different because CIECAM02UCS accounts for the adapting field luminance, relative tristimulus values of the sample, relative luminance of the background and the degree of adaptation, whereas the CIE1976 UCS color space did not. In this subsection first the predicted and participant order are explained. Second the luminance order is explained, third the random order and finally the additive noise order is explained. The correlation coefficients of these orders compared with either the predicted or participant order are shown in tables 4.1, 4.2, 4.3 and 4.4.

4.6.1 Predicted order comparison

The hue angles of the predicted order for both color spaces CIE 1976 UCS and CIECAM02UCS were first converted to radians. Second, the order based on the participants in hue angles were also converted to radians. After converting all variables into radians, the hue angles in radians of the participants were compared with the hue angles in radians of either the CIE 1976 UCS or CIECAM02UCS color space. To prevent an otherwise bias between tray groups, the hue angles of both the predicted cap order and the responses were both separated into four different groups, each group representing a different tray. Each tray was namely constrained by two anchor caps, so there would always be a high correlation between the responses and predicted order if they were not separated for different trays. So the predicted order in hue radians of the two color spaces were compared with the ranked responses of the participants in hue radians see tables 4.1, 4.2, 4.3 and 4.4. In the tables the luminance order and random order did not change between age group because these two orders were compared with the predicted order for the color spaces which was independent for age. The participant order did change between age groups, because the participant order was dependent on age. The order based on additive noise did also change between age groups because the additive noise was compared with the participant order and not with the predicted order. In the tables for the participant order the correlation coefficients decreased with a decrease in light level. Also for both color spaces for the participant order the correlation coefficients at the lowest light level were larger for the younger age group than the older age group for all trays.

Table 4.1: Correlation coefficients for each light level and tray for hue angles calculated in the CIECAM02UCS color space for the younger age group.

Light Level	Tray	Participant Order	Luminance Order	Random Order	Noise (k)		
					100	10	1
.7	**1**	.9187	.8998	-.0001	.8977	.7465	.2374
	2	.9408	-.4538	.0002	.9199	.7689	.2439
	3	.8452	-.1697	-.0010	.8243	.6771	.2143
	4	.9792	-.4012	-.0005	.9688	.8807	.3211
5.6	**1**	.9906	.8991	-.0003	.9672	.7999	.2520
	2	.9960	-.4511	-.0003	.9748	.8198	.2630
	3	.9892	-.1725	.0003	.9643	.7895	.2458
	4	.9978	-.3955	-.0004	.9872	.8971	.3273
17.9	**1**	.9971	.8990	-.0014	.9738	.8057	.2531
	2	.9994	-.4507	.0015	.9782	.8225	.2638
	3	.9956	-.1731	.0010	.9706	.7947	.2474
	4	.9994	-.3949	-.0008	.9888	.8982	.3274
45.9	**1**	.9983	.8990	.0017	.9747	.8059	.2531
	2	.9987	-.4507	.00002	.9774	.8219	.2637
	3	.9982	-.1731	-.0002	.9731	.7966	.2477
	4	.9994	-.3947	.0007	.9888	.8985	.3277
307	**1**	.9997	.8991	.0018	.9763	.8083	.2542
	2	.9989	-.4467	.0015	.9762	.8133	.2572
	3	.9975	-.1772	-.0005	.9740	.8056	.2544
	4	.9993	-.3933	-.0002	.9883	.8963	.3253

Table 4.2: Correlation coefficients for each light level and tray for hue angles calculated in the CIECAM02UCS color space for the older age group.

Light Level	Tray	Participant Order	Luminance Order	Random Order	Noise (k)		
					100	10	1
.7	**1**	.7493	.8998	-.0001	.7321	.6092	.1936
	2	.8456	-.4538	.0002	.8269	.6918	.2182
	3	.6223	-.1697	-.0010	.6070	.4990	.1556
	4	.9354	-.4012	-.0005	.9256	.8413	.3078
5.6	**1**	.9892	.8991	-.0003	.9659	.7990	.2514
	2	.9909	-.4511	-.0003	.9698	.8155	.2615
	3	.9673	-.1725	.0003	.9431	.7719	.2401
	4	.9956	-.3955	-.0004	.9850	.8952	.3267
17.9	**1**	.9959	.8990	-.0014	.9706	.8030	.2529

Table 4.2: Correlation coefficients for each light level and tray for hue angles calculated in the CIECAM02UCS color space for the older age group.

Light Level	Tray	Participant Order	Luminance Order	Random Order	Noise (k)		
					100	10	1
	2	.9989	-.4507	.0015	.9757	.8204	.2631
	3	.9986	-.1731	.0010	.9698	.7943	.2471
	4	.9996	-.3949	-.0008	.9875	.8970	.3269
45.9	**1**	.9959	.8990	.0017	.9725	.8040	.2524
	2	.9989	-.4507	.00002	.9777	.8221	.2638
	3	.9986	-.1731	-.0002	.9735	.7969	.2478
	4	.9996	-.3947	.0007	.9889	.8986	.3278
307	**1**	.9996	.8991	.0018	.9762	.8083	.2542
	2	.9993	-.4467	.0015	.9766	.8136	.2575
	3	.9979	-.1772	-.0005	.9744	.8059	.2544
	4	.9998	-.3933	-.0002	.9889	.8967	.3255

4.6.2 Random order comparison

Furthermore, a fully random order sequence of cap ordering was created at each tray for 2000 repeats. This sequence was then converted into hue angles and afterwards also converted into radians. The predicted ordering according to Farnsworth, the CIE 1976 UCS and CIECAM02UCS color spaces in radians were compared with the random order sequence. The correlation coefficient that was reported was then determined by taking the average over all repeats. As expected no large correlations were found between any of these orderings, see tables 4.1, 4.2, 4.3 and 4.4. Additionally (not reported in the table), the ordering of the participants were compared with the random order sequence and the largest absolute correlation coefficient was .0018. This means that the participants did not place the color caps in a random order.

4.6.3 Luminance order comparison

Expected was that participants would not be fully random in their ordering of the color caps at scotopic and mesopic vision. Participants were expected to order the color caps based on hue angles at photopic vision, but at the mesopic vision, where rods also contribute to vision, other cues could be utilized instead. Therefore, the actual luminance of the color caps at the eye level with the LMK camera were measured. The actual luminance was then used as another rank order to compare with the order based on the participants, see tables 4.1, 4.2, 4.3 and 4.4. Tray 1 had a large correlation with the predicted order that the participant ordering of tray 1 was possibly influenced by the luminance differences. At tray 4, however, the luminance order is negatively correlated with the predicted order, but

participants had a larger correlation coefficient for this tray at lower light levels. Therefore, indicating that participants, at least for tray 4, did not use the luminance differences on the tray to order the color caps.

Table 4.3: Correlation coefficients for each light level and tray for hue angles calculated in the CIE 1976 UCS color space for the younger age group.

Light Level	**Tray**	**Participant Order**	**Luminance Order**	**Random Order**	**Noise (k)**		
					100	10	1
.7	**1**	.9228	.8864	-.0019	.8884	.6760	.1927
	2	.9354	-.4634	-.0010	.9170	.7805	.2529
	3	.8193	-.0891	-.0009	.8022	.6780	.2172
	4	.9812	-.4519	.0009	.9725	.8983	.3428
5.6	**1**	.9913	.8843	-.0009	.9533	.7221	.2046
	2	.9954	-.4588	.0010	.9772	.8404	.2774
	3	.9868	-.0973	-.0013	.9644	.8042	.2543
	4	.9982	-.4420	.0001	.9896	.9156	.3504
17.9	**1**	.9971	.8842	.0003	.9589	.7266	.2056
	2	.9994	-.4584	.0005	.9811	.8438	.2785
	3	.9956	-.0977	.0013	.9730	.8114	.2565
	4	.9996	-.4416	-.0007	.9910	.9168	.3510
45.9	**1**	.9983	.8840	-.0010	.9602	.7276	.2058
	2	.9985	-.4578	.0014	.9804	.8437	.2789
	3	.9979	-.0989	.0014	.9751	.8122	.2566
	4	.9994	-.4404	.0015	.9908	.9166	.3508
307	**1**	.9996	.8842	-.0010	.9621	.7318	.2078
	2	.9988	-.4539	-.0007	.9793	.8353	.2718
	3	.9973	-.1026	-.0003	.9763	.8228	.2647
	4	.9993	-.4406	-.0004	.9905	.9147	.3485

Table 4.4: Correlation coefficients for each light level and tray for hue angles calculated in the CIE 1976 UCS color space for the older age group.

Light Level	**Tray**	**Participant Order**	**Luminance Order**	**Random Order**	**Noise (k)**		
					100	10	1
.7	**1**	.7618	.8864	-.0019	.7333	.5578	.1579
	2	.8352	-.4634	-.0010	.8189	.6967	.2257
	3	.6086	-.0891	-.0009	.5955	.5041	.1619
	4	.9397	-.4519	.0009	.9314	.8601	.3287

Table 4.4: Correlation coefficients for each light level and tray for hue angles calculated in the CIE 1976 UCS color space for the older age group.

Light Level	Tray	Participant Order	Luminance Order	Random Order	Noise (k)		
					100	10	1
5.6	**1**	.9893	.8843	-.0009	.9514	.7207	.2038
	2	.9901	-.4588	.0010	.9720	.8361	.2764
	3	.9592	-.0973	-.0013	.9374	.7819	.2465
	4	.9960	-.4420	.0001	.9874	.9134	.3498
17.9	**1**	.9939	.8842	.0003	.9558	.7241	.2049
	2	.9967	-.4584	.0005	.9785	.8414	.2779
	3	.9953	-.0977	.0013	.9727	.8113	.2567
	4	.9986	-.4416	-.0007	.9901	.9159	.3508
45.9	**1**	.9956	.8840	-.0010	.9575	.7257	.2052
	2	.9989	-.4578	.0014	.9807	.8440	.2790
	3	.9983	-.0989	.0014	.9755	.8126	.2569
	4	.9996	-.4404	.0015	.9911	.9169	.3509
307	**1**	.9995	.8842	-.0010	.9619	.7317	.2077
	2	.9992	-.4539	-.0007	.9797	.8357	.2720
	3	.9980	-.1026	-.0003	.9770	.8235	.2650
	4	.9998	-.4406	-.0004	.9910	.9152	.3487

4.6.4 Additive noise comparison

In addition to the random order sequence an additive noise model was created. This model accounted for the suggested ordering of a color space and made displacements for each color cap based on a normal distribution where the mu was the hue angle in degrees and the k was the additive noise. k indicated the concentration around the mean (mu) and was analogous to the variance. For k the values 100, 10 and 1 were chosen based on a large, medium and small concentration around the mean. The new hue angles were determined by a simulation of 2000 repeats wherein each time different hue angles were chosen from a mises distribution. The mises distribution represents a circular analogue of the normal distribution [58]. For each of the repeats the new additive noise ordering for each color space were compared to the ordering of the participant in radians, see tables 4.1, 4.2, 4.3 and 4.4. Figure 4.12, illustrates the different hue angles for all the 2000 repeats where the radius indicated the amount of times this hue angle was chosen. These results indicate that when the concentration of the 2000 repeats around the hue angles increases the correlation coefficient also increases. Meaning that when noise is added with this model the correlation coefficient does not increase even at the lowest light level.

(a) Large concentration (k=100) around mean

(b) Small concentration (k=0.1) around mean

Figure 4.12: Mises distribution around the hue angles of the CIECAM02UCS color space where the observed concentration is analogous to the variance for a sequence of 2000 simulations.

4.7 Thurstonian analysis

The Thurstonian analysis resulted in scale values for the color cap ordering for each tray, age group and light level. An example of such Thurstonian order of the color caps is shown in figure 4.13 where the order was determined from left to right.

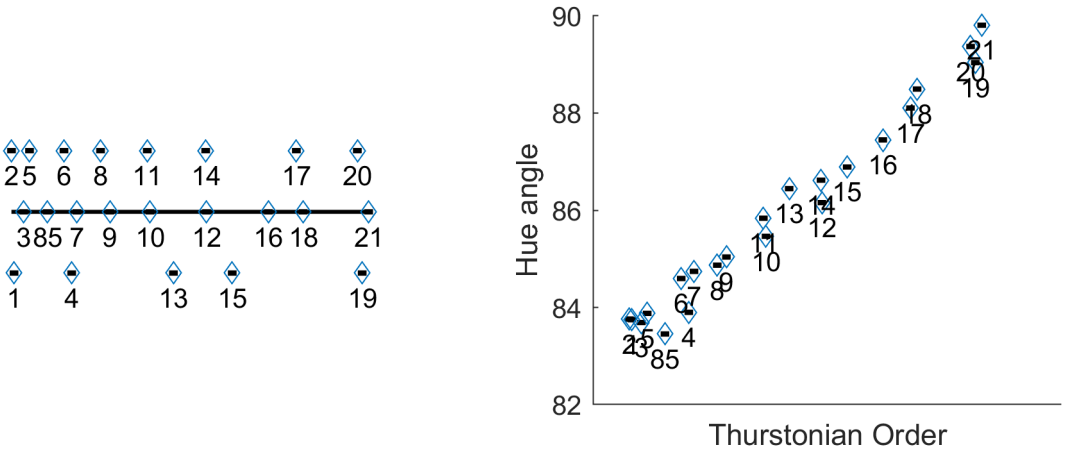

(a) Thurstonian order of the color caps with 95% confidence intervals

(b) Thurstonian order plotted against the hue angle of the color caps

Figure 4.13: Thurstonian order for the younger age group for tray 1 at the lowest light level.

The caps were shifted on y-axis in the left figure for better visibility of the color cap numbers but the y-axis there had no other meaning whatsoever. In both the left and right figure the x-axis is arbitrary and only indicates the Thurstonian order of color caps from left to right, starting at 1 (the most left) and ending at 21 (the most right). This

Thurstonian order was then plotted against different colorimetric characteristics such as hue angle or the L, M and S cone activation's. The hue angle seemed to correlate well with the scale values, however, the L, M and S cone activation's or any combinations of these did not well correlate with the scale values. Other trays, age groups and light levels were analyzed but not reported, because no other good correlation than the hue angle characteristic was found.

4.8 Bipolarity and axis analysis

The method for analyzing the FM-100 Hue test score that was proposed by Kenneth Knoblauch produced components that were related to the Fourier component of the error distribution at two cycles per revolution. Using the formulas described in the method section the amplitude, modulation, bipolarity, axis of bipolarity and mean error were calculated.

Figure 4.14, shows the model fit to the standard FM-100 Hue test score for the the younger age groups and five illuminance's plotted according the Kinnear method [62]. The two cycle sine wave had different parameter estimates for each age group and light level. In figure 4.15 all the model parameters were plotted as a function of illuminance on a 10-log scale. Noticeable from the parameter estimates was that the amplitude changed significantly between the lowest and highest light level, whereas the axis of bipolarity did not change much. The magnitude of the amplitude difference also increased with age, whereas the phase angle cap number difference did not change much. Additionally, the mean FM-100 Hue test score and modulation (bipolarity) parameter estimates showed to increase by a decrease in illuminance.

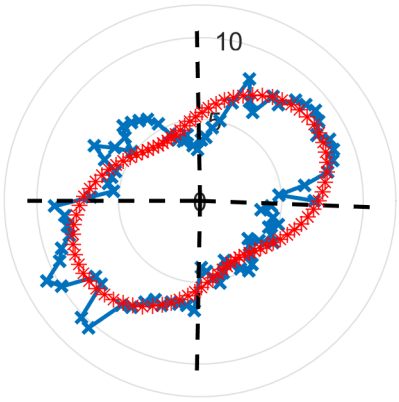

(a) 0.7 lux

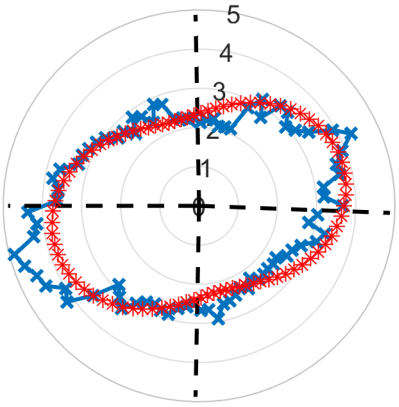

(b) 5.6 lux

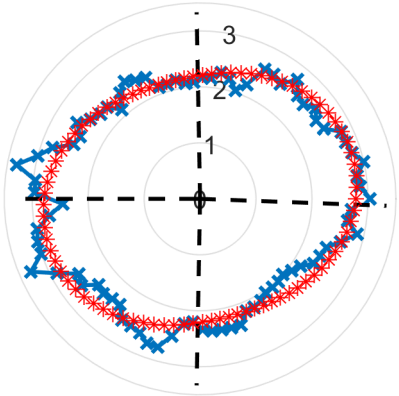

(c) 17.9 lux

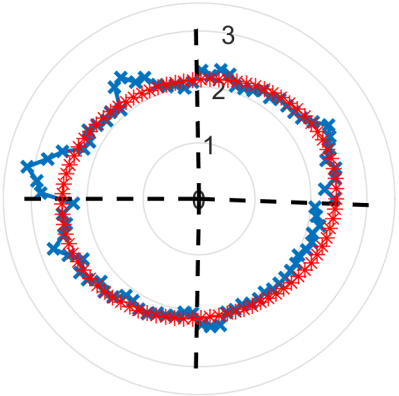

(d) 34.9 lux

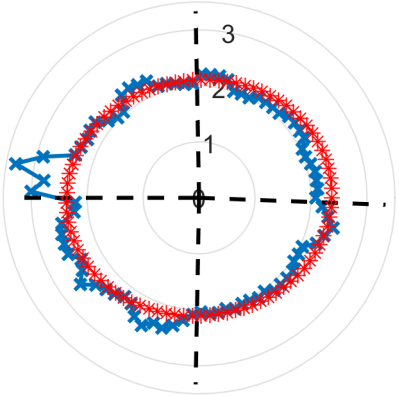

(e) 307 lux

Figure 4.14: Error distributions of the younger age group for the five illuminance levels and the plotted two cyle sine wave in red asterisks.

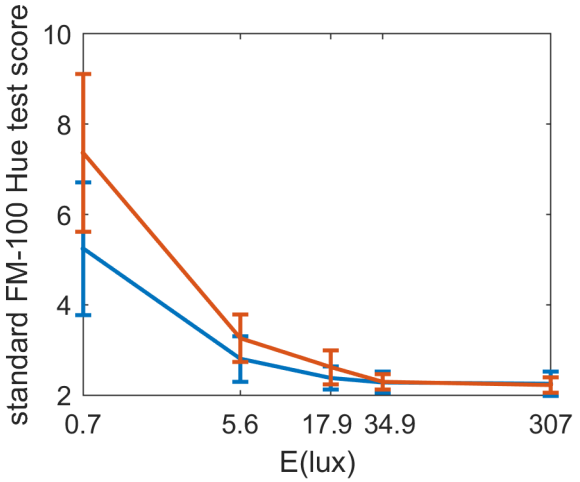

(a) Standard FM-100 Hue test score

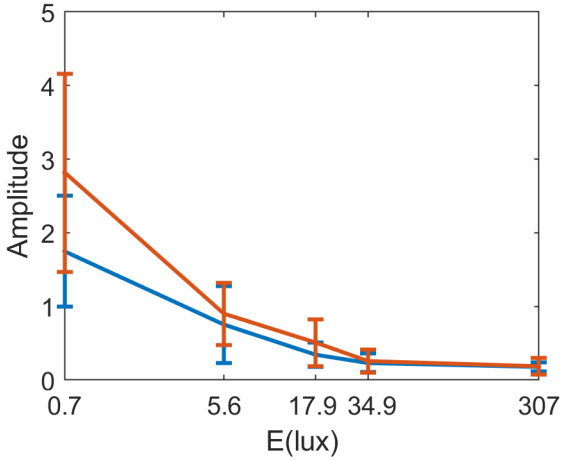

(b) Amplitude

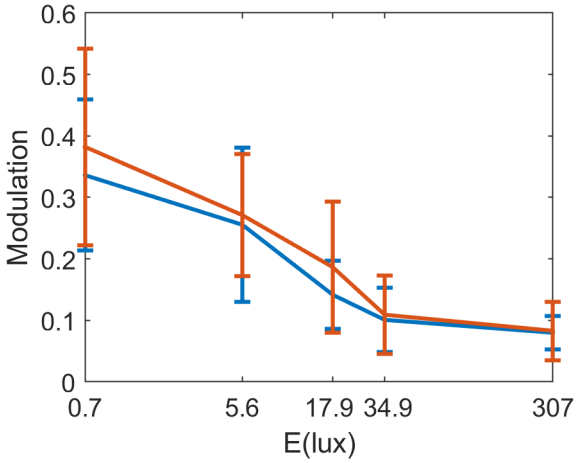

(c) Modulation

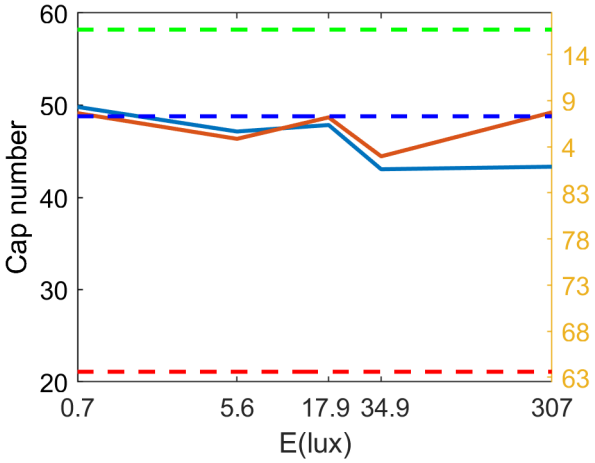

(d) Axis of bipolarity

Figure 4.15: Components of the two cycle sine wave plotted for the older (red) and younger (blue) age groups against the illuminance on a 10-log scale.

Chapter 5

Modelling

In this section, an attempt to model the variation in cap order at the different light levels was made. Two color appearance models are explored and optimized for color discrimination at different light levels. The first color appearance model is CIECAM02UCS, which is an often used color appearance model at photopic vision. The second color appearance model is CAM04LMS, which included also the rod activation at the mesopic light levels. Both color appearance models were investigated over all subjects and not between age groups. This was done because both models did not account for the age factor in their calculations. Finally, the threshold detection ellipses are modelled and explained for all light levels and between the two age groups.

5.1 (Mesopic) Color Discrimination Models

5.1.1 (Mesopic) CIECAM02UCS

5.1.1.1 L, M and S cone fudamentals

Like in the CIECAM02UCS model the CIE 1931 XYZ chromaticity coordinates were first converted into L- M- and S- cone activation with the Hunt-Pointer-Estevez transformation matrix (MHPE) shown in equation 5.1 [64].

$$\begin{pmatrix} L \\ M \\ S \end{pmatrix} = \begin{pmatrix} 0.38971 & 0.68897 & -0.07868 \\ -0.22981 & 1.18340 & 0.04641 \\ 0 & 0 & 1 \end{pmatrix} \begin{pmatrix} X_2 \\ Y_2 \\ Z_2 \end{pmatrix} \tag{5.1}$$

5.1.1.2 Optimizing CIECAM02UCS for Mesopic condition

The current model that is often used to describe the color appearance of an object is the CIECAM02UCS model. This model, however, did not optimally predict the color discrimination at low light levels with the average lowest correlation coefficient at tray 3 of $\frac{.8452+.6223}{2} = .7338$, from tables 4.3 and 4.4. Therefore, an adjustment for this color model was made by adding other factors to their equations. The factors added to the

equations depended on the light level and allowed for better correlation to the response data. The equations that were adjusted by these factors were the correlate for red-green and yellow-blue. These equations for the correlate for red-green and yellow-blue had the form of equations 5.2 and 5.3 [43]. In this equation L'_a, M'_a and S'_a indicate the modified post-adaptation cone responses.

$$a = L'_a - \frac{12}{11}M'_a + \frac{1}{11}S'_a \tag{5.2}$$

$$b = \frac{1}{9}(L'_a + M'_a - 2S'_a) \tag{5.3}$$

When accounting for the light level (E) and tray number (T) with the added weighing coefficients (k_1, k_2, k_3, k_4, k_5 and k_6) the equation had the form of equations 5.4 and 5.5. The weighing coefficients for all light levels were determined by a nonlinear solver 'fmincon' in Matlab and dependent on the light level and tray number. Two sets of hue angles in radians were created. The first set was chosen to be an uniformly distributed 85 set of hue angles with distances of 360/85 degrees between each hue angle. This set was chosen to represent the 85 color caps for an assumed uniform distribution between them. Future studies should further investigate the actual perceived hue angle difference at each light level to increase the accuracy of this model. The other set of hue angles came from the participant ordered color caps that were transformed into hue angles by the adjusted CIECAM02UCS model. The nonlinear solver of Matlab then would maximize the correlation between two hue angle sets in radians by changing the weighing coefficients. The results of the maximized correlation coefficient is shown in table 5.2 for the weighing coefficients shown in table 5.1. The new optimized CIECAM02UCS model only slightly improved the lowest correlation coefficient at tray 3 from .7338 to .7375. The weighing coefficients of the model indicate the correlate for yellow-blue was less important (.0025, .0027 and .0753) in predicting the color cap order than the correlate for red-green (1.00, .979 and 1.02) at the lowest light level.

$$a = (k_1(E,T)L'_a - \frac{12}{11}k_2(E,T)M'_a + \frac{1}{11}k_3(E,T)S'_a) \tag{5.4}$$

$$b = \frac{1}{9}(k_4(E,T)L'_a + k_5(E,T)M'_a - 2k_6(E,T)S'_a) \tag{5.5}$$

Table 5.1: Optimization weighing coefficients of the CIECAM02UCS model at different illuminance's and tray numbers.

Tray		**Illuminance (lux)**				
		0.7	**5.6**	**17.9**	**34.9**	**307**
1	$k_1(E,T)$	1.00	1.00	1.00	1.00	1.00
	$k_2(E,T)$	.993	1.03	1.03	.994	1.00
	$k_3(E,T)$	.555	1.14	1.19	1.23	1.41
	$k_4(E,T)$	.167	.774	.919	1.48	2.13

Table 5.1: Optimization weighing coefficients of the CIECAM02UCS model at different illuminance's and tray numbers.

Tray		**Illuminance (lux)**				
		0.7	**5.6**	**17.9**	**34.9**	**307**
	$k_5(E,T)$	.212	.850	.985	1.46	2.04
	$k_6(E,T)$	.0653	.777	.923	1.27	1.57
2	$k_1(E,T)$	1.00	1.00	1.00	1.00	1.00
	$k_2(E,T)$	256	.931	.982	.960	.971
	$k_3(E,T)$	222	.0058	.604	.308	.443
	$k_4(E,T)$	339	1.99	1.20	1.24	1.33
	$k_5(E,T)$	289	.0195	1.08	1.05	1.05
	$k_6(E,T)$	37.0	.933	1.13	1.07	1.17
3	$k_1(E,T)$	1.00	1.00	1.00	1.00	1.00
	$k_2(E,T)$	.979	1.03	.976	1.01	.995
	$k_3(E,T)$	1.02	1.41	.817	1.09	.901
	$k_4(E,T)$	.0025	1.36	2.36	1.45	1.52
	$k_5(E,T)$	.0027	1.44	.549	1.40	1.39
	$k_6(E,T)$	.0753	1.32	1.35	1.39	1.41
4	$k_1(E,T)$	1.00	1.00	1.00	1.00	1.00
	$k_2(E,T)$	.929	.775	.869	.834	.783
	$k_3(E,T)$	.0827	.602	.863	.769	.668
	$k_4(E,T)$	.505	.345	.677	.584	.540
	$k_5(E,T)$	.370	.329	.740	.579	.518
	$k_6(E,T)$	.678	.834	1.05	1.03	.769

Table 5.2: Averaged correlation coefficients of the newly weighted CIECAM02UCS model at the different illuminance's and tray numbers.

Tray	**0.7 lux**	**5.6 lux**	**17.9 lux**	**34.9 lux**	**307 lux**
1	.8327	.9883	.9945	.9962	.9992
2	.8975	.9905	.9954	.9960	.9964
3	.7375	.9742	.9944	.9971	.9967
4	.9570	.9946	.9977	.9990	.9990

5.1.2 (Mesopic) CAM04LMS

Another color appearance model was used to predict the responses of the participants. This model was created by Shin, Matsuki, Yaguchi and Shiori (2004) [65] and is based on the L, M and S cone fundamentals and a weighting function to include the rods at the lower light levels for the mesopic vision. First the L, M and S at photopic vision were derived from the modified color matching functions by Judd (equations 5.6, 5.7, 5.8 and 5.9) [35] and the transformation matrix determined by Pokorny and Smith (equation 5.10) [66]. Where $S(\lambda)$ is the spectral reflectance, $I(\lambda)$ the spectral irradiance, and the $\bar{x}'(\lambda)$, $\bar{y}'(\lambda)$ and $\bar{z}'(\lambda)$ the color matching functions by Judd.

$$X_{judd} = k \int_{\lambda} S(\lambda) I(\lambda) \bar{x}'(\lambda) d\lambda \tag{5.6}$$

$$Y_{judd} = k \int_{\lambda} S(\lambda) I(\lambda) \bar{y}'(\lambda) d\lambda \tag{5.7}$$

$$Z_{judd} = k \int_{\lambda} S(\lambda) I(\lambda) \bar{z}'(\lambda) d\lambda \tag{5.8}$$

where

$$k = \int_{\lambda} I(\lambda) \bar{y}'(\lambda) d\lambda \tag{5.9}$$

$$\begin{pmatrix} L \\ M \\ S \end{pmatrix} = \begin{pmatrix} 0.15514 & 0.54312 & -0.03286 \\ -0.15514 & 0.45684 & 0.03286 \\ 0 & 0 & 1 \end{pmatrix} \begin{pmatrix} X_{judd} \\ M_{judd} \\ S_{judd} \end{pmatrix} \tag{5.10}$$

Besides the L, M and S cone activation, the rod activation by means of a scotopic luminance factor was determined, see equations 5.11 and 5.12. Where $V'(\lambda)$ indicates the scotopic luminosity function.

$$Y' = k' \int_{\lambda} S(\lambda) I(\lambda) V'(\lambda) d\lambda \tag{5.11}$$

where

$$k' = \frac{100}{\int_{\lambda} I(\lambda) V'(\lambda) d\lambda} \tag{5.12}$$

After determining the scotopic luminance factor and the L, M, and S cone activation the correlate for red-green, yellow-blue and the achromatic responses were determined by equations 5.13, 5.14 and 5.15.

$$A(E) = \alpha(E) K_W \frac{L+M}{(L+M)_W} + \beta(E) K'_W (\frac{Y'}{Y'_W})^{\gamma} \tag{5.13}$$

$$r/g(E) = l(E)(L - 2M) + a(E)Y' \tag{5.14}$$

$$b/y(E) = m(E)(L + M - S) + b(E)Y' \tag{5.15}$$

The coefficients $\alpha(E)$ and $\beta(E)$ depend on the illuminance E of the illumination and demonstrate the amount of photopic and scotopic contribution to the correlate for achromatic. The coefficients $l(E)$ and $a(E)$ also depend on the illuminance E of the illumination and demonstrate the amount of photopic and scotopic contribution to the correlate for red-green. The coefficients $m(E)$ and $b(E)$ depend on the illuminance E of the illumination and demonstrate the amount of photopic and scotopic contribution to the correlate for blue-yellow. The coefficients $\alpha(E)$, $\beta(E)$, $l(E)$, $a(E)$, $m(E)$ and $b(E)$ were determined by Shin et al. for the illuminance conditions 0.01, 0.1, 1, 10, 100 and 1000 lux as weights for the rod and cone signals. These coefficients, however, were not provided for the illuminance conditions used in this study. In this color appearance model the weighing coefficients $l(E)$, $a(E)$, $m(E)$ and $b(E)$), see table 5.3, therefore were determined by a nonlinear solver 'fmincon' in Matlab for the illuminance conditions 0.7, 5.6, 17.9, 34.9 and 307 lux. This optimization of the weighing coefficients was done similar to the previous optimization with the adjusted CIECAM02UCS model. For which the correlation coefficients between the predicted ordering of the model in hue angles and an uniformly distributed set of hue angles was maximized. The correlation coefficients are shown for each tray and light level in table 5.4. The weighing coefficients were determined by this optimization because the originally reported weighing coefficients were at different illuminance levels than the illuminance levels used in our experiment. Based on the model by Shin et al. (2004) [65], The solver was limited for values between 0 and 1 for the constants $l(E)$ and $m(e)$. The other two constants ($a(E)$ and $b(E)$) were limited between -1 and 1. The weighing coefficients that were determined by the optimization were very different from the weighing coefficients reported by Shin et al. (2004). Especially the small differences of the weighing coefficients between each illuminance level were noticeably different. In the paper by Shin et al. (2004) larger differences of the weighing coefficient between each illuminance level were reported. The large difference in the weighing coefficients might be a result of the different tasks that were used in this study and that of Shin et al. (2004). The correlation coefficients for the determined weighing coefficients, shown in table 5.4, were similar to those found with the (adjusted) CIECAM02UCS model.

Table 5.3: Weighing coefficients of the color appearance model at different illuminance's.

	0.7 lux	**5.6 lux**	**17.9 lux**	**34.9 lux**	**307 lux**
$l(E)$	.654	.655	.651	.645	.645
$m(E)$	.0817	.115	.121	.122	.1215
$a(E)$	.0258	.0173	.0152	.0171	.0171
$b(E)$	-.0152	-.0117	-.0098	-.0103	-.0103

Table 5.4: Averaged correlation coefficients of the newly weighted color appearance model at the different illuminance's and tray numbers.

Tray	0.7 lux	5.6 lux	17.9 lux	34.9 lux	307 lux
1	.8233	.9833	.9900	.9921	.9952
2	.9010	.9884	.9930	.9932	.9941
3	.7219	.9706	.9928	.9957	.9953
4	.9545	.9898	.9916	.9925	.9928

5.2 Threshold detection ellipses

The mesopic discrimination model described above only indicates what transformation of the color space would best predict the data, however, did not take into account the noise at the photoreceptor or post-receptor level. Therefore, based on the research by Lucassen, Lambooij, Sekulovski and Vogels about the spatio-chromatic sensitivity explained by post-receptoral contrast [67], (noise) detection threshold ellipses were examined, modelled and optimized.

First, the color caps reflectance spectra R(λ) were used to calculate the cone excitation's of each cap for a chosen illumination I(λ) by using the equations 5.16, 5.17, 5.18 and 5.19 for the CIE 2006 $\bar{l}$, $\overline{m}$ and $\overline{s}$ 2 degree cone fundamentals for a 53 and 24 years old standard observer. The CIE 2006 $\bar{l}$, $\overline{m}$ and $\overline{s}$ cone fundamentals were normalized for their area under the curve, see equation 5.19.

$$L = \int_{\lambda} R(\lambda)I(\lambda)\bar{L}(\lambda)d\lambda \tag{5.16}$$

$$M = \int_{\lambda} R(\lambda)I(\lambda)\bar{M}(\lambda)d\lambda \tag{5.17}$$

$$S = \int_{\lambda} R(\lambda)I(\lambda)\bar{S}(\lambda)d\lambda \tag{5.18}$$

where

$$\begin{aligned} \bar{L}(\lambda) &= \frac{\bar{l}_2(\lambda)}{\int_{\lambda} \bar{l}_2(\lambda)d\lambda} \\ \bar{M}(\lambda) &= \frac{\bar{m}_2(\lambda)}{\int_{\lambda} \bar{m}_2(\lambda)d\lambda} \\ \bar{S}(\lambda) &= \frac{\bar{s}_2(\lambda)}{\int_{\lambda} \bar{s}_2(\lambda)d\lambda} \end{aligned} \tag{5.19}$$

The L, M and S cone excitation's were then transformed into chromatic channels based on the CIECAM02 definition for the correlates for red-green and yellow-blue. CIECAM02 defined the correlate for red-green to indicate the amount of distance of the L-M channel from the definition for unique yellow (L-M = $\frac{M-S}{11}$), shown in equation 5.20.

$$a = L - \frac{12}{11}M + \frac{1}{11}S = C_1 - \frac{1}{11}C_2 \tag{5.20}$$

CIECAM02 defined the correlate for yellow-blue to indicate the amount of distance of the L-M channel from the definition for unique red (L-M = M-S) and unique green (L-M = S-L), shown in equation 5.21.

$$b = \frac{1}{9}(L + M - 2S) = \frac{1}{9}(C_2 - C_1 + C_1 - C_3) \tag{5.21}$$

where

$$\begin{aligned} C_1 &= L - M \\ C_2 &= M - S \\ C_3 &= S - L \end{aligned} \tag{5.22}$$

The resulting chromaticity channels for the correlate for yellow-blue and red-green were rotated clockwise such that the correlate for blue-yellow was aligned with the indication for the tritan axis through color cap number 5.1 and 48.8 [61].

$$A = cos(28.1)a + sin(28.1)b \tag{5.23}$$

$$B = -sin(28.1)a + cos(28.1)b \tag{5.24}$$

In this A B chromaticity space all color caps were plotted and ellipses were determined at each color cap. The overlap between each of these ellipses would then indicate the probability of a displacement between each of these color caps.

To determine the size of the ellipses, first the average chromatic euclidean distance in the color space between all color caps at each illuminance level (E) was calculated by using equation 5.25.

$$Mean\ Distance(E) = \frac{\sum_{i=1}^{84} \sqrt{(A_{i,E} - A_{i+1,E})^2 + (B_{i,E} - B_{i+1,E})^2}}{84} \tag{5.25}$$

Second, the distance threshold was then determined as 30 % from the average chromatic euclidean distance between all color caps shown in equation 5.26. Initially the distance threshold was chosen such that the threshold detection ellipses had no overlap at the highest illuminance condition because very little displacements at the highest illuminance level were observed.

$$Distance\,Threshold(E) = \frac{3}{10} Mean\ Distance(E) \tag{5.26}$$

Third, by using the distance formula indicated by equation 5.27 the detection thresholds were determined for 12 angular directions at the point at which the distance was equal to the distance threshold. The 12 angular directions were at increasing intervals of 30 degrees starting at 0 degree. Furthermore, in the probability summation the A and B chromaticity channels were weighted by the detection coefficients $D_A(E)$ and $D_B(E)$ that depended on the illuminance level. The points at which the distance was equal to the distance threshold determined the size of the ellipse. Initially the detection coefficients started at 1 and the distance threshold at 30 % such that at the highest illuminance condition no overlap between the threshold detection ellipses were observed. The detection coefficients then could be lowered resulting in an increase in the threshold detection ellipses and therefore an increase in the overlap of the ellipses. An increase in the overlap of the ellipses then would result in a higher predicted probability of displacement between color caps which then could be optimized with the actual probability observed from the participant data.

$$Distance(E) = \sqrt{(D_A(E)\Delta A)^2 + (D_B(E)\Delta B)^2} \tag{5.27}$$

Fourth, the 12 resulting points for each color cap at which the distance was equal to the distance threshold in the chromaticity space were used to fit a threshold detection ellipse. An example of these threshold detection ellipses is shown in figure 5.1.

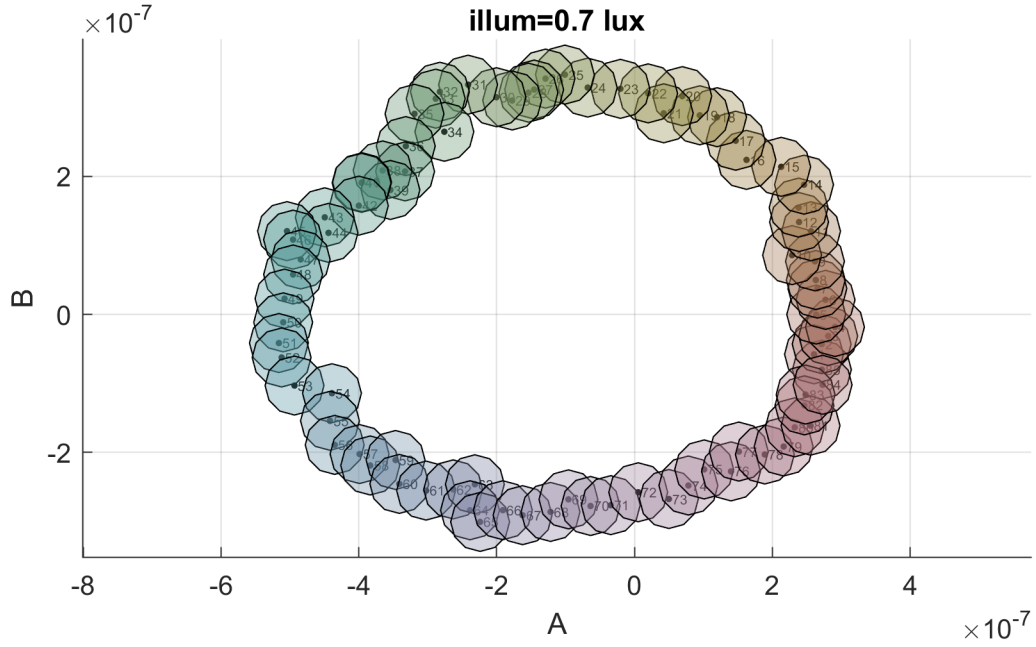

Figure 5.1: Example of the threshold detection ellipses at the lowest light level for D_A and D_B set at 0.23.

The probability of a displacement depended on the amount of overlap between ellipses which is illustrated in figure 5.2 where only the overlap between ellipses is shown.

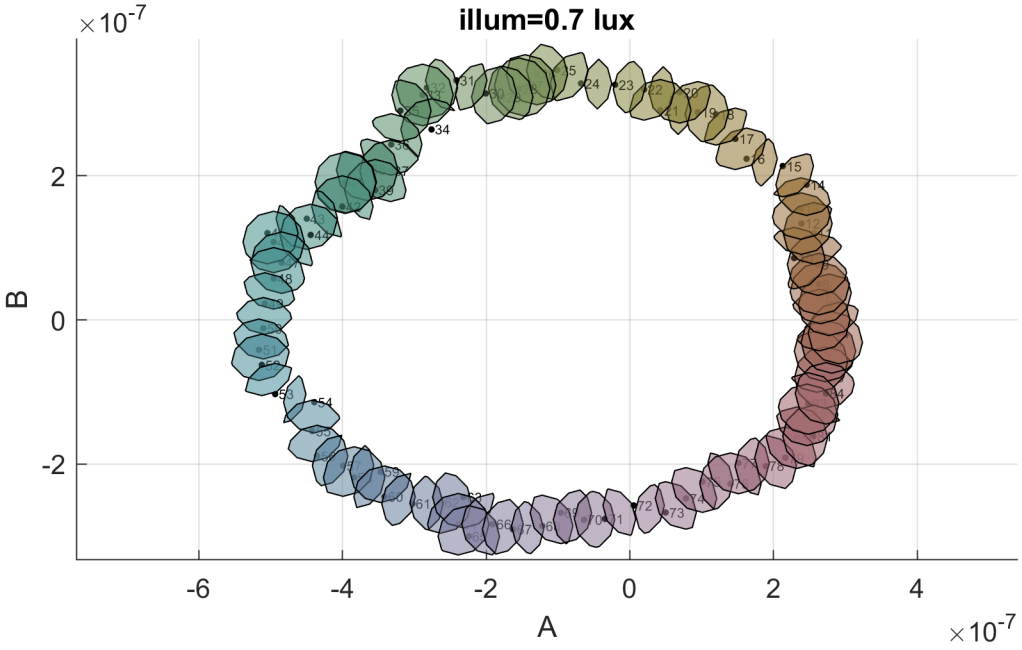

Figure 5.2: Example of the overlap area of the threshold detection ellipses at the lowest light level for D_A and D_B set at 0.23.

Fifth, the probability of a displacement was calculated based on the overlap in ellipse area. This overlapping area was divided then by a circle with the radius being the average cap distance to get the normalized percentage of overlap. This was necessary because otherwise an increase in the ellipse would not necessarily result in an increase in the probability of displacement. Furthermore the resulting percentage of overlap was then divided by the amount of color caps inside the threshold detection ellipse, shown in equation 5.28.

$$Probability_{i,E} = \frac{Overlapping\ Ellipse\ Area}{\pi Mean\ Distance(E)^2} \frac{1}{Number of Caps\ in\ Ellipse} \tag{5.28}$$

The predicted probability of displacements by the overlap in the threshold detection ellipses were then compared with the probability of displacements of the participants for the younger and older age group. The probability of displacements by the participants were determined by dividing the whole displacement matrix for each group (shown in figures 4.1 and 4.2) by 12. The detection functions $D_A(E)$ and $D_B(E)$ were then optimized by a grid search for the smallest root mean squared difference between the predicted probability and the probability based on the displacements of the participants at each tray, shown in figure 5.3.

The optimized detection functions resulted in the threshold detection ellipses which were plotted for each color cap for the A B chromaticity channels in figure 5.4 for the younger age group and figure 5.5 for the older age group. Furthermore the overlap between the threshold detection ellipses between the color caps were also plotted for the A B chromaticy channels in figure 5.6 for the younger age group and figure 5.7 for the older age group.

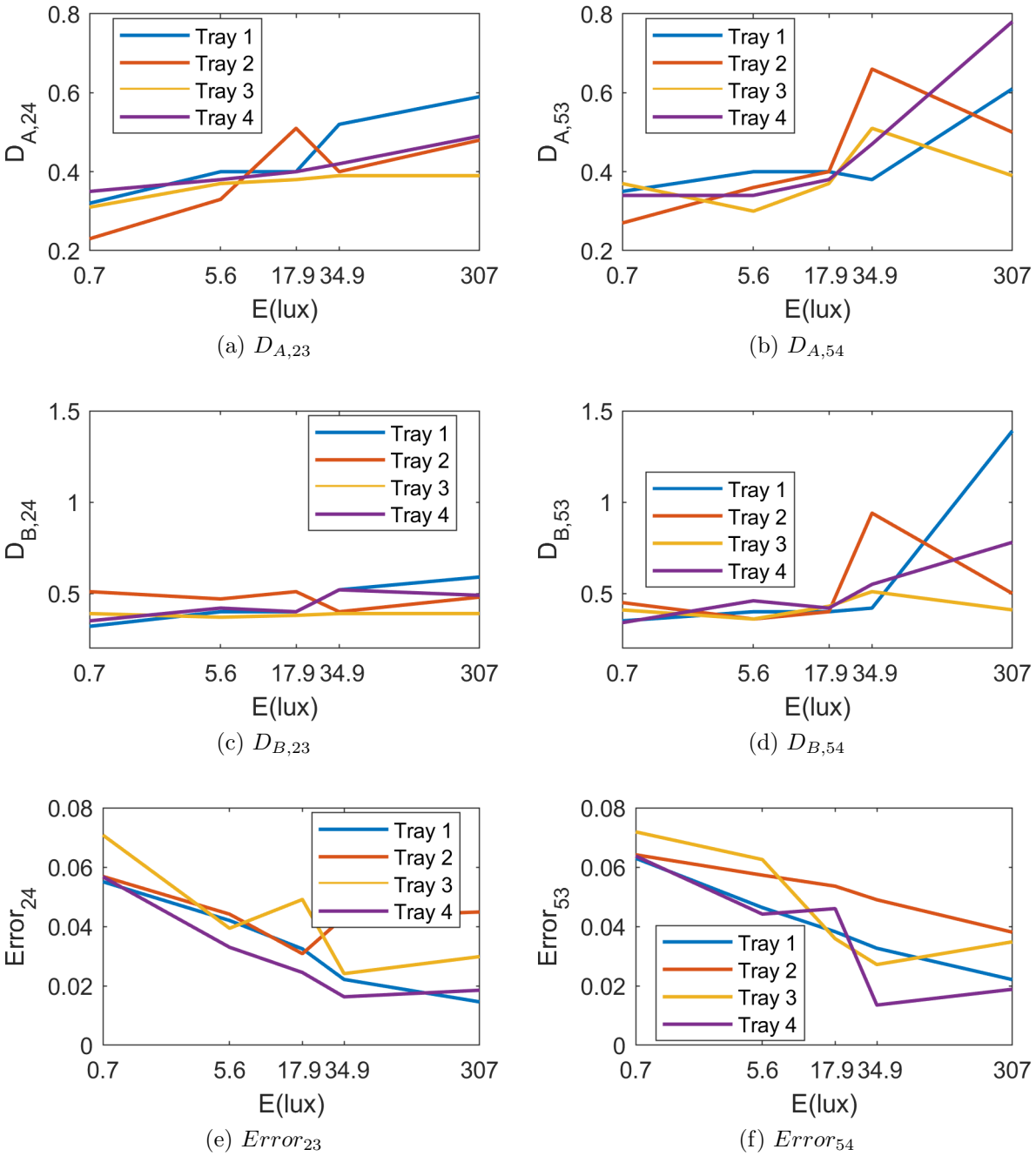

(a) $D_{A,23}$ (b) $D_{A,54}$

(c) $D_{B,23}$ (d) $D_{B,54}$

(e) $Error_{23}$ (f) $Error_{54}$

Figure 5.3: Error and detection functions plotted against the illuminance level on a 10-log scale for each age group.

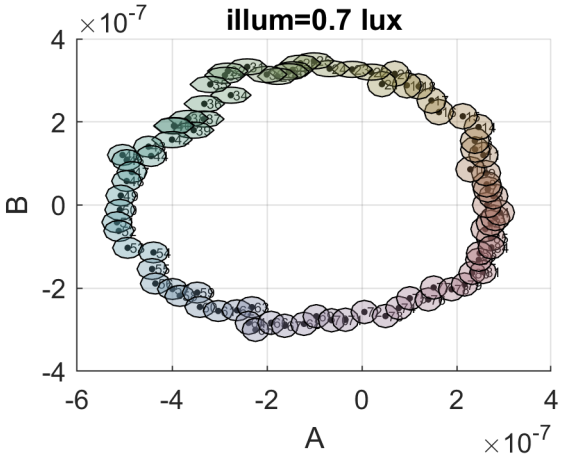

(a) 0.7 lux

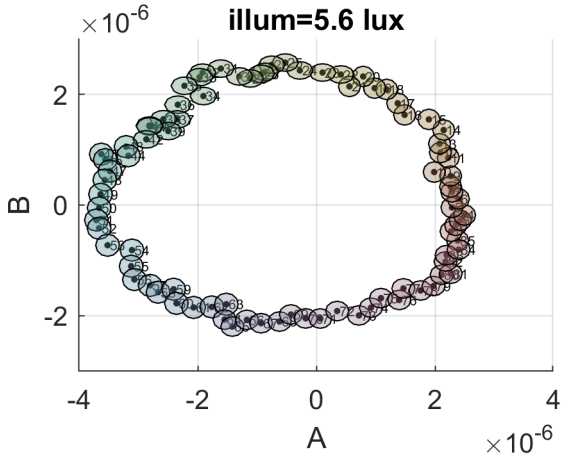

(b) 5.6 lux

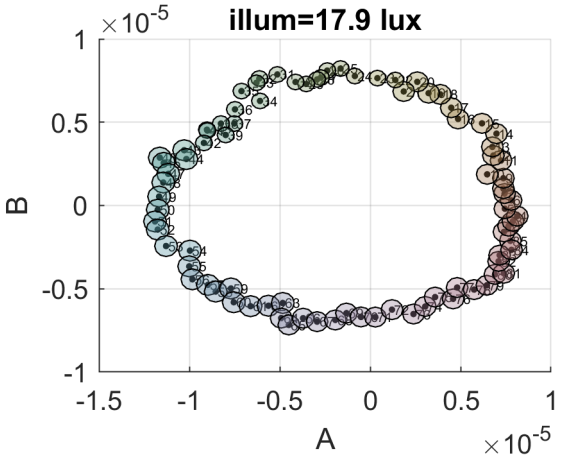

(c) 17.9 lux

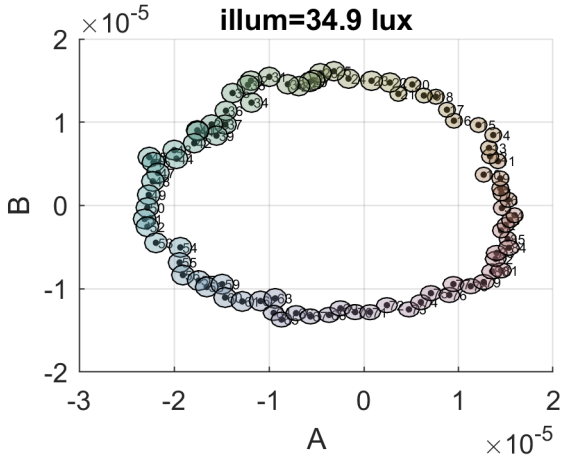

(d) 45.9 lux

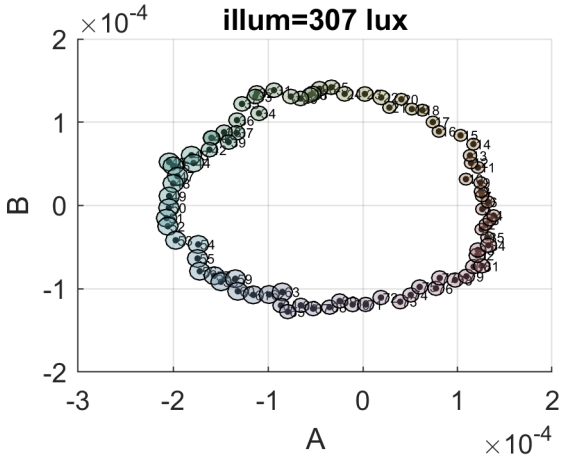

(e) 307 lux

Figure 5.4: Threshold detection ellipses for the younger age group.

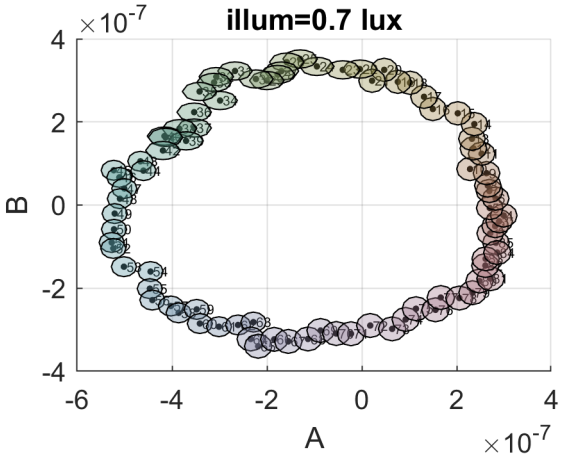

(a) 0.7 lux

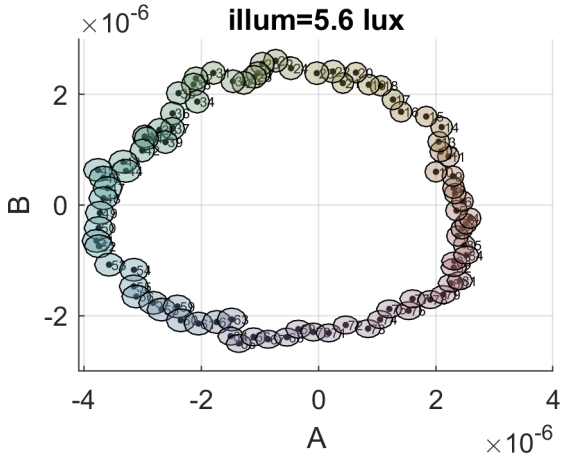

(b) 5.6 lux

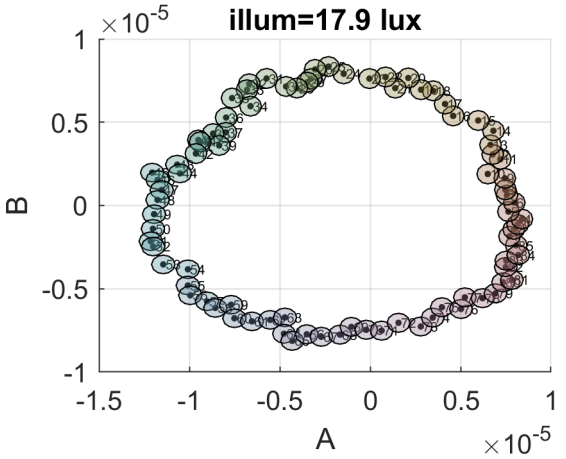

(c) 17.9 lux

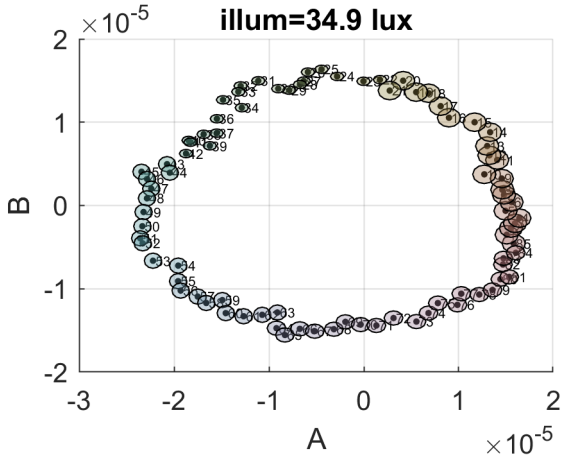

(d) 45.9 lux

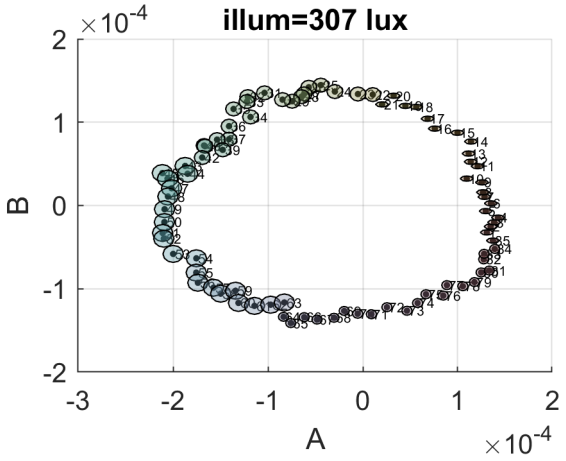

(e) 307 lux

Figure 5.5: Threshold detection ellipses for the older age group.

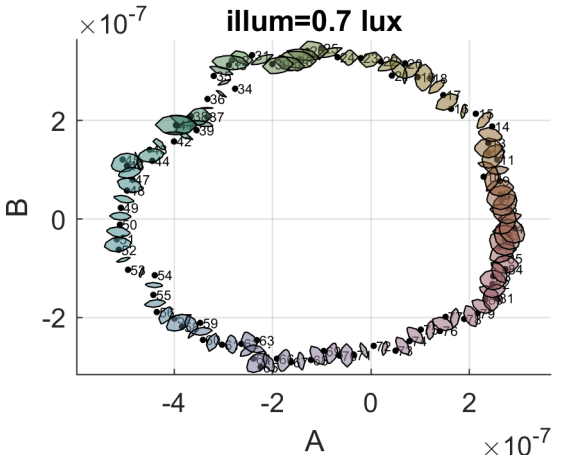

(a) 0.7 lux

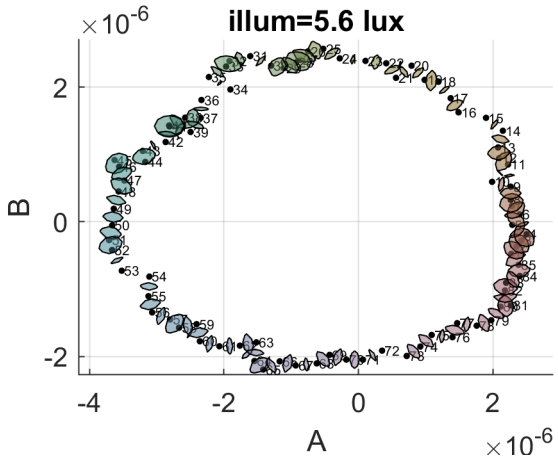

(b) 5.6 lux

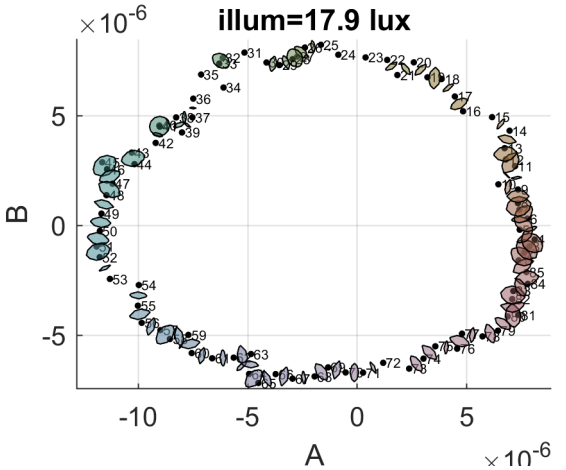

(c) 17.9 lux

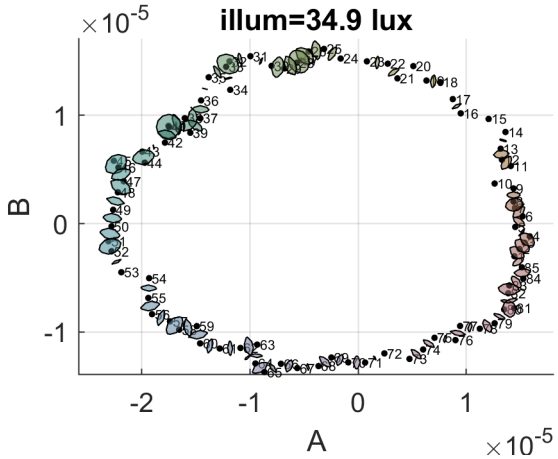

(d) 45.9 lux

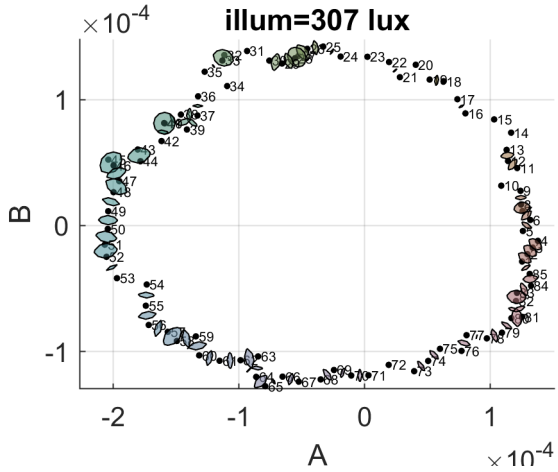

(e) 307 lux

Figure 5.6: Overlap between the threshold detection ellipses for the younger age group.

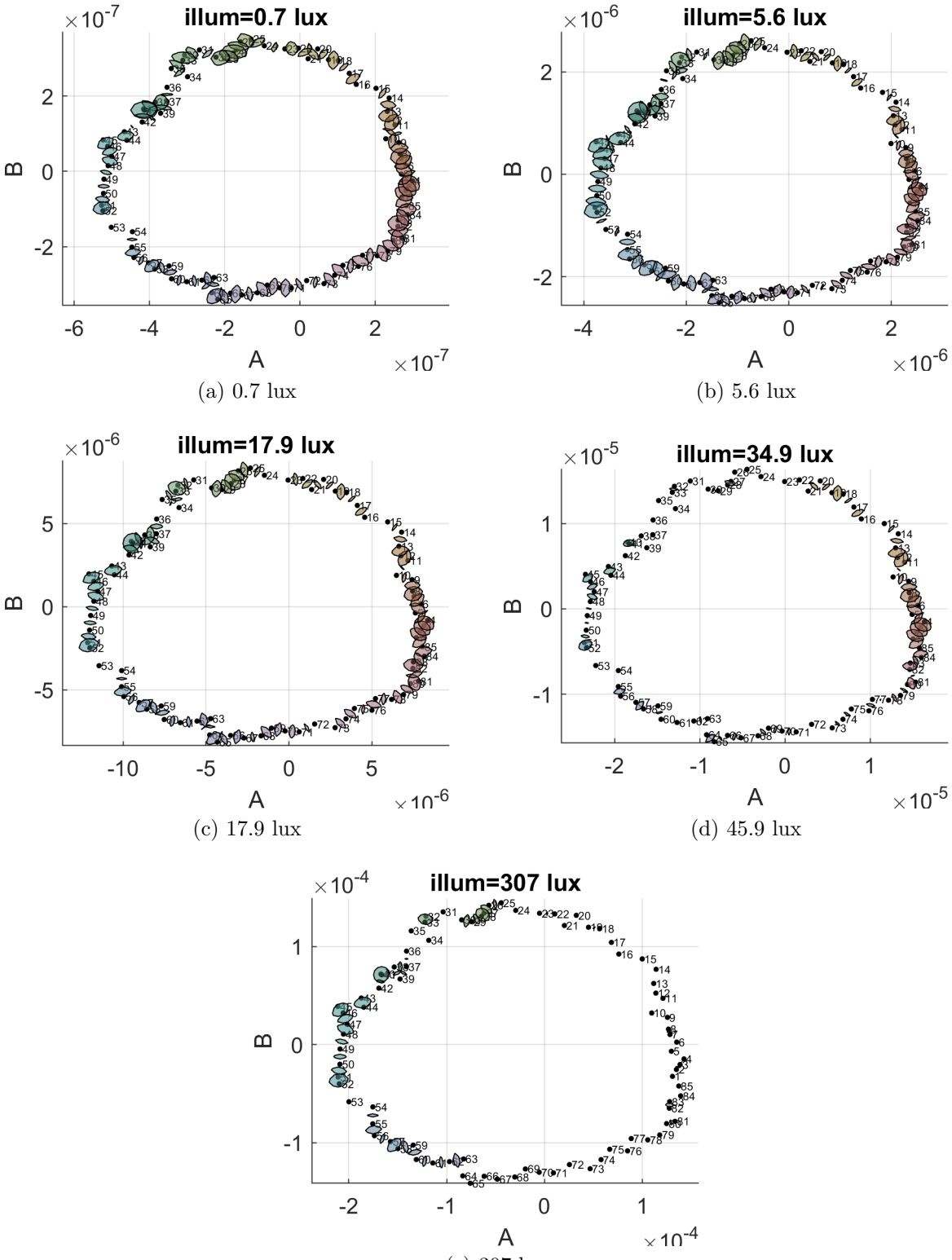

(a) 0.7 lux

(b) 5.6 lux

(c) 17.9 lux

(d) 45.9 lux

(e) 307 lux

Figure 5.7: Overlap between the threshold detection ellipses for the older age group.

Chapter 6

Discussion and Conclusion

6.1 Discussion

6.1.1 Discussion of Results

The main purpose of the present study was to measure the chromatic discrimination for a set of ordered color caps at different light levels and between two age groups. Previous research about color discrimination has shown that it is influenced by (il)luminance, spectral power distribution and age [18] [13] [16] [20]. In the present study, efforts were made to characterize the accuracy of different color spaces with hue angles, confusing distances and the circular statistics as an alternative to the well known FM100-Hue error score. Furthermore, in the present study, an effort was made to model the L-, M- and S-cone activation to better represent the chromatic discrimination at the lower light levels in the mesopic vision region.

In this study, the Farnsworth-Munsell 100 Hue color vision test was used as a measure of the chromatic discrimination. The Farnsworth-Munsell 100 Hue color vision test was originally designed to be uniformly distributed in the Munsell book of colors. The color caps of this color vision test were indicated as an almost perfect circle in the CIE 1931 xyY color space. The uniformity of the CIE 1931 xyY color space has now been refuted by many researchers and other color spaces such as the CIE 1976 UCS and the CIECAM02UCS color appearance space were introduced with improved uniformity. It is therefore not surprising that the chromatic coordinates form an imperfect circle around the illuminant and the distances between the neighbouring color caps were not equal everywhere in the CIE 1976 UCS and CIECAM02UCS color spaces. When ordering the color caps based on the hue angle calculated by the color spaces no differences were observed between the predicted order based on the color space and the order specified by Farnsworth himself. Though the hue angle difference between the color caps was not perfectly uniform it was the best standardized measure for chromatic discrimination available in the lab at that time.

In line with previous studies, the results of the experiment show that there are significant differences in chromatic discrimination when reducing the light level into the mesopic vision region for the FM100 Hue error score. For all light level conditions except the lowest, the correlation coefficient between the predicted order and the participant order determined by the circular statistics were around 0.9 or higher. The most remarkable and lowest correlation coefficients were at the first 3 trays at the lowest lighting condition, which were smaller than 0.9 and around or below 0.8. In this study, based on the paper from Kinnear and Sahraie about the new Farnsworth-Munsell 100 hue test norms of normal observers for each year of age 5—22 and for age decades 30—70 [20], differences between two age groups for 18—30 and 45—60 years old were investigated. In line with this study, the results of our study showed that there were significant differences in chromatic discrimination between the two age groups. Most interesting though was the significant interaction effect of light level and age group. Observed from the post hoc analysis observed was that the older participant group had more difficulty in doing the FM100 hue color vision test than the younger participant group. This would suggest that people between the age of 45 and 60 years old would need significantly more light for chromatic discrimination than people that are between the age of 18 and 30 years old. Based on the paper by Yuodelis and Hendrickson about the development of the human fovea (1986) [68] and the paper of Knoblauch (1987) [19], the interaction effect of age group and light level could be explained by the decrease in the cone density by age. Knoblauch suggested that other motivational factors might also had an influence on this interaction effect, however, by adding breaks between the trials and the test being interactive these motivational factors were minimized. Furthermore based on the research by Walkey, Barbur, Harlow and Makous (2001) [69], the tritan like effect observed at low light levels could be explained by the scarcity of S-cones in the retina.

Jiaye Li in her master thesis about visibility and predictability of perceived colour differences describes the confusion distances and observer variability within observers for a specific set of repeats. Thresholds were fitted in the CIECAM02UCS color spaces for the intra-observer variation in the confusion distances from the color cap orderings. In this study, an attempt was made to fit thresholds for the inter-observer variation in color cap ordering, however, without any success. There was to much variation between participants in their color cap orderings to accurately determine any thresholds even at the lowest euclidean distance between two color caps.

Furthermore, the results from the circular statistics were somewhat questionable because assumed was that each color cap had a certain hue angle calculated in the CIECAM02UCS and CIE 1976 color space and that those hue angles wouldn't change at different light levels. The hue angles that were linked to a color cap number were calculated in the CIECAM02UCS and CIE 1976 UCS color space by using the known reflectance values of the color caps like explained in the methodology. To then determine the correla-

tion coefficient the hue angles corresponding to the numerated color cap orders that were determined by the response of the participant, the luminance distribution and randomization were compared to the hue angles that corresponded to the correct order. Thus the correlation coefficient here would basically tell how well the predicted rank order corresponded to the other rank orders in hue angles. Although this information was important it wouldn't necessarily justify using circular statistics for the participant, luminance and random order. The assumption that each color cap had a fixed hue angle was only made for the participant, luminance and random order, and not for the additive noise. The additive noise did change the hue angle at each color caps based on the variance around the fixed hue angle at photopic vision. The additive noise did explain the amount of variance that was needed to have a comparable correlation coefficient to that of the participant order. However, when directly comparing the participant order with the additive noise no higher correlation coefficient was found than comparing the participant order with the predicted order in radians.

The results from the Thursthonian analysis were difficult to interpret. The Thursthonian analysis provided an estimate of the cap order by its probability, however, did not account for any noise at the photoreceptor or post-receptoral level. The Thursthonian order, like in the circular statistics, provided the best estimate of the order of the participants. The main difference though was that in the Thursthonian order assumed was that every color cap was compared with each other, which might not have been the case. So the results of the Thurstonian analysis were questionable, however, did indicate what the predicted order would be if all participants did compare all of the color caps with each other. The Thrusthonian order was plotted against the achromatic, opponent channels and the rod activation of the color caps, but besides the hue angle in the opponent channels no other photoreceptor or post-receptoral level seemed to explain the data.

The results from the bipolarity and axis analysis were similar to the results obtained by Knoblauch [19]. The results indicated a tritanlike defect in the older age groups and at lower illuminance levels. When the illuminance levels were lowered the errors along the tritan axis, through approximated color cap numbers 5.1 and 48.8 [61], increased. Furthermore, the bipolarity, amplitude, and modulation all increased for a lower illuminance level and in the older age group. This would further indicate evidence for the tritan like effects caused by weak S-cone mediated hue signals at mesopic light levels.

6.1.2 Discussion of Models

In the mesopic model color discrimination models there was some small improvement gained by adding extra factors to equations for the highest correlation coefficient improvement of 0.0037 at tray 3 for the adjusted CIECAM02 UCS adjusted model. These correlation coefficients were determined by comparing the fixed hue angles from the original CIECAM02

UCS model for the Farnsworth predicted cap order and comparing that to the hue angles that came out of the adjusted CIECAM02 UCS model. The problem with minimizing the correlation coefficient between the adjusted and original model was that the adjusted model was optimized for the same hue angle differences between the color caps in the original model. This assumption, however, was not tested and future research should further investigate the actual threshold differences between each combination of color cap.

Furthermore, based on the research by Lucassen, Lambooij, Sekulovski, and Vogels about the spatio-chromatic sensitivity explained by post-receptoral contrast [67], (noise) detection threshold ellipses were examined, modelled and optimized. With the detection threshold ellipses, the large variation at the lower light levels in the ordering of the color caps was explained by a general decrease in the detection coefficients and an inequality in the two chromatic channels. The detection coefficient D_A along the tritan axis was generally lower at the lower light levels compared to the detection coefficient D_B and resulted in a larger ellipse region into that chromatic channel direction. This would again indicate the inaccuracy of the human visual system to discriminate colors along the tritan axis at mesopic light levels. Between the two age groups less of a differences between the detection coefficients was observed, however, the error (unexplained variance) for the older age group was higher than the younger age group at the lowest level. This was probably due to that the cap order for the older participants was much more dispersed and less represented a normal distribution (shown in figure 4.1). The cap order for the younger participants much better represented a normal distribution (shown in figure 4.2). The model was not perfect in the prediction of the data, but in general performed decently well as shown in figure 5.3 with an error of less than 0.08.

6.1.3 Implications

The results of this study were important to further understand how lighting systems could be optimized for different age groups and light levels. The study was performed in commission of the Signify Research Group that aims for high lighting quality systems. The study therefore not only contributed to the theoretical research on chromatic discrimination at the mesopic vision but also could be used for the improvement of light applications. Light applications, for example, could be improved for a better user experience by accounting for differences in chromatic discrimination between age group when the lights are dimmed. Another application would be in the street lighting and emergency lighting which could be designed differently depending on the targeted consumers. When consumers, for example, would be younger than 30 at night less light would be needed for chromatic discrimination compared to when the consumer would be older than 45. Furthermore, theoretically, this study could help better understand the effect of chromatic discrimination at lower light levels on the human color vision. Also, with the threshold detection ellipses the ability to discriminate color caps can be predicted for different illuminations. Predicting the ability to discriminate color caps can be useful for creating standards for emergency, street and

commercial lighting.

6.1.4 Discussion of Limitations

6.1.4.1 Limitations of Equipment

An important limitation of this study was the restriction in the number of LEDs in the LED cube and that most of these LEDs had a very peaked distribution. As shown in the method section the spectral power distribution did not perfectly match with illuminant C and small deviations in the chromaticity coordinates between the color caps under standard illuminant C and the recreated illuminant C resulted. These deviations, however, were very minimal and it is unlikely that this would have any significant effect on the results of this study. The recreated illuminant C was similar in the chromaticity coordinates with the standard illuminant C and the color cap position in the CIE 1976 UCS color space hardly changed.

Another limitation of this study was the reduction of the light level. The LED cubes had a limited sensitivity for only 10 bits per channel. This limited sensitivity carried the consequence of having to use two polarization filters placed on top of each other. The angle of one of the polarization filters than determined the amount of light that could be filtered. The polarization filters first provided the problem in the lower wavelengths at which it did not filter as much as at the other wavelengths. This problem was accounted for by calculating the ratio between the amount that was not filtered and then multiplying a LED with that ratio that had a peak at the lower wavelengths. The second problem was that even with the polarization filters at opposite angles of each other we couldn't go lower than 0.7 lux (0.2 cd/m^2).

In this study, the FM100 hue test kit was used to determine the chromatic discrimination. The FM100 hue test kit, however, was limited in the number of color caps that were included and there was only one type of tray provided. Using other color cap sets and different trays could have an influence on the results, however, because of the comparability of this study with other studies the standard FM100 hue test kit was used.

6.1.4.2 Limitations of Methodology

The methodology suggested by Farnsworth was used in this study, however, some participants might have had different strategies in ordering the color caps. The participants were instructed to order the color caps based on their color, however, some participants might have used different cues such as brightness for some of the color cap placements. Another limitation in this methodology was the inability to control the eye movements. When looking at the eye movements of some of the participants while they were performing the task, noteworthy was that most participants made rapid eye movement comparing

most of the color caps with each other. When they had all the color caps aligned participants seemed to make fewer eye movements and probably were looking at the overall color cap ordering instead of each individual color cap. Furthermore, there was no time limit in doing the task where some participants spend a very long time on the task and others were quicker in ordering the color caps. Just like in the Farnsworth methodology participants were instructed to perform the task in a somewhat quick way, however, they were not limited in their time in doing the task.

6.1.4.3 Confounding Factors

Apart from the limitations of methodology and equipment, the confounding factors were also considered. As mentioned before the whole experiment took a long time to finish, therefore, visual fatigue might have affected the responses of the participants. Due to the visual fatigue participants possibly ordered the last few conditions with less precision than the first few conditions. To minimize any visual fatigue the participants were offered a break halfway through the experiment to rest there eyes before continuing.

Another confounding factor in this study was the adaptation issue for which was unclear whether participants would either locally adapt to the color cap stimuli or adapt more globally to the average of the surrounding. Also, participants were first adapted for 5 minutes to the light level of the proceeding trial which was based on the chromatic adaptation curve. The light adaptation was known to be quicker so probably a smaller adaptation time would have been possible, but to be sure the participants had a large enough adaptation time five minutes were chosen.

The background of the environment at the bottom of the light box where the color caps were displayed was made black to minimize any influence of contrast between the color caps and the background. Choosing another background, however, could have had an influence on the cap order responses of the participants. Besides the background, the surrounding walls of the light box were chosen to be white to improve the uniformity of light hitting the color caps at different positions in the light box. Additionally, the white walls were chosen to help improve the adaptation to the illumination condition. Different (colored) surroundings probably would have had an effect on the responses of the participants.

6.1.5 Conclusion

This study aimed to produce a guideline to determine at which light levels the current available colorimetric models can accurately predict chromatic discrimination. Therefore, the hue angles and the FM100 hue error score were examined at different light levels. The colorimetric models correlated well with the participant data for correlation coefficients above .96 except at the lowest light level. Much more errors were observed in tray numbers 1 and 3 at the lowest light level for both the younger and older age group. This suggested that

the two colorimetric models that were investigated the CIECAM02UCS and CIE 1976 UCS color spaces are less accurate in predicting the chromatic discrimination at mesopic vision. Based on other literature this was explained by a reduction of chromatic sensitivity at the mesopic vision and the reduction in the quantal catch of the cone receptors. Especially the lowest correlation .6223 at the lowest light level at tray number 3 for the older age group was explained by this reduction in quantal catch and the scarcity of s-cones in the retina.

To answer the main research question of this study "How is our ability to discriminate object colors affected by our age and by the illumination level?" and to test the hypotheses "There is a significant effect of illuminance on chromatic discrimination" and "There is a significant effect of age on chromatic discrimination" a repeated measures ANOVA was performed. The repeated measures ANOVA revealed significant main effects for Tray and Light and significant interaction effects between Light and AgeGroup and between Light and Tray. Additionally, the repeated measure ANOVA revealed significant differences between participants. Both hypotheses were confirmed for the main effects of light level and age, however, there were interaction effects between the light level and age group. Looking at the post hoc analysis the interaction effect can be explained by older participants having more difficulty with the FM100 hue color vision test at lower light levels. Thus in the mesopic vision region researchers should account for the age difference of participants when conducting chromatic discrimination experiments. Finally, threshold detection ellipses explained the data with a root mean squared difference in probability of cap displacement of lower than 0.08. The threshold detection ellipses were larger along the tritan axis at the lowest light level which agreed with previously reported tritan like effects caused by weak S-cone mediated hue signals.

Bibliography

[1] Wandell B. and Thomas S. Foundations of vision. *Psyccritiques*, 42(7), 1997. xixi, 11

[2] Rinner O. and Gegenfurtner K. R. Time course of chromatic adaptation for color appearance and discrimination. *Vision Research*, 40(14):1813–1826, jun 2000. 1, 16

[3] Fairchild M. D. and Reniff L. Time course of chromatic adaptation for color-appearance judgments. *Journal of the Optical Society of America A*, 12(5):824, may 1995. 1, 16

[4] Jameson D. and Hurvich L. M. *Color Adaptation: Sensitivity, Contrast, After-images*, pages 568–581. Springer Berlin Heidelberg, Berlin, Heidelberg, 1972. 1

[5] Zaidi Q. *Color and brightness induction: from Mach bands to three-dimensional configurations*. New York: Cambridge Univ. Press, 1999. 1

[6] Baron R. A., Rea M. S., and Daniels S. G. Effects of indoor lighting (illuminance and spectral distribution) on the performance of cognitive tasks and interpersonal behaviors: The potential mediating role of positive affect. *Motivation and Emotion*, 16(1):1–33, mar 1992. 1

[7] Elliot A. J. and Maier M. A. Color Psychology: Effects of Perceiving Color on Psychological Functioning in Humans. *Annual Review of Psychology*, 65(1):95–120, jan 2014. 1

[8] Steele R. V. The story of a new light source. *Nature photonics*, 1(1):25, 2007. 1

[9] Cho J., Park J. H., Kim J. K., and Schubert E. F. White light-emitting diodes: History, progress, and future. *Laser & photonics reviews*, 11(2):1600147, 2017. 1

[10] Brown W. R. J. The Influence of Luminance Level on Visual Sensitivity to Color Differences. *J. Opt. Soc. Am.*, 41(10):684–688, 1951. 2

[11] Wyszecki G. and Fielder G. H. New Color-Matching Ellipses. *J. Opt. Soc. Am.*, 61(9):1135–1152, sep 1971. 2

[12] Yeh T., Pokorny J., and Smith V. C. Chromatic Discrimination with variation in Chromaticity and Luminance - Data and Theory. *Vison Research*, 33(13):1835–1845, sep 1993. 2, 105, 106, 107, 108, 109, 110, 111, 112

[13] Pridmore R. W. and Melgosa M. Effect of luminance of samples on color discrimination ellipses: Analysis and prediction of data. *Color Research & Application*, 30(3):186–197, 2005. 2, 3, 83

[14] Jennings B. J. and Barbur J. L. Colour detection thresholds as a function of chromatic adaptation and light level. *Ophthalmic and Physiological Optics*, 30(5):560–567, 2010. 2

[15] Royer M. P., Houser K. W., and Wilkerson A. M. Color discrimination capability under highly structured spectra. *Color Research & Application*, 37(6):441–449, 2012. 2, 106, 107, 108, 109, 111, 112

[16] Cheng W., Ju J., Sun Y., and Lin Y. The effect of led lighting on color discrimination and preference of elderly people. *Human Factors and Ergonomics in Manufacturing & Service Industries*, 26(4):483–490, 2016. 2, 83

[17] Boyce P.R. and Simons R.H. Hue discrimination and light sources. *Lighting Research & Technology*, 9(3):125–140, 1977. 2

[18] Yebra A., Garcia J. A., Nieves J. L., and Romero J. Chromatic discrimination in relation to luminance level. *Color Research & Application*, 26(2):123–131, apr 2001. 3, 83, 106, 107, 108, 109, 110, 111, 112

[19] Knoblauch K., Saunders F., Kusuda M., Hynes R., Podgor M., Higgins K. E., and De Monasterio F. M. Age and illuminance effects in the farnsworth-munsell 100-hue test. *Applied Optics*, 26(8):1441–1448, 1987. 3, 84, 85

[20] Kinnear P. R. and Sahraie A. New farnsworth-munsell 100 hue test norms of normal observers for each year of age 5–22 and for age decades 30–70. *British Journal of Ophthalmology*, 86(12):1408–1411, 2002. 3, 83, 84

[21] Kokoschka S. Das v lambda-dilemma in der photometrie. In *Proceedings of 3.*, volume 3, 1997. 3, 7

[22] Eloholma M., Viikari M., Halonen L., Walkey H., Goodman T., Alferdinck J., Freiding A., Bodrogi P., and Várady G. Mesopic modelsfrom brightness matching to visual performance in night-time driving: a review. *Lighting Research & Technology*, 37(2):155–173, jun 2005. 3, 7

[23] Roufs J. A. J. Light as a true visual quantity : principles of measurement, 1978. 3, 7

[24] Fairchild M. D. *Color appearance models*. John Wiley & Sons, 2013. 5

[25] Marc R. E. and Sperling H. G. Chromatic Organization of Primate Cones. 6

[26] Schmidt T. M., Chen S., and Hattar S. Intrinsically photosensitive retinal ganglion cells: many subtypes, diverse functions. *Trends in Neurosciences*, 34(11):572–580, nov 2011. 6

[27] Normann R. A. and Werblin F. S. Control of retinal sensitivity. I. Light and dark adaptation of vertebrate rods and cones. *The Journal of general physiology*, 63(1):37–61, jan 1974. 6

[28] Rodieck R. W. and Rodieck R. W. *The first steps in seeing*. Sinauer Associates Sunderland, MA, 1998. 8

[29] Starr C., Evers C., and Starr L. *Biology: concepts and applications*. Cengage Learning, 2010. 9

[30] Wright W. D. A re-determination of the trichromatic coefficients of the spectral colours. *Transactions of the Optical Society*, 30(4):141–164, mar 1929. 11

[31] Guild J. The Colorimetric Properties of the Spectrum. *Philosophical Transactions of the Royal Society A: Mathematical, Physical and Engineering Sciences*, 230(681-693):149–187, jan 1931. 11

[32] Smith T. and Guild J. The C.I.E. colorimetric standards and their use. *Transactions of the Optical Society*, 33(3):73–134, jan 1931. 12

[33] Stockman A. and Sharpe L. T. Into the twilight zone: the complexities of mesopic vision and luminous efficiency. *Ophthalmic and Physiological Optics*, 26(3):225–239, may 2006. 12

[34] Stockman A. and Sharpe L. T. The spectral sensitivities of the middle- and long-wavelength-sensitive cones derived from measurements in observers of known genotype. *Vision Research*, 40(13):1711–1737, jun 2000. 12

[35] Judd D. B. Report of U.S. secretariat committee on colorimetry and artificial daylight. *Proceedings of the 12th Session of the CIE, 1951*, 1:11, 1951. 13, 70

[36] Vos J. J. Colorimetric and photometric properties of a 2 fundamental observer. *Color Research & Application*, 3(3):125–128, 1978. 13

[37] Stiles W. S. and Burch J. M. Interim Report to the Commission Internationale de l'Eclairage, Zurich, 1955, on the National Physical Laboratory's Investigation of Colour-matching. *Optica Acta: International Journal of Optics*, 2(4):168–181, dec 1955. 13

[38] Stiles W. S. and Burch J. M. N.P.L. Colour-matching Investigation: Final Report. *Optica Acta: International Journal of Optics*, 6(1):1–26, jan 1959. 13

[39] Speranskaya I. N. Determination of spectrum color coordinates for twenty-seven normal observers. *Opt. Spectrosc.*, 7:424–428, 1959. 13

[40] Bieske K. and Vandahl C. A study about colour-difference thresholds. *Lux et Color Vespremiensis*, 2008. 14

[41] Narendran N., Vasconez S., Boyce P., and Eklund N. Just-Perceivable Color Differences between Similar Light Sources in Display Lighting Applications. *Journal of the Illuminating Engineering Society*, 29(2):68–77, jul 2000. 14

[42] MacAdam D. L. Visual sensitivities to color differences in daylight. *Josa*, 32(5):247–274, 1942. 14

[43] Moroney N., Fairchild M. D., Hunt R. W. B., Li C., Luo M. R., and Newman T. The ciecam02 color appearance model. In *Color and Imaging Conference*, volume 2002, pages 23–27. Society for Imaging Science and Technology, 2002. 14, 68

[44] Kohn A. Visual Adaptation: Physiology, Mechanisms, and Functional Benefits. *Journal of Neurophysiology*, 97(5):3155–3164, may 2007. 15

[45] Ruseckaite R., Lamb T. D., Pianta M. J., and Cameron A. M. Human scotopic dark adaptation: Comparison of recoveries of psychophysical threshold and ERG b-wave sensitivity. *Journal of Vision*, 11(8):2–2, jul 2011. 15

[46] Baker H. D. Initial Stages of Dark and Light Adaptation. *Journal of the Optical Society of America*, 53(1):98, jan 1963. 15

[47] Kalloniatis M. and Luu C. Light and dark adaptation. In *Webvision: The Organization of the Retina and Visual System [Internet]*. University of Utah Health Sciences Center, 2007. 15

[48] Reuter T. Fifty years of dark adaptation 19612011. *Vision Research*, 51(21-22):2243–2262, nov 2011. 15

[49] Dowling J. E. Neural and Photochemical mechanisms of visual adaptation in the rat. *The Journal of general physiology*, 46(6):1287–301, jul 1963. 15

[50] Hayhoe M. M., Levin M. E., and Koshel R. J. Subtractive processes in light adaptation. *Vision Research*, 32(2):323–333, feb 1992. 15

[51] Engeldrum P. G. *Psychometric scaling: a toolkit for imaging systems development*. Imcotek press, 2000. 16, 41, 100

[52] Taylor M. M. and Creelman C. D. PEST: Efficient Estimates on Probability Functions. *The Journal of the Acoustical Society of America*, 41(4A):782–787, apr 1967. 16

[53] Watson A. B. and Pelli D. G. Quest: A Bayesian adaptive psychometric method. *Perception & Psychophysics*, 33(2):113–120, mar 1983. 16

[54] Esposito T. and Houser K. A new measure of colour discrimination for leds and other light sources. *Lighting Research & Technology*, 51(1):5–23, 2019. 37, 55

[55] Schütt H. H., Harmeling S., Macke J. H., and Wichmann F. A. Painfree and accurate bayesian estimation of psychometric functions for (potentially) overdispersed data. *Vision Research*, 122:105–123, 2016. 40

[56] Kuss M., Jäkel F., and Wichmann F. A. Bayesian inference for psychometric functions. *Journal of Vision*, 5(5):8–8, 2005. 40

[57] Fründ I., Haenel N. V., and Wichmann F. A. Inference for psychometric functions in the presence of nonstationary behavior. *Journal of vision*, 11(6):16–16, 2011. 40

[58] Berens P. Circstat: a matlab toolbox for circular statistics. *J Stat Softw*, 31(10):1–21, 2009. 40, 62

[59] Jammalamadaka S. R. and Sengupta A. *Topics in circular statistics*, volume 5. world scientific, 2001. 40

[60] Montag E. D. Empirical formula for creating error bars for the method of paired comparison. *Journal of Electronic Imaging*, 15(1):010502, 2006. 41

[61] Knoblauch K. On quantifying the bipolarity and axis of the farnsworth-munsell 100-hue test. *Investigative ophthalmology & visual science*, 28(4):707–710, 1987. 42, 73, 85

[62] Kinnear P. R. Proposals for scoring and assessing the 100-hue test. *Vision research*, 10(5):423–433, 1970. 42, 64

[63] Rao C. R. *Linear statistical inference and its applications*, volume 2. Wiley New York, 1973. 43

[64] Hunt R. W. G. and Pointer M. R. A colour-appearance transform for the cie 1931 standard colorimetric observer. *Color Research & Application*, 10(3):165–179, 1985. 67

[65] Shin J., Matsuki N., Yaguchi H., and Shioiri S. A color appearance model applicable in mesopic vision. *Optical review*, 11(4):272–278, 2004. 70, 71

[66] Smith V. C. and Pokorny J. Spectral sensitivity of the foveal cone photopigments between 400 and 500 nm. *Vision research*, 15(2):161–171, 1975. 70

[67] Lucassen M., Lambooij M., Sekulovski D., and Vogels I. Spatio-chromatic sensitivity explained by post-receptoral contrast. *Journal of vision*, 18(5):13–13, 2018. 72, 86

[68] Yuodelis C. and Hendrickson A. A qualitative and quantitative analysis of the human fovea during development. *Vision research*, 26(6):847–855, 1986. 84

[69] Walkey H. C., Barbur J. L., Harlow J. A., and Makous W. Measurements of chromatic sensitivity in the mesopic range. *Color Research & Application*, 26(S1):S36–S42, 2001. 84

[70] Asano Y., Fairchild M. D., and Blondé L. Individual Colorimetric Observer Model. *PLOS ONE*, 11(2):1–19, 2016. 100, 101

[71] Hansen T., Giesel M., and Gegenfurtner K. R. Chromatic discrimination of natural objects. *Journal of Vision*, 8(1), 2008. 101, 105, 106, 107, 108, 109, 111, 112

[72] Shevell S. K. The dual role of chromatic backgrounds in color perception. *Vision Research*, 18(12):1649–1661, 1978. 101

[73] Bodrogi P., Brückner S., Khanh T. Q., and Winkler H. Visual assessment of light source color quality. *Color Research & Application*, 38(1):4–13, feb 2013. 105, 106, 107, 108, 109, 111, 112

[74] Mayr S., Köpper M., and Buchner A. Comparing colour discrimination and proofreading performance under compact fluorescent and halogen lamp lighting. *Ergonomics*, 56(9):1418–29, sep 2013. 106, 107, 108, 109, 110, 111, 112

[75] M. S. Rea and FreyssinierNova J. P. Color rendering: A tale of two metrics. *Wiley Online Library*, 2008. 106, 107, 108, 109, 110, 111, 112

[76] Acosta I., León J., and Energies P. B. Daylight Spectrum Index: A New Metric to Assess the Affinity of Light Sources with Daylighting. *Energies*, 2018. 106, 107, 108, 109, 111, 112

[77] Babilon S. *On the Color Rendition of White Light Sources in Relation to Memory Preference*. PhD thesis, Technische Universität, 2018. 106, 107, 108, 109, 111, 112

[78] Boissard S. and Fontoynont M. Optimization of LEDbased light blendings for object presentation. *Wiley Online Library*, 2009. 106, 107, 108, 109, 111, 112

[79] Danilova M. V. and Mollon J. D. Symmetries and asymmetries in chromatic discrimination. *Journal of the Optical Society of America A-Optics Image science and Vision*, 31(4):A247–A253, apr 2014. 106, 107, 108, 109, 111, 112

[80] Esposito T. Modeling color rendition and color discrimination with average fidelity, average gamut, and gamut shape. 2016. 106, 107, 108, 109, 111, 112

[81] Hood S. Light emitting diode color rendition properties. 2013. 106, 107, 108, 109, 111, 112

[82] Jiang L., Jin P., and Express P. L. Color discrimination metric based on cone cell sensitivity. *Optics express*, 2015. 106, 107, 108, 109, 111, 112

[83] Jost S., Cauwerts C., and Avouac P. CIE 2017 color fidelity index Rf: a better index to predict perceived color difference? *Journal of the Optical Society of America A-Optics Image Science and Vision*, 35(4):B202–B213, apr 2018. 106, 107, 108, 109, 111, 112

[84] Lin Y., Wei M., Smet K. A. G., Tsukitani A., Bodrogi P., and Khanh T. Q. Colour preference varies with lighting application. *Lighting Research & Technology*, 49(3):316–328, may 2017. 106, 107, 108, 109, 111, 112

[85] O'Connor D. A. and Davis R. G. Lighting for the Elderly: The Effects of Light Source Spectrum and Illuminance on Color Discrimination and Preference. *LEUKOS*, 2(2):123–132, oct 2005. 106, 107, 108, 109, 110, 111, 112

[86] Pardis Taherzadeh. *Ivestigating the influence of spectral power distribution characteristics on hue differentiation task performance.* PhD thesis, Bilkent University, 2018. 106, 107, 108, 109, 111, 112

[87] Vrabel P. L., Bernecker C. A., and Mistrick R. G. Visual Performance and Visual Clarity under Electric Light Sources: Part IIVisual Clarity. *Journal of the Illuminating Engineering Society*, 27(1):29–41, jan 1998. 106, 107, 108, 109, 111, 112

[88] Wei M., Houser K. W., David A., and Krames M. R. Colour gamut size and shape influence colour preference. *Lighting Research & Technology*, 49(8):992–1014, dec 2017. 106, 107, 108, 109, 111, 112

[89] Wei M., Houser K. W., Allen G. R., and Beers W. W. Color Preference under LEDs with Diminished Yellow Emission. *LEUKOS*, 10(3):119–131, jul 2014. 106, 107, 108, 109, 110, 111, 112

[90] Žukauskas A., Vaicekauskas R., Vitta P., Tuzikas A., Petrulis A., and Shur M. Color rendition engine. *Optics express*, 2012. 106, 107, 108, 109, 111, 112

.1 Literature Review

The studies about chromatic discrimination indicate that the luminance and chromaticity of the light source have an effect on the chromatic discrimination of illuminated surfaces. However, because different color renditions are used it is uncertain how well these studies truly represent color discrimination under another light source, like daylight. Thus, to indicate the color rendition characteristics for color discrimination a well representative color fidelity metric is important. To better understand the relation between color discrimination, color rendering and the already existing research on this topic, a literature study was performed. This literature study focuses on both color rendering and color discrimination. By an extensive literature search and analysis, two different literature questions are answered:

1. What complex viewing conditions were determined and how were they represented in previous studies on the discrimination of color objects?

2. How is color fidelity measured and what is needed to obtain an accurate color rendering index?

To answer literature question 1, the display, stimulus and viewing characteristics are reported, to most accurately describe the viewing conditions and the representation of stimuli for the discrimination studies of color objects. To answer literature question 2, the study and method characteristics of the color rendering studies are analyzed, to determine the characteristics for color fidelity measurements and the conditions that are necessary to obtain an accurate color rendering index. In the following subsections first, the methodology of the literature review is explained with the evaluation and search criteria. The results of this literature review are reported in the second subsection and discussed in the third subsection. Finally, a summary of the most important findings is provided in the last subsection of this literature review.

.1.1 Methodology

In this section the assessment criteria of this literature review are described first. After the assessment criteria description, the data analysis method is described. Thereafter, the search process of where the papers were found and how they were recovered is described. Finally, the inclusion and exclusion criteria are provided that were used to get the final selection of papers.

.1.1.1 Assessment criteria

Five assessment criteria were chosen (see Table 1) to be able to answer the literature questions and to gather insight into the differences between the studies that investigated color discrimination. The criteria were (I) study characteristics, (II) method characteristics, (III) display characteristics, (IV) stimulus characteristics and (V) viewing condition. In

the following subsection, each criterion is explained for why it was chosen and what exactly this criterion entails.

Table 1: Overview of the assessment criteria with their subcategories.

Study Characteristics	**Method Characteristics**	**Display Characteristics**	**Stimulus Characteristics**	**Viewing Condition**
Observers	Constant stimuli	Light emitting	Uniform and gratings	Adaptation
Between and within	Limits	Illuminated surfaces	Luminance and chromaticity	Field size
Age	Adjustment		Color rendering	Surrounding
	Survey			
	Paired Comparisons			

.1.1.1.1 Study characteristics This criterion is important to understand the general design of the studies. The design of a study is important to mention because slight differences between studies could have profound consequences on the actual effects that are explained. The study characteristics were investigated for three categories. The first, (1) number of observers, was chosen because known is that the number of observers largely determines the actual statistical power and generalizability of the effect reported in a study. The second, (2) between and within observer effects, was chosen because the latter two effects are very different and important to distinguish. The third and final study characteristic, (3) age variability, was chosen because shown is that younger people (∼20) perceive colors differently than older people (∼70) [70].

.1.1.1.2 Method characteristics This criterion is important to understand how effects are measured. How the tasks are designed can be crucial and sometimes limited by what the researcher wants to measure. The method characteristics were investigated for four different categories. The categories were chosen based on the description of psychophysical methods by Engeldrum, which explains the advantages, limitations, and disadvantages of these methods in his book about psychometric scaling [51]. Many of the methods described by Engeldrum are used in color research for many different tasks (e.g. alternative forced choice tasks and staircase procedures). The categories are (1) method of constant stimuli, (2) method of limits, (3) method of adjustment, (4) survey. In addition to the methods described by Engeldrum, a commonly used task called (5) paired comparisons, was used as a method characteristic.

.1.1.1.3 Display characteristics This criterion is important to understand how stimuli are presented to the observer. The presentation of stimuli is very important to how the observer perceives the stimulus. The display characteristics were investigated for two different categories. In this literature study, the display of the stimulus is characterized by (1) light emitting stimuli and by (2) illuminated surfaces.

.1.1.1.4 Stimulus characteristics The criterion stimulus characteristics is important to understand what the dependent and independent variables in the study are. These variables explain the main effect. In this study, the stimulus is referred to the controlled physical properties of the light that were emitted or used to illuminate objects. The stimulus characteristics were investigated for three different categories. The first, (1) uniform and complex objects, was chosen because complex objects can induce different results than just using uniform stimuli [71]. The second, (2) (il)luminance and chromaticity, was chosen because some studies chose different (il)luminance levels and chromaticities for their stimuli. The third, (3) color rendering, was chosen because this an effect on the appearance of surfaces. Color rendering is, however, limited to a single number describing only how well a light source renders the colors of a chosen test sample set when compared to a specific reference light source within a specific color space. Other indexes such as the gamut area index, color quality scale, chromatic discrimination index, and color preference scale were therefore also considered, however, excluded from the analysis because of simplicity and because many studies only reported the color rendering index.

.1.1.1.5 Viewing conditions This criterion is important to understand to what extent the studies controlled the condition of how the stimulus was displayed. The viewing conditions were investigated for three different categories. The first, (1) adaptation, was chosen because it is important to know to what the observer was adapted to before, and while doing the task. Adaptation itself is not necessarily a viewing condition, but since the perceived stimulus under certain viewing conditions is highly influenced by the adaptation to the scene, or the adaptation that preceded the stimulus presentation, adaptation was included as a viewing condition characteristic. The second, (2) field size, was chosen because different field sizes induce differences in the appearance of the stimulus [70] and the sensitivity of the visual system is dependent on stimuli/field size. When the stimulus used in the study was limited to field size, the direct viewing angle was reported in this literature review. When the field size of the stimulus was not specified or limited, the whole size of the experimental setup was examined. The third, (3) surrounding, was chosen because the appearance of the stimulus also depends on the direct surrounding it was viewed in [72]. When the direct surrounding of the stimulus was not specified the whole surrounding of the participant was examined.

.1.1.1.6 Conclusion section To identify the main findings the conclusion sections of the studies were investigated and categorized by their main topic. The conclusion section includes the most important results and shows the progress in research for the different

domains.

.1.1.2 Data analysis

Most of the data that was gathered for each assessment criterion was displayed in tables. The tables were used to provide a good overview of all the subcategories within each assessment criterion. The subcategory, (il)luminance, and chromaticity, of the stimulus characteristic was displayed by means of a color space. The data was plotted for their chromaticity coordinates and the variation in (il)luminance level was reported. Furthermore, the subcategory, uniform, and gratings (contrast), of the stimulus characteristic was displayed by figures of different contrasts. Additionally, in this same assessment characteristic, color rendering was also additionally visualized by figures of different spectral power distributions.

.1.1.3 Search Process

For this literature review, the search process existed of using specified search terms (key words) in seven different databases. The literature from the databases was examined in order by four steps (see Table 2), starting at the more general databases including a lot of different articles, followed up by the topic-specific databases and afterward the topic-specific journals were searched. Finally, the resulting literature list was further assessed by the criteria and reported in this literature review. The general databases, Web of Science, Google Scholar and ScienceDirect were chosen based on their wide selection of articles. The topic-specific databases consisted of the PsycInfo and PubMed databases. The PubMed database provides more detailed publications within the life sciences and biomedical fields, whereas the PsycInfo database provides more detailed publication within the psychology field. The topic-specific journals consisted of the Journal of Illuminating Engineering Society and the Journal of Vision. Additional to the databases, references found in other relevant literature (reviews) were also used and assessed.

Table 2: The four steps with the databases and journals used in the search process.

General Databases		
Web of Science	*Google Scholar*	*ScienceDirect*
Topic-specific databases		
PsycInfo	*PubMed*	
Topic-specific journals		
Journal of Illuminating Engineering Society		*Journal of Vision*
Literature assessment		

During the search process two combinations of search terms were specified. The first topic that was specified is (1.1) Color fidelity and the second topic is (2.1) Color discrim-

ination. The two topics were chosen to explore the relationship between color discrimination and color fidelity. Where the discrimination of colored objects is dependent on the spectral power distribution of the illumination. In the actual search process sometimes instead of color rendering and color discrimination, the terms (1.2) Color rendering and (2.2) Chromatic discrimination were used only when the intended search terms did not provide enough relevant articles. Chromatic discrimination and color discrimination are in essence the same, however, can provide very different search results. Color fidelity and color rendering are also related and therefore color fidelity or color rendering was used as input in the search database. At the first step of the search process for the Google scholar and sciencedirect databases the combinations were searched for matches in the full text to provide for a broad amount of articles. For the Web of science database the combinations were only search for matches in the title as otherwise too many articles were found. At the second step of the search process the PsychInfo database was searched for matches in the title, whereas for the PubMed database matches were searched in the full text. For the PubMed database matches were searched in the full text as otherwise too few articles were found. At the third step of the search process for both Journals the matches were searched in the full text to assure that all relevant articles were included. Furthermore, the input in each search engine of each database different slightly in combinations of color fidelity, color rendering, color discrimination and chromatic discrimination, see Table 3.

Table 3: Overview of all the search topics and databases/journals that were used.

Database/ Journal	**Fields**	**Combinations**	**Input in search engine**	**Date of last search**
Google Scholar	Full text	Color rendering and color discrimination	"Color fidelity" AND "Color discrimination"	27/2/2019
ScienceDirect	Full text	Color rendering and color discrimination	"Color rendering" AND "Color discrimination"	27/2/2019
Web Of Science	Title	Color rendering and color discrimination	"Color fidelity" OR "Chromatic discrimination"	27/2/2019
PsycInfo	Title	Color rendering and color discrimination	"Color rendering" OR "Color discrimination"	27/2/2019
PubMed	Full Text	Color rendering and color discrimination	"Color rendering" AND "color discrimination"	27/2/2019

Table 3: Overview of all the search topics and databases/journals that were used.

Database/ Journal	**Fields**	**Combinations**	**Input in search engine**	**Date of last search**
Journal Of illuminating Engineering Society	Full Text	Color rendering and color discrimination	"Color rendering" AND "Color discrimination"	27/2/2019
Journal Of Vision	Full Text	Color rendering and color discrimination	"Color rendering" AND "Color discrimination"	27/2/2019

.1.1.4 Inclusion and exclusion criteria

In the final step of the search process, the resulting set of articles in all databases and journals were examined for their relevance to the literature questions. Studies that performed psychophysical research, and that were relevant to color rendering or color discrimination were included in the literature review. Studies that explained a patent or examined color rendering or color discrimination for non-human subjects were therefore excluded. Also, other single citations for which no document was publicly available or non-English documents were excluded. Finally, dictionary or glossary type of document including no psychophysical research were not examined in the results of this literature review. The found studies were examined based on their abstract and title. When insufficient information could be extracted from the abstract and title, the whole article was examined.

.1.2 Results

This section shows the number of search results that were found (see Table 4). After deduction to eligible unique articles a total of 22 studies were analyzed for each of the six assessment criteria. For each of these assessment criteria the results were further described for each category. The new articles indicated the number of articles that were not found in the earlier steps of the search process at other databases. Sometimes an article would occur in multiple databases, then the article would be attributed to and considered "new" at the first database it was found at in the search process. The eligible unique articles indicated the number of articles that met all criteria.

Table 4: Number of articles, new articles and eligible unique articles found with each database.

Database	**Articles**	**New articles**	**Eligible unique articles**
Google Scholar	165	147	14
ScienceDirect	42	41	-
Web Of Science	128	120	5
PsycInfo	30	30	-
PubMed	22	21	1
Journal of Illuminating Engineering Society	39	33	2
Journal of Vision	9	9	-
Total	**435**	**402**	**22**

.1.2.1 Overview

Most of the search results were derived from the general databases, Google Scholar, ScienceDirect and Web of Science From the hits of the databases, non-English documents were removed and only the remaining (new) articles were investigated. After applying the inclusion and exclusion criteria only a handful of articles were considered to be eligible and unique for the literature review. The general database Google Scholar offered the most eligible unique articles, namely 14. Some of these eligible unique articles from Google Scholar were also found in other databases, however, for simplicity they were not considered as new articles. Although it is worth mentioning that some of the eligible unique articles that were found in these general databases originated from the Journal of Illuminating Engineering Society. For the general database ScienceDirect, the topic-specific database PsycInfo and the Journal of Vision none eligible unique articles were found. From the general database Web of Science 5 eligible unique articles were found, for the topic-specific database PubMed 1 eligible unique article was found and the final two eligible unique articles were chosen from the Journal of Illuminating Engineering Society. In total 22 unique articles were examined.

.1.2.2 Study characteristics

First, the study characteristics were examined for the number of observers, the between and within observer effects and finally the age of the participants for each study.

.1.2.2.1 Number of observers Figure 1 shows the number of observers, male and female, for each of the 22 unique articles. Most studies reported the male/female ratio of the observers, except for study [73], [71] and [12]. Also observable is that the number of

observers varies a lot between the studies and in some studies also the male/female ratio is unequally distributed.

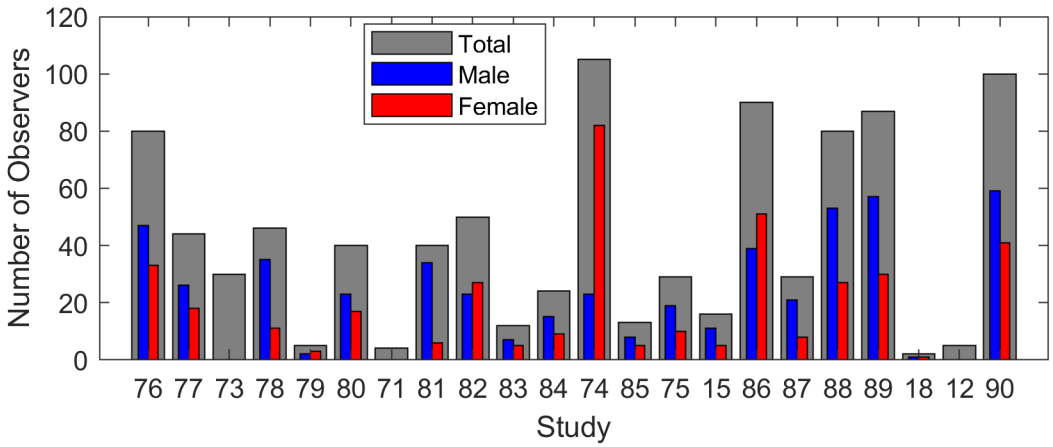

Figure 1: Histograms of the Male and Female ratio of each study nested within the total number of observers for that particular study.

.1.2.2.2 Between and within Most of the studies that were performed focused on within subjects effects whereas only the studies [74] and [75] (also) looked at between subject effects, see Table 5.

Table 5: Frequency table of the two different study types that investigate either between or within subject effects.

Study Type	**Study**	**Frequency**
Between Subjects	[74] [75]	2
Within Subjects	[76] [77] [73] [78] [79] [80] [71] [81] [82] [83] [84] [85] [75] [15] [86] [87] [88] [89] [18] [12] [90]	20

.1.2.2.3 Age The age of all studies varied between 14 and 78 years old. Figure 2 shows the age range for every study where the average age of the participants was indicated for the studies that reported this number. Study [85] did not report any mean, minimum and/or maximum age.

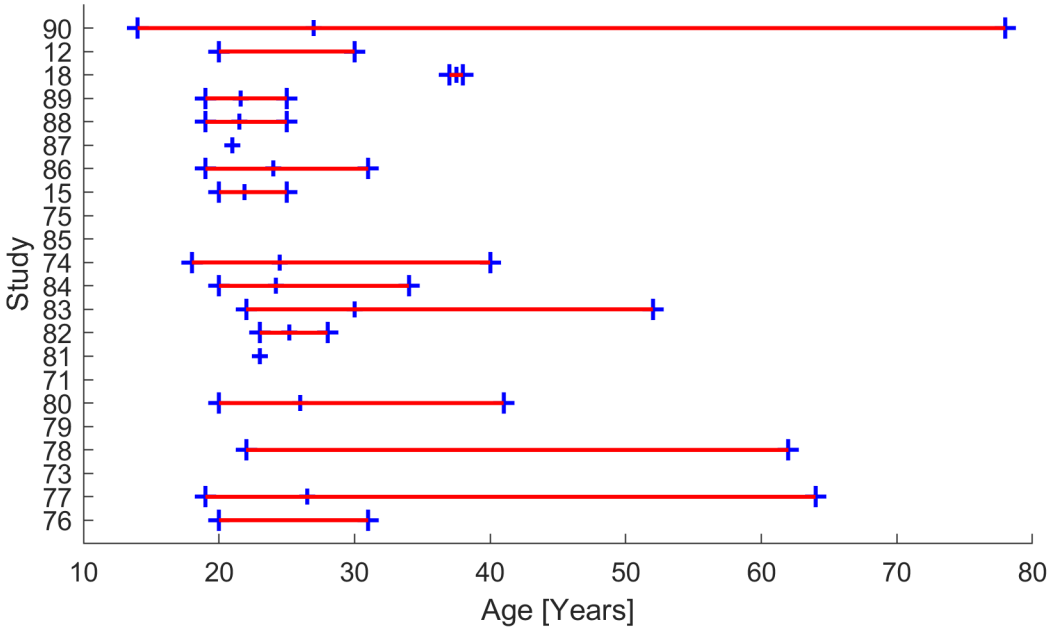

Figure 2: Minimum, mean and maximum age, if reported, plotted for each study.

.1.2.3 Method characteristics

Second, the method characteristics were examined for the different types of methods that were used. Within this section, also, reoccurring tasks were reported such as the Farnsworth-Munsell 100 Hue (FM100) test were reported.

Table 6: Frequency table of different methods that were used for each study.

Method used	Study	Frequency
Constant Stimuli	[79] [71] [82] [83] [18] [12]	6
Limits	-	0
Adjustment	[78] [89] [90]	3
Survey	[76] [77] [73] [80] [81] [84] [85] [86] [87] [88] [89]	11
Paired comparison	[80] [74] [85] [75] [15] [86]	6

Table 6, shows the methods and/or tasks that were used in each study. Most of the studies implemented a survey to collect data. Studies [80] and [71] combined the survey with another method. None of the studies reported having performed the method of limits. Furthermore, only 3 studies reported having used the method of adjustment. For

the paired comparison task characteristic three similar hue differentiation tasks were found, the FM100-Hue task appeared to be used in studies [80], [74], [75] and [15], the task was used in study [86] and the L'Anthony task in study [85]. Additionally, to the constant stimuli method, studies [79], [71], [18] and [12] used an alternative forced choice task combined with a staircase procedure.

.1.2.4 Display characteristics

Third, the display characteristics were examined for the stimulus to be from a light emitting display or illuminated on a surface.

Table 7: Frequency table of the two display types that were used in studies, either light emitting or an illuminated surfaces.

Display Type	Study	Frequency
Light emitting	[79] [71] [12]	3
Illuminated surfaces	[76] [77] [73] [78] [80] [81] [82] [83] [84] [74] [85] [75] [15] [86] [87] [88] [89] [18] [90]	19

Table 7, shows the amount of studies that used a light emitting display or an illuminated surface for the stimulus presentation. Nineteen studies used an illuminated surface and three studies used a light emitting display. Two of these three studies that used the light emitting display were directly presenting the stimuli via a specified computer display, whereas study [12] used a mirror to present the light emitting computer display indirectly.

.1.2.5 Stimulus characteristics

Fourth, the stimulus characteristics were examined for the object type, the luminance and the chromaticitys that were used and, if reported, the color rendering indices of the light sources. The stimulus characteristics, luminance, chromaticity and color rendering were determined for the light source that was used to emit the light spectra used in the study.

.1.2.5.1 Uniform and complex objects Most studies used uniform objects as their stimulus, whereas some studies investigated more complex objects, see Table 8. The complex objects could be further classified under different categories. Most of these studies investigating complex objects used either objects from a restaurant, retail, supermarket or museum setting. In the restaurant setting mostly plates with food or other restaurant objects were chosen. In the retail setting different kinds of clothing were chosen such as shoes and dresses. In the supermarket setting different kinds of fruits, vegetables and

drinks such as coca cola cans were chosen. In the museum setting mostly different kinds of paintings were observed under different light settings. The uniform patches consisted of different Munsell patches such as in the FM100 Hue test or different kinds of color checkers such as the Macbeth color checker.

Table 8: Frequency table of the two different types of objects that were used as a stimulus in the studies.

Object type	**Study**	**Frequency**
Light emitting	[76] [77] [73] [80] [82] [84] [85] [88] [89] [90]	10
Illuminated surfaces	[76] [73] [78] [79] [71] [81] [83] [74] [85] [75] [15] [86] [87] [18] [12]	15

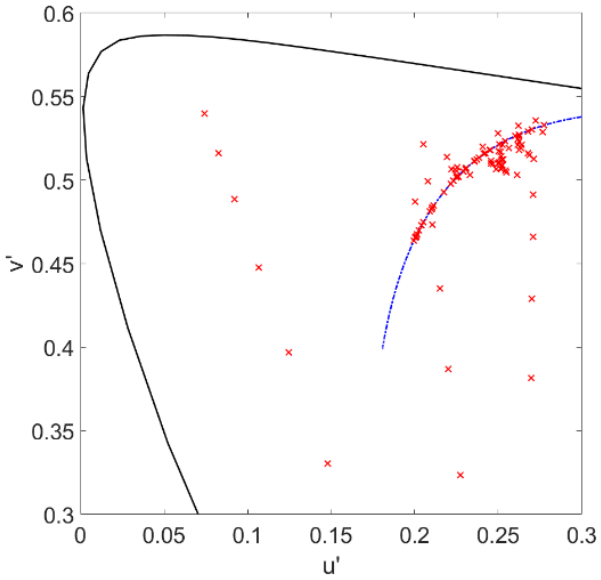

Figure 3: Distribution of the chromaticity coordinates in the CIE 1976 UCS diagram reported in the studies that were examined.

.1.2.5.2 Luminance and Chromaticity Most of the chromaticities that were reported were of the lighting itself or the uniform surfaces. In Figure 3 all the chromaticity points are plotted in the CIE 1976 UCS diagram, which is considered to be the most uniform in visual discrimination, for their u and v chromaticity coordinates. Furthermore, in Figure 3, also the black body curve is indicated, which represents most of the whitish

colors. Remarkable, but not so much surprising, is that most of the lights were scattered around this black body curve. Most lights that were investigated were chosen to represent normal office, home or street lighting and thus chosen to be close to or on the black body curve. Furthermore, only the studies [74] [85] [75] [89] [18] [12] varied the (il)luminance values, whereas the other studies had constant illuminance values for above 250 lux at the stimulus plane.

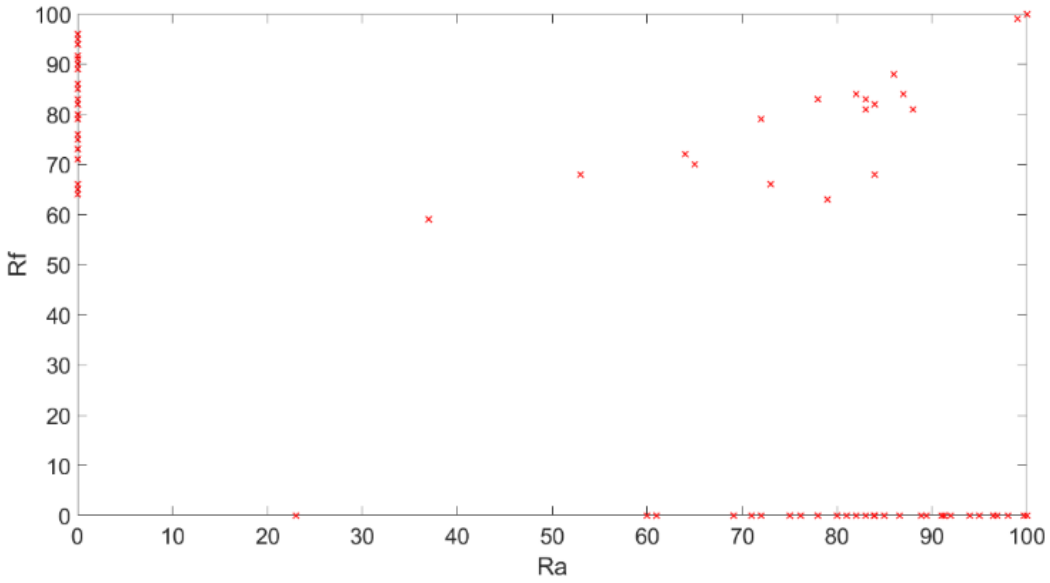

Figure 4: Distribution of the color rendering (Ra and Rf) values of the lights that were reported in the studies.

.1.2.5.3 Color rendering The color rendering was overall less reported in the studies and when they were reported mostly either the Rf or the Ra values were given. Figure 4 shows the distribution of the color rendering indices of the lights that were used in the studies, any missing values of either an Rf value or Ra value an 0 value was chosen. Most of the studies used Rf and Ra values in between 60 and 100.

.1.2.6 Viewing condition

Fifth, the viewing condition of the stimulus was examined for the (pre-)adaptation to a stimulus before the experiment, the field size of the stimulus and the direct surrounding of the stimulus.

.1.2.6.1 Adaptation

Table 9: Frequency table of the different (pre-)adaptations that were reported in the studies.

(pre-)Adaptation	Study	Frequency
Dark	[78] [82]	2
Light	[80] [71] [83] [84] [74] [15] [86] [88] [89] [18] [90]	11
Chromatic	[71] [12]	2
Not reported	[76] [77] [73] [81] [75] [87]	6

Table 9, shows the different types of adaptation that were employed in the studies to control for the light conditions that the participants were previous to the experiment exposed to. Studies [15] and [88] indicated to also have used so-called washout periods between stimulus presentations, to prevent any influence of previous stimulus exposure. Washout periods were mainly used to bleach the cones and prevent any afterimage or previous adaptation onto the chromatic discrimination under the next light source. The (pre-)adaptation periods varied a lot between the studies, most used a 2- or 3-minute exposure to a chosen reference light source, whereas some studies had a shorter 30 seconds or 1 minute exposure and others had a longer exposure of 5 or 10 minutes.

.1.2.6.2 Field size

Table 10: Frequency table of the different field sizes that were reported in the studies.

Field Size	Study	Frequency
2 degree	[71] [18] [12]	3
3 degree	[79]	1
Light box	[76] [73] [78] [80] [81] [82] [83] [85] [75] [86] [88] [90]	12
Room	[77] [84] [74] [15] [87] [89]	6

Table 10, shows the different kinds of field sizes that were used to control for the foveal and parafoveal vision of the participants in seeing the stimulus. Most studies did a standard light box to present the stimulus in, however, some controlled the stimulus region for a 2- or 3-degree field of vision. Some studies did not use a light box or small patch to show the stimulus but used a whole room where they presented the stimulus in. The light boxes varied from 60x60x30 cm to roughly 150x80x80 cm. The rooms varied between 120x225x250 cm to 305x366x274 cm.

.1.2.6.3 Surrounding

Table 11: Frequency table of the different surroundings that were reported in the studies.

Environment	Study	Frequency
Dark	[78] [80] [83] [74] [15] [86] [87] [88] [89] [12] [90]	11
Light	[77] [79] [18]	3
Chromatic	[71]	1
Not reported	[76] [73] [81] [82] [84] [85] [75]	7

Table 11, shows the different direct surroundings to which the stimulus was presented. Most studies used a dark room, where for the direct surrounding of the stimulus no other room light or ambient light beside the chosen lighting was presented. A few studies had the stimulus surrounded by a white or neutral environment and some other studies did not specified the direct surrounding of the stimulus. Furthermore, the reflectance of the illuminated surface was in most studies a neutral painted background.

.1.2.7 Overall conclusions

Finally, the overall conclusion section of the studies was examined. Interestingly, most of the studies that investigated color rendering used a survey to determine preference lighting and to discriminate between different color rendering indexes such as the Ra and Rf. Most of the studies investigating chromatic discrimination used the FM100 hue task or the method of constant stimuli to determine thresholds and error in chip placement. The scoring formula for determining the error rate was determined by Farnsworth in creating the FM100 hue task. This error rate, however, was determined for illuminant C and all the studies using the FM100 hue task in this literature study used different illuminants. The studies using the FM100 hue task and reporting this error rate, however, did not correct for the different chromaticities and (il)luminance's of the illuminants. Some of the error rates reported, therefore, could be (partially) explained by these differences between illuminants. The studies [77] [80] [84] [74] [85] [88] [89] indicate that there are different preferences for different lighting spectra and color rendering indexes. Generally lighting with spectra that increased Chroma compared to the reference light source are more preferred [80]. Furthermore, studies [79] [80] [71] [74] [85] [75] [15] [86] [18] [12] reported that there are differences in chromatic discrimination for different (ill)luminance levels and/or for different chromaticities. The studies [76] [80] [90] indicate the importance for a general color fidelity metric, which has a well representative reference illuminant, uses the most perceptual uniform color space with the most accurate chromatic adaptation transform and is created with reflectance spectra of well representative color samples. Additionally, studies [76] [77] [80] [75] [15] [88] [90] indicate the importance of an alternative metric, called the color gamut. These studies report that a single color fidelity metric is not enough to accurately determine the color rendering of a light source and that also the color gamut should be included. Furthermore, studies [74] and [75] indicate that the color fidelity index defined by the CIE, is not sufficient in describing color discrimination.

.1.2.8 Discussion

In this literature review not all Journals that investigate lighting were included because of the lack of availability of the papers. Furthermore, the search terms were very broad and might have been the cause of missing some important papers that could have been found with different search terms. Also, the inclusion of only studies that performed psychophysical experiments reduced the amount of unique eligible articles. Many studies investigated color rendering by means of Monte Carlo simulations or by modelling combinations of different spectral power distribution and reflectance patches, which eventually were not included because they were technically no psychophysical experiments. The resulting amount of literature that was analyzed varied conceptually between a definite focus on color rendering versus papers discussing mainly color discrimination. The color discrimination described in the papers variated between threshold based studies and color difference studies. The threshold based studies mainly were in controlled environments where the spectrum was often not reported and only small patches were presented. The color difference studies, however, mostly took into account spectra differences and often accounted for different color renderings. In these studies sometimes either only the Ra or Rf color fidelity values were reported for the used lighting. Most of these studies also reported the spectral power distributions, however, due to a lack of the actual numerical values of these spectras, they were not recreated. Recreation of all the spectra for each study seemed not feasible for the time and resources available for this literature study.

.1.3 Conclusion

The aim of this literature review was to look at how the complex environment is being controlled in color rendering and color discrimination studies. Most studies did control for similar variables such as the stimulus characteristics and display characteristics. However, the viewing condition and the color rendering were often not reported or hardly controlled in the experiment. To answer the first literature question of the literature study What complex viewing conditions were determined and how were they represented in previous studies about the discrimination of color objects?. In previous studies about the discrimination of color objects that were investigated in this literature review, notable is that the viewing conditions that were mentioned and controlled varied a lot between the studies. Most studies did account for some form of adaptation and the field size was often limited but not fully controlled. Furthermore, the surrounding was in most studies carefully painted gray to represent the average of most reflectances a person would be exposed to in a regular indoor environment. The direct surrounding however was often not controlled or changed in comparison to the stimulus presented. So in most cases the box was chromatically somewhat homogenously lit with just a few irregularities of the position of the stimulus within the light box. The homogeneity of the illuminated surfaces of the light box did depend on how the luminaire was placed, which was in most cases in the top of the light box. Furthermore, some studies indicated to have used different tasks using different stimuli, however, the tests encountered, FM100-hue test, Krkc test and the LAnthony test

were very similar to each other. In every test the stimulus was assumed to stimulate all three cone types based on the L- and M- cone excitation (red-green axis) and the S-cone excitation (tritan axis). Also the stimuli used in these tests were of a matte surface. To answer the second literature question of this literature study How is color fidelity measured and what is needed to obtain an accurate color rendering index?. The studies investigated in this literature study that mention color fidelity and color rendering were very indifferent about choosing a single color fidelity metric for an overall color rendering index. Some studies indicate the importance of a second metric called the color gamut and most studies either reported the Ra or Rf values for the color fidelity and Rg or gamut area index (GAI) values for the color gamut. To indicate the color fidelity and color gamut mostly the studies used a subsample of standardized color samples, so for the Ra 8 color samples are determined by the CIE and for the Rf 99 color samples are determined by the IES TM-30. Both the color fidelity metrics indicate the need for a well representative reference illuminant, the need to use the most perceptually uniform color space that uses the most accurate chromatic adaptation transform and that a well representative color sample set is used to determine the differences of a current light source with a reference light source. Most of the studies that investigated color preference for a specific color rendering used rather a mix of complex objects and uniform targets. The uniform targets were mostly Macbeth Color Checkers. The complex objects could be categorized under restaurant, retail, supermarket or museum settings. Also, the color fidelity metrics did not seem to be good predictors for chromatic discrimination under different light spectra. A general color fidelity metric and color gamut metric is necessary to indicate how good a light source will render colors compared to a reference light source. In addition to the color fidelity and color gamut, future research should also investigate differences in chromatic discrimination for different spectra for different light levels to better understand how the light source influences the ability to discriminate colors.

.2 Instructions Form

Signify Classified - Internal

First the Ishihara's color deficiency test is performed in the left light box if you do not want to know whether you are color deficient please inform the researcher beforehand.

Second, you are asked to perform the FM100 Hue test.

This task is as follows.

You will be presented with four trays containing color caps see the figure below.

Each tray will be presented to you individually under different illuminations, where we will first start in the left light box and afterwards, we will move over to the right light box.

Each tray will be emptied, and the color caps of that tray are first shuffled and then placed in front of you like in the figure below. While the researcher is placing a new tray inside the light box you are asked to look away to prevent you from having any biased response.

Then when the color caps are shuffled, you are asked to first make a rough ordering just in front of the tray like in the below left figure. When you are satisfied with the color ordering you can place the color caps back on the tray like in the below right figure. Now you can look at the result and you can make some last adjustments on the tray if necessary.

When satisfied with the result you can notify the experimenter that you are ready for the next tray. After you have performed four trays in a cycle, there will be a 5-minute adaptation to a next light setting. The task will continue until each of the four trays are ordered at every of the five light settings.

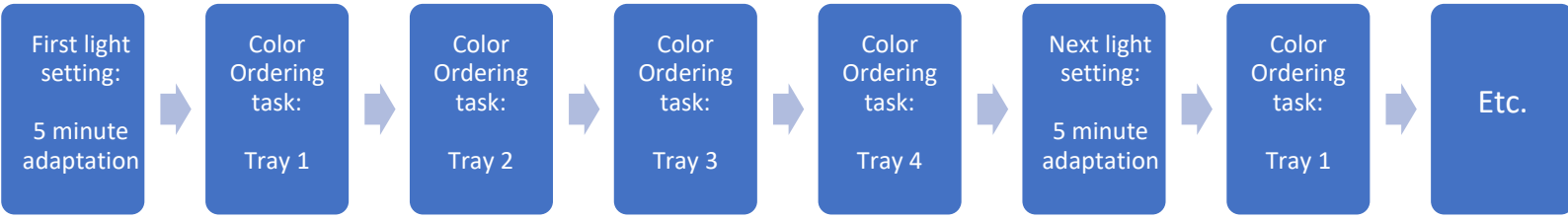

<u>Some general remarks when doing the experiment:</u>

Do not look on the back of the color caps, in case of the back of a color cap being shown try to notify the experimenter of this.

When doing the ordering of the color caps do not touch the top part of the color caps. The consistency of the test depends on the painted surfaces of the color caps not to be filthy/touched.

Thanks for participating in this experiment!

.3 Informed Consent Form TU/e

TU/e Technische Universiteit Eindhoven University of Technology

Informed consent form

This document gives you information about the study of the effect of (il)luminance and color rendering on color perception. Before the study begins, it is important that you learn about the procedure followed in this study and that you give your informed consent for voluntary participation. Please read this document carefully.

Aim and benefit of the study

The aim of this study is to measure color differences for different light levels. This information is used to improve the quality of lighting systems.

This study is done by Rik Spieringhs, a student under the supervision of Raymond Cuijpers of the Human-Technology Interaction group.

Procedure

During this study, the participant's task is to perform the FM-100 Hue task for different light levels. The different light levels are presented sequentially in the light box. Your response (the order of the color caps in the FM-100 Hue test) is recorded.
Between trials an adaptation period of two to five minutes will follow.
The actual experiments will be carried out in a laboratory at the HTC7 building of Signify Research (Eindhoven).

Risks

The study does not involve any risks or detrimental side effects.

Duration

The study will last approximately 60 minutes.

Voluntary

Your participation is completely voluntary. You can refuse to participate without giving any reasons and you can stop your participation at any time during the study. You can also withdraw your permission to use your experimental data up to 24 hours after the study is finished. All this will have no negative consequences whatsoever.

Participant's Initials ____

Confidentiality

All research conducted at the Human-Technology Interaction Group adheres to the Code of Ethics of the NIP (Nederlands Instituut voor Psychologen – Dutch Institute for Psychologists).
We will not be sharing personal information about you to anyone outside of the research team. No video or audio recordings are made that could identify you. The information that we collect from this study is used for writing scientific publications and will be reported at group level. It will be completely anonymous and it cannot be traced back to you. Only the researchers will know your identity and we will lock that information up with a lock and key.

Further information

If you want more information about this study you can ask Rik Spieringhs (contact email: r.m.spieringhs@student.tue.nl). If you have any complaints about this study, please contact the supervisor, Raymond Cuijpers (contact email: r.h.cuijpers@tue.nl) or Marcel Lucassen (contact email: marcel.lucassen@signify.com).

Certificate of Consent

I, (NAME)…….. have read and understood this consent form and have been given the opportunity to ask questions. I agree to voluntary participate in this research study carried by the research group Human Technology Interaction of the Eindhoven University of Technology.

_____ _____

Participant's Signature Date

Participant's Initials _____

.4 Informed Consent Form and Privacy Notice Signify

Signify Classified - Internal

INFORMED CONSENT

INFORMED CONSENT

During this study, your task is to perform a color discrimination task for different light levels. The different light levels are presented sequentially in the light box. Your response on this color discrimination task is recorded and will be analysed afterwards.

- √ I have understood the information about this research study and all my questions have been answered by the responsible researcher.
- √ I had sufficient time to consider my participation in this project and I am fully aware that my participation in this project is voluntarily.
- √ I know that I can decide not to participate or stop my participation at any time without giving a reason for this decision.
- √ I understand and agree that my personal data will be processed in accordance with the Privacy Notice for Research Participants (as included in Annex 1 below).
- √ I understand that any and all information related to the study, including, but not limited to, information brochures, study descriptions, prototypes, user manuals, instructions as well as information generated by myself during the study, e.g. measurement results, user feedback constitutes confidential information of Signify. I hereby agree to keep this information confidential, use it exclusively for the purpose of my participation in the study and not to disclose such information to any third party.
- √ All confidential information revealed or submitted by Signify will remain property of Signify.
- √ I agree to participate as a volunteer in this research study.

 CONFIDENTIAL

You may decline without providing any reasons, you may also retract permission during the test, or afterwards. Modification or withdrawal of your consent can be done directly to the researcher during the study, or (afterwards) via an email to the researcher or by filling in a request on https://www.signify.com/global/privacy, citing the name of the study and the date of your participation.

SIGNATURES

I declare to have read the consent form to agree with its content and to participate in the study.

Name study participant	Signature	Date

Responsible researcher

I have answered all questions about the research study and discussed the meaning and scope of this informed consent and signed it in the presence of the study participant.

Name researcher	Signature	Date

ANNEX 1
SIGNIFY
Privacy Notice for Research Participants

Last Updated: January 2019

INTRODUCTION
Your privacy is important to Signify.

We have drafted this Privacy Notice (also referred to as "Notice") in an easy and comprehensible way in order to help you understand who we are, what personal data we collect about you, why we collect it, and what we do with it. Keep in mind that personal data (in this Notice also referred to as "data" or "your data") means any information or set of information from which we are able, directly or indirectly, to personally identify you, in particular by reference to an identifier, e.g. name and surname, email address, phone number, etc.
Please keep in mind that since Signify is an international company, this Notice may be replaced or supplemented in order to fulfill local requirements, as well as in order to provide you with additional information on how we process your data through specific Signify products, services, systems or applications.
We strongly encourage you to take some time to read this Notice in full. If you do not agree to this privacy notice, please do not provide us with your data.

WHEN DOES THIS PRIVACY NOTICE APPLY?
This Notice covers how we collect and use your data when you participate in our research studies (e.g. interviews, surveys, experiments, etc.) or otherwise interact with us in your capacity as research participants.

WHO IS SIGNIFY?
As Signify , we are a global organization leader in the general lighting market with a unique competitive position and recognized expertise in the development, manufacturing and application of innovative lighting products, systems and services.
When this Notice mentions "we," "us," or the "Company," it refers to the controller of your data under this Notice, namely the Signify affiliate which is performing the research study, as well as Signify Netherlands B.V. (Registration number 17061150 - High Tech Campus 48, 5656 AE, Eindhoven, The Netherlands). Please note that the Signify affiliates include the subsidiary companies in which Signify N.V. has control, either through direct or indirect ownership.

WHAT TYPES OF DATA WE COLLECT ABOUT YOU?
Depending on the type of research study you participate in, we may process different data about you. Below you will find an overview of the categories of data that we may collect:

Information you provide to us directly

Categories of data	***Examples of types of data***
Personal identification data	Name, surname, date of birth, gender
Contact information data	Email, phone number, address, country
Any other information that you decide to voluntarily share	Feedback, opinions, reviews, comments, uploaded files, other information provided for our research study

Lastly, if you visit our premises, for security reasons we might also record your data through video or other electronic, digital or wireless surveillance system or device (e.g. CCTV).

Note that your directly identifiable data obtained during the research study will be separated from the research data and will be replaced by an assigned number/code. Access to the key/link between the

assigned number/code and your directly identifiable data will be limited to the responsible researcher and might only be disclosed to regulatory authorities or ethical committees, if required.

Information we collect automatically

When you participate in research studies performed with the support of devices, we may collect information sent to us by your computer, mobile phone or other access device. For example, we may collect:

Categories of data	***Examples of types of data***
Device information	Hardware model, IMEI number and other unique device identifiers, MAC address, IP address, operating system version, and settings of the device you use to access the services
Log information	Time and duration of your use of our digital channel or product
Location information	Your actual location (derived from your IP address or other location-based technologies), that may be collected when you enable location-based products or features such as through our apps
Other information about your use of our digital channels or products	Apps you use or websites you visit, links you click within our advertising e-mail, motion sensors data

We will not use the above information in our research analysis.

HOW DO WE USE YOUR DATA?
We may use your data for different legitimate reasons and business purposes.
Below you will find an overview of the purposes for which we may process your data:

Purposes	***Examples***
Research purposes	Testing to improve our prototypes, products, services, systems and applications
Providing support (upon your request)	Providing support via communication channels, such as customer or contact center support.
Security and protection of our interests/assets	Deploying and maintaining technical and organizational security measures, conducting internal audits and investigations, conducting assessments to verify conflict of interests
Compliance with legal obligations	Disclosing data to government institutions or supervisory authorities as applicable in all countries in which we operate, such as tax and national insurance deductions, record-keeping and reporting obligations, conducting compliance audits, compliance with government inspections and other requests from government or other public authorities, responding to legal process such as subpoenas, pursuing legal rights and remedies, and managing any internal complaints or claims
Defense of legal claims	Establishment, exercise or defense of legal claims to which we are or may be subject
Product development	To improve the services, products and communications we provide.

You are not obliged to provide us with your data. In case you chose not to provide us with your data, we will not process your data in the context of the relevant research study.

ON WHAT LEGAL BASIS DO WE USE YOUR DATA?

In order to be able to process your data, we may rely on different legal bases, including:

- Your consent (only when legally required or permitted). If we rely on your consent as a legal basis for processing your data, you may withdraw your consent at any time;
- The necessity for us to comply with legal obligations and to establish, exercise, or defend our self from legal claims;
- The necessity to pursue our legitimate interests (e.g. to ensure that our networks and information are secure);
- The necessity to respond to your requests;
- The necessity to protect the vital interests of any person;
- Any other legal basis anyhow permitted by local laws.

WHEN DO WE SHARE YOUR DATA?

We do not share any of your data except in the limited cases described here.
If it is necessary for the fulfillment of the purposes described in this Notice, we may disclose your data to the following entities:

- *Service providers*: like many businesses, we may outsource certain data processing activities to trusted third party service providers to perform functions and provide services to us, such as ICT service providers.
- *Public and governmental authorities*: when required by law, or as necessary to protect our rights, we may share your data with entities that regulate or have jurisdiction over Signify .
- *Other parties in connection with corporate transactions*: we may also, from time to time, share your data in the course of corporate transactions, such as during a sale of a business or a part of a business to another company, or any reorganization, merger, joint venture, or other disposition of our business, assets, or stock (including in connection with any bankruptcy or similar proceeding).

WHEN DO WE TRANSFER YOUR DATA ABROAD?

Due to our global nature, data you provide to us may be transferred to or accessed by Signify affiliates and trusted third parties from many countries around the world. As a result, your data may be processed outside the country where you live, if this is necessary for the fulfillment of the purposes described in this Notice.
If you are located in a country member of the European Economic Area, we may transfer your data to countries located outside of the European Economic Area. Some of these countries are recognized by the European Commission as providing an adequate level of protection. With regard to transfers from the European Economic Area to other countries that are not are recognized by the European Commission as providing an adequate level of protection, we have put in place adequate measures to protect your data, such as organizational and legal measures (e.g. binding corporate rules and approved European Commission standard contractual clauses). You may obtain a copy of these measures by contacting the Signify Privacy Office (you will find the contact details in the below section “what are your choices?”).

HOW LONG DO WE KEEP YOUR DATA?

We keep your data for the period necessary to fulfill the purposes for which it has been collected (for details on these purposes, see above section “How do we use your data?”). Please keep in mind that in certain cases a longer retention period may be required or permitted by law. The criteria used to determine our retention periods include:

- How long is the data needed for our research study?
- Are we subject to a legal, contractual, or similar obligation to retain your data? Examples can include mandatory data retention laws in the applicable jurisdiction, government orders to

.5 Output of STATA

```
. import excel "D:\Signify\DATA\FMerrorData_2.xlsx", sheet("Sheet1") firstrow

. set matsize 800

.
. gen FM2 = log(FM)

.
. anova FM2 AgeGroup/P|AgeGroup Light Light#AgeGroup/Light#P|AgeGroup Tray Tray#AgeGroup/Tray#P
> d(Tray Light)
```

Number of obs =	**480**	R-squared	=	**0.9538**	
Root MSE =	**.124183**	Adj R-squared	=	**0.9161**	

Source	Partial SS	df	MS	F	Prob>F
Model	**84.001765**	**215**	**.39070588**	**25.34**	**0.0000**
AgeGroup	**1.6336371**	**1**	**1.6336371**	**6.66**	**0.0171**
P|AgeGroup	**5.3982511**	**22**	**.24537505**		
Light	**61.524243**	**4**	**15.381061**	**272.02**	**0.0000**
Light#AgeGroup	**1.8984223**	**4**	**.47460558**	**8.39**	**0.0000**
Light#P|AgeGroup	**4.9758231**	**88**	**.05654344**		
Tray	**3.8006739**	**3**	**1.2668913**	**54.71**	**0.0000**
Tray#AgeGroup	**.08958062**	**3**	**.02986021**	**1.29**	**0.2854**
Tray#P|AgeGroup	**1.5284478**	**66**	**.0231583**		
Light#Tray	**2.9225759**	**12**	**.24354799**	**15.79**	**0.0000**
Light#Tray#AgeGroup	**.23010993**	**12**	**.01917583**	**1.24**	**0.2533**
Residual	**4.0712467**	**264**	**.01542139**		
Total	**88.073012**	**479**	**.1838685**		

```
Between-subjects error term:  P|AgeGroup
                     Levels:  24        (22 df)
     Lowest b.s.e. variable:  P
     Covariance pooled over:  AgeGroup  (for repeated variables)

Repeated variable: Tray
                                         Huynh-Feldt epsilon        =  0.9308
                                         Greenhouse-Geisser epsilon =  0.7892
                                         Box's conservative epsilon =  0.3333
```

			Prob > F			
Source	df	F	Regular	H-F	G-G	Box
Tray	**3**	**54.71**	**0.0000**	**0.0000**	**0.0000**	**0.0000**
Tray#AgeGroup	**3**	**1.29**	**0.2854**	**0.2860**	**0.2865**	**0.2684**
Tray#P|AgeGroup	**66**					

```
Repeated variable: Light
                                         Huynh-Feldt epsilon        =  0.4647
                                         Greenhouse-Geisser epsilon =  0.4147
                                         Box's conservative epsilon =  0.2500
```

			Prob > F			
Source	df	F	Regular	H-F	G-G	Box
Light	**4**	**272.02**	**0.0000**	**0.0000**	**0.0000**	**0.0000**
Light#AgeGroup	**4**	**8.39**	**0.0000**	**0.0011**	**0.0018**	**0.0084**
Light#P|AgeGroup	**88**					

Repeated variables: Light#Tray

Huynh-Feldt epsilon = **0.8778**
Greenhouse-Geisser epsilon = **0.5641**
Box's conservative epsilon = **0.0833**

Source	df	F	Prob > F Regular	H-F	G-G	Box
Light#Tray	**12**	**15.79**	**0.0000**	**0.0000**	**0.0000**	**0.0006**
Light#Tray#AgeGroup	**12**	**1.24**	**0.2533**	**0.2615**	**0.2838**	**0.2768**
Residual	**264**					

```
.
. estat esize
```

Effect sizes for linear models

Source	Eta-Squared	df	[95% Conf.	Interval]
Model	**.9537742**	**215**	**.8996545**	**.9286451**
AgeGroup P|AgeGroup	**.2323184**	**1**	**.0065421**	**.4746104**
Light	**.9251757**	**4**	**.8916966**	**.9400117**
Light#AgeGroup Light#P|AgeGroup	**.2761645**	**4**	**.1041294**	**.3893018**
Tray	**.7131895**	**3**	**.5764165**	**.7778026**
Tray#AgeGroup Tray#P|AgeGroup	**.0553641**	**3**	**.**	**.1539732**
Light#Tray	**.4178796**	**12**	**.3046067**	**.4700432**
Light#Tray#AgeGroup	**.0534971**	**12**	**.**	**.0690435**

```
.
. margins, within(AgeGroup)
```

Predictive margins — Number of obs = **480**

Expression : **Linear prediction, predict()**
within : **AgeGroup**
Empty cells : **reweight**

	Margin	Delta-method Std. Err.	t	P>|t|	[95% Conf.	Interval]
AgeGroup						
1	**4.069776**	**.008016**	**507.71**	**0.000**	**4.053993**	**4.08556**
2	**4.186454**	**.008016**	**522.26**	**0.000**	**4.17067**	**4.202237**

```
.
. margins, within(Light)
```

Predictive margins — Number of obs = **480**

Expression : **Linear prediction, predict()**
within : **Light**
Empty cells : **reweight**

	Margin	Delta-method Std. Err.	t	P>|t|	[95% Conf.	Interval]
Light						
1	**4.816474**	**.0126744**	**380.02**	**0.000**	**4.791518**	**4.841429**
2	**4.135159**	**.0126744**	**326.26**	**0.000**	**4.110203**	**4.160115**
3	**3.957266**	**.0126744**	**312.23**	**0.000**	**3.932311**	**3.982222**
4	**3.876386**	**.0126744**	**305.84**	**0.000**	**3.85143**	**3.901342**
5	**3.85529**	**.0126744**	**304.18**	**0.000**	**3.830334**	**3.880246**

```
.
. margins, within(Light AgeGroup)

Predictive margins                                  Number of obs     =        480

Expression   : Linear prediction, predict()
within       : Light AgeGroup
Empty cells  : reweight
```

	Margin	Delta-method Std. Err.	t	P>|t|	[95% Conf.	Interval]
Light#AgeGroup						
1 1	**4.647496**	**.0179243**	**259.29**	**0.000**	**4.612203**	**4.682789**
1 2	**4.985451**	**.0179243**	**278.14**	**0.000**	**4.950159**	**5.020744**
2 1	**4.057789**	**.0179243**	**226.39**	**0.000**	**4.022496**	**4.093081**
2 2	**4.21253**	**.0179243**	**235.02**	**0.000**	**4.177237**	**4.247822**
3 1	**3.91011**	**.0179243**	**218.15**	**0.000**	**3.874818**	**3.945403**
3 2	**4.004422**	**.0179243**	**223.41**	**0.000**	**3.96913**	**4.039715**
4 1	**3.873598**	**.0179243**	**216.11**	**0.000**	**3.838305**	**3.90889**
4 2	**3.879174**	**.0179243**	**216.42**	**0.000**	**3.843882**	**3.914467**
5 1	**3.859889**	**.0179243**	**215.34**	**0.000**	**3.824596**	**3.895182**
5 2	**3.850691**	**.0179243**	**214.83**	**0.000**	**3.815398**	**3.885984**

```
.
. margins, within(Tray)

Predictive margins                                  Number of obs     =        480

Expression   : Linear prediction, predict()
within       : Tray
Empty cells  : reweight
```

	Margin	Delta-method Std. Err.	t	P>|t|	[95% Conf.	Interval]
Tray						
1	**4.187321**	**.0113363**	**369.37**	**0.000**	**4.164999**	**4.209642**
2	**4.102754**	**.0113363**	**361.91**	**0.000**	**4.080433**	**4.125075**
3	**4.227277**	**.0113363**	**372.90**	**0.000**	**4.204956**	**4.249598**
4	**3.995109**	**.0113363**	**352.42**	**0.000**	**3.972788**	**4.01743**

```
.
. margins, within(Light Tray)

Predictive margins                                  Number of obs     =        480

Expression   : Linear prediction, predict()
within       : Light Tray
Empty cells  : reweight
```

	Margin	Delta-method Std. Err.	t	P>|t|	[95% Conf.	Interval]
Light#Tray						
1 1	4.976381	.0253487	196.32	0.000	4.926469	5.026292
1 2	4.684954	.0253487	184.82	0.000	4.635042	4.734865
1 3	5.091186	.0253487	200.85	0.000	5.041274	5.141097
1 4	4.513375	.0253487	178.05	0.000	4.463463	4.563286
2 1	4.183786	.0253487	165.05	0.000	4.133874	4.233697
2 2	4.093603	.0253487	161.49	0.000	4.043691	4.143514
2 3	4.265679	.0253487	168.28	0.000	4.215767	4.31559
2 4	3.997569	.0253487	157.70	0.000	3.947658	4.047481
3 1	4.01283	.0253487	158.31	0.000	3.962919	4.062742
3 2	3.936016	.0253487	155.27	0.000	3.886105	3.985928
3 3	4.002478	.0253487	157.90	0.000	3.952566	4.052389
3 4	3.877742	.0253487	152.98	0.000	3.82783	3.927653
4 1	3.92795	.0253487	154.96	0.000	3.878039	3.977862
4 2	3.906259	.0253487	154.10	0.000	3.856348	3.95617
4 3	3.878419	.0253487	153.00	0.000	3.828508	3.928331
4 4	3.792916	.0253487	149.63	0.000	3.743004	3.842827
5 1	3.835656	.0253487	151.32	0.000	3.785744	3.885567
5 2	3.892939	.0253487	153.58	0.000	3.843027	3.94285
5 3	3.898624	.0253487	153.80	0.000	3.848713	3.948535
5 4	3.793942	.0253487	149.67	0.000	3.74403	3.843853

```
.
. margins, within(Light AgeGroup) pwcompare(effects) mcompare(bonferroni)

Pairwise comparisons of predictive margins

Expression   : Linear prediction, predict()
within       : Light AgeGroup
Empty cells  : reweight
```

	Number of Comparisons
Light#AgeGroup	45

	Contrast	Delta-method Std. Err.	Bonferroni t	Bonferroni P>|t|	Bonferroni [95% Conf.	Bonferroni Interval]
Light#AgeGroup						
(1 2) vs (1 1)	.3379555	.0253487	13.33	0.000	.2543794	.4215315
(2 1) vs (1 1)	-.5897074	.0253487	-23.26	0.000	-.6732834	-.5061314
(2 2) vs (1 1)	-.4349664	.0253487	-17.16	0.000	-.5185424	-.3513904
(3 1) vs (1 1)	-.7373857	.0253487	-29.09	0.000	-.8209617	-.6538096
(3 2) vs (1 1)	-.6430735	.0253487	-25.37	0.000	-.7266495	-.5594975
(4 1) vs (1 1)	-.7738984	.0253487	-30.53	0.000	-.8574744	-.6903224
(4 2) vs (1 1)	-.7683216	.0253487	-30.31	0.000	-.8518976	-.6847456
(5 1) vs (1 1)	-.7876071	.0253487	-31.07	0.000	-.8711831	-.704031
(5 2) vs (1 1)	-.7968049	.0253487	-31.43	0.000	-.8803809	-.7132288
(2 1) vs (1 2)	-.9276629	.0253487	-36.60	0.000	-1.011239	-.8440869
(2 2) vs (1 2)	-.7729219	.0253487	-30.49	0.000	-.8564979	-.6893459
(3 1) vs (1 2)	-1.075341	.0253487	-42.42	0.000	-1.158917	-.9917651
(3 2) vs (1 2)	-.981029	.0253487	-38.70	0.000	-1.064605	-.897453
(4 1) vs (1 2)	-1.111854	.0253487	-43.86	0.000	-1.19543	-1.028278
(4 2) vs (1 2)	-1.106277	.0253487	-43.64	0.000	-1.189853	-1.022701
(5 1) vs (1 2)	-1.125563	.0253487	-44.40	0.000	-1.209139	-1.041986
(5 2) vs (1 2)	-1.13476	.0253487	-44.77	0.000	-1.218336	-1.051184
(2 2) vs (2 1)	.154741	.0253487	6.10	0.000	.071165	.238317
(3 1) vs (2 1)	-.1476782	.0253487	-5.83	0.000	-.2312542	-.0641022
(3 2) vs (2 1)	-.0533661	.0253487	-2.11	1.000	-.1369421	.0302099
(4 1) vs (2 1)	-.184191	.0253487	-7.27	0.000	-.267767	-.100615
(4 2) vs (2 1)	-.1786142	.0253487	-7.05	0.000	-.2621902	-.0950382
(5 1) vs (2 1)	-.1978996	.0253487	-7.81	0.000	-.2814756	-.1143236
(5 2) vs (2 1)	-.2070974	.0253487	-8.17	0.000	-.2906735	-.1235214

(3 1) vs (2 2)	-.3024192	.0253487	-11.93	0.000	-.3859952	-.2188432
(3 2) vs (2 2)	-.2081071	.0253487	-8.21	0.000	-.2916831	-.1245311
(4 1) vs (2 2)	-.338932	.0253487	-13.37	0.000	-.422508	-.255356
(4 2) vs (2 2)	-.3333552	.0253487	-13.15	0.000	-.4169312	-.2497792
(5 1) vs (2 2)	-.3526406	.0253487	-13.91	0.000	-.4362167	-.2690646
(5 2) vs (2 2)	-.3618384	.0253487	-14.27	0.000	-.4454145	-.2782624
(3 2) vs (3 1)	.0943121	.0253487	3.72	0.011	.0107361	.1778881
(4 1) vs (3 1)	-.0365127	.0253487	-1.44	1.000	-.1200887	.0470633
(4 2) vs (3 1)	-.0309359	.0253487	-1.22	1.000	-.114512	.0526401
(5 1) vs (3 1)	-.0502214	.0253487	-1.98	1.000	-.1337974	.0333546
(5 2) vs (3 1)	-.0594192	.0253487	-2.34	0.892	-.1429952	.0241568
(4 1) vs (3 2)	-.1308249	.0253487	-5.16	0.000	-.2144009	-.0472489
(4 2) vs (3 2)	-.1252481	.0253487	-4.94	0.000	-.2088241	-.0416721
(5 1) vs (3 2)	-.1445335	.0253487	-5.70	0.000	-.2281095	-.0609575
(5 2) vs (3 2)	-.1537313	.0253487	-6.06	0.000	-.2373074	-.0701553
(4 2) vs (4 1)	.0055768	.0253487	0.22	1.000	-.0779992	.0891528
(5 1) vs (4 1)	-.0137087	.0253487	-0.54	1.000	-.0972847	.0698673
(5 2) vs (4 1)	-.0229065	.0253487	-0.90	1.000	-.1064825	.0606695
(5 1) vs (4 2)	-.0192855	.0253487	-0.76	1.000	-.1028615	.0642906
(5 2) vs (4 2)	-.0284833	.0253487	-1.12	1.000	-.1120593	.0550928
(5 2) vs (5 1)	-.0091978	.0253487	-0.36	1.000	-.0927738	.0743782

.

.6 GLA Calculation tool output of CRI-based colour renditions for standard illuminant C

Signify Classified - Internal

Output of GLA Calculation Tool for CIE 13.3 CRI and Associated CRI-based Colour Rendition Properties

Test Source:	Illuminant C	
Notes:	Tables 5 & 9.1 - Relative spectral power distribution of CIE illuminant C in CIE publication 015-2018 "Colorimetry"	
Date / Time:	**Wednesday, 26 June 2019**	**10:21:57**

Correlated Colour Temperature (T_{cp}) in K	6774	CIE1931 chromaticity coordinate, x	0.3101
Distance to Blackbody Locus (D_{uv})	-0.0022	CIE1931 chromaticity coordinate, y	0.3162
General Colour Rendering Index (R_a)	**97**	CIE1976 chromaticity coordinate, u'	0.2009
Colour Gamut Index (G_a)	**103**	CIE1976 chromaticity coordinate, v'	0.4609

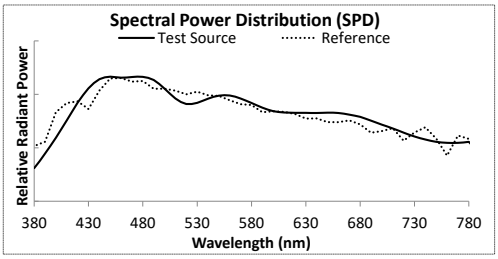

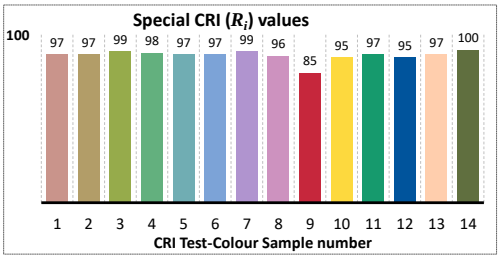

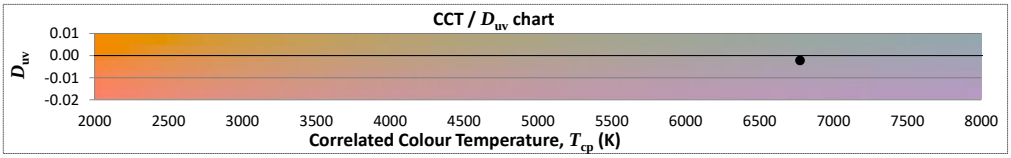

Two-dimensional R_a-G_a Graphic

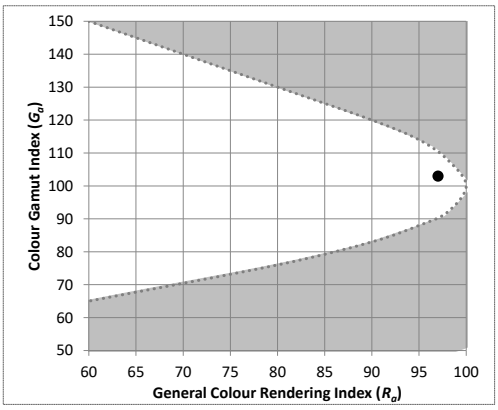

Colour-shift graphic

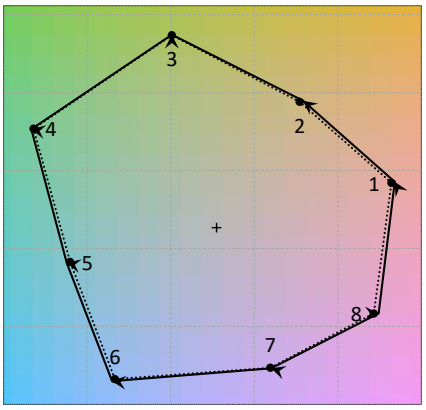

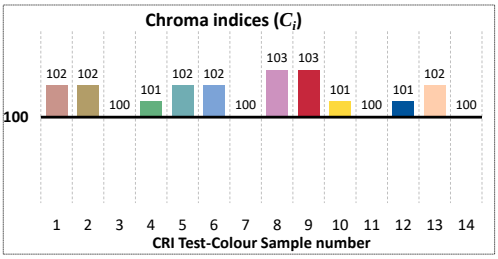

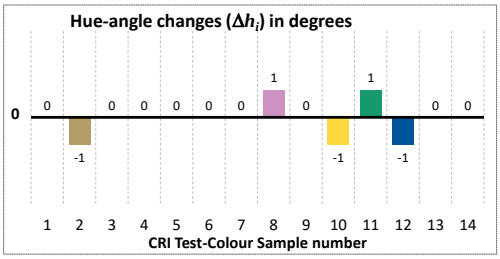

.7 GLA Calculation tool output of CRI-based colour renditions for approximated illuminant C_a (0.728 lux)

Signify Classified - Internal

Output of GLA Calculation Tool for CIE 13.3 CRI and Associated CRI-based Colour Rendition Properties

Test Source:	Recreated Illuminant C	
Notes:	0.728 lux	
Date / Time:	**Wednesday, 26 June 2019**	**14:09:05**

Correlated Colour Temperature (T_{cp}) in K	7146	CIE1931 chromaticity coordinate, x	0.3046
Distance to Blackbody Locus (D_{uv})	-0.0003	CIE1931 chromaticity coordinate, y	0.3141
General Colour Rendering Index (R_a)	**96**	CIE1976 chromaticity coordinate, u'	0.1978
Colour Gamut Index (G_a)	**100**	CIE1976 chromaticity coordinate, v'	0.4589

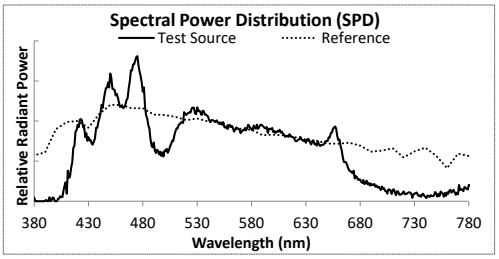

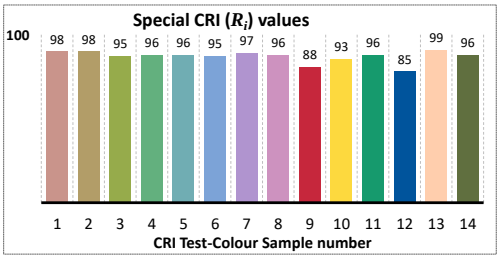

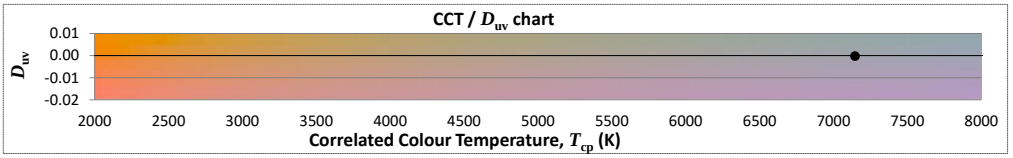

Two-dimensional R_a-G_a Graphic

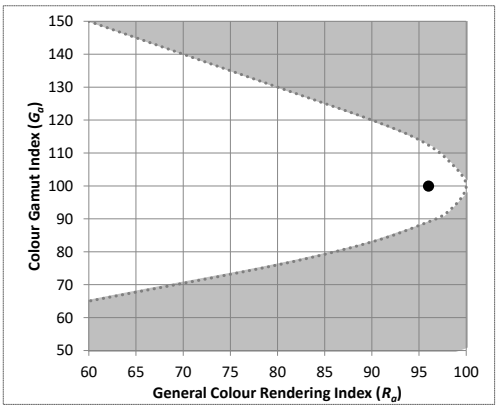

Colour-shift graphic

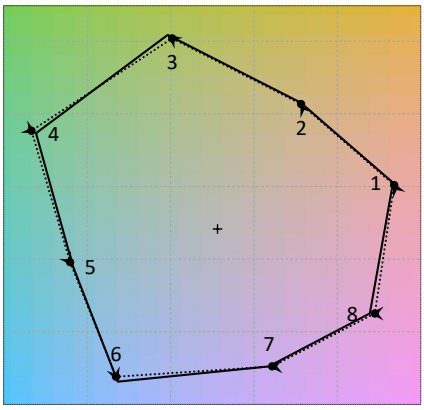

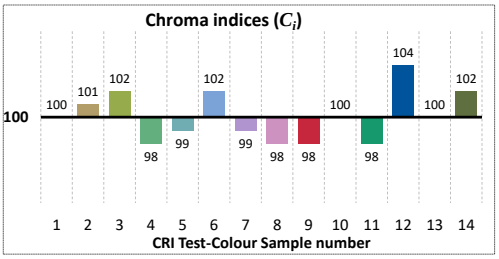

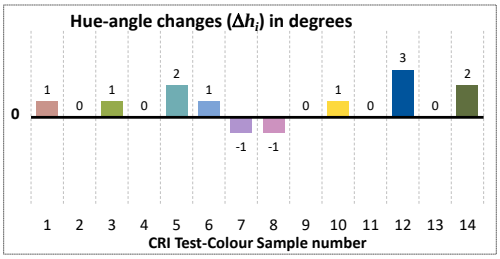

.8 GLA Calculation tool output of CRI-based colour renditions for approximated illuminant C_a (5.56 lux)

Signify Classified - Internal

Output of GLA Calculation Tool for CIE 13.3 CRI and Associated CRI-based Colour Rendition Properties

Test Source:	Recreated Illuminant C	
Notes:	5.56 lux	
Date / Time:	**Wednesday, 26 June 2019**	**14:09:23**

Correlated Colour Temperature (T_{cp}) in K	6695	CIE1931 chromaticity coordinate, x	0.3113
Distance to Blackbody Locus (D_{uv})	-0.0027	CIE1931 chromaticity coordinate, y	0.3163
General Colour Rendering Index (R_a)	**96**	CIE1976 chromaticity coordinate, u'	0.2017
Colour Gamut Index (G_a)	**101**	CIE1976 chromaticity coordinate, v'	0.4612

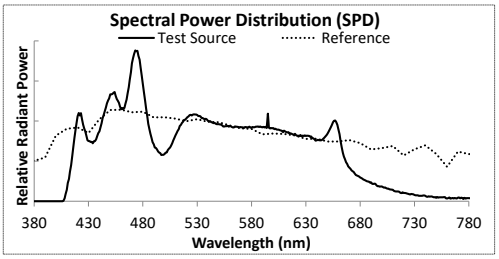

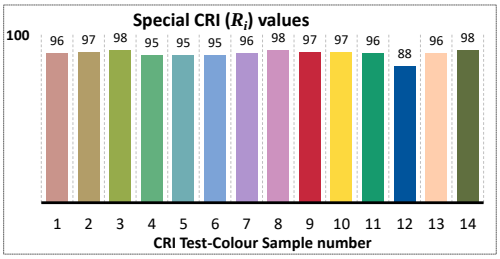

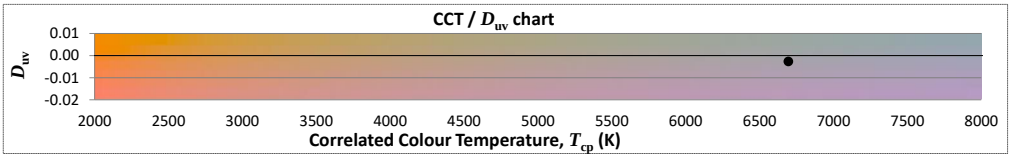

Two-dimensional R_a-G_a Graphic

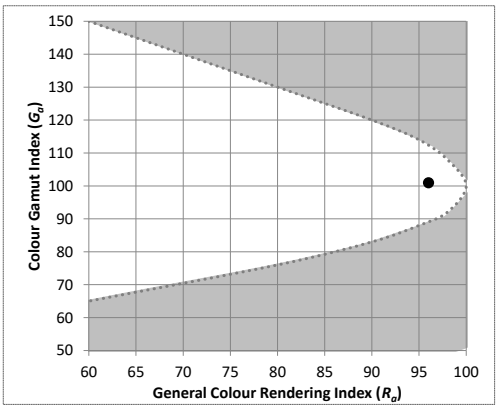

Colour-shift graphic

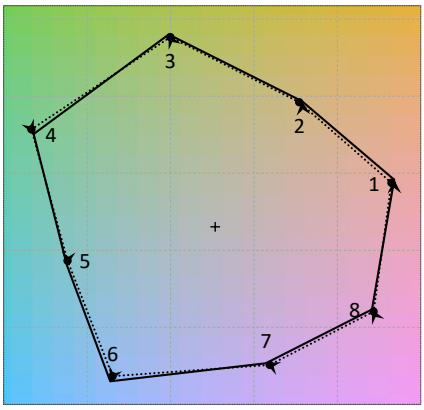

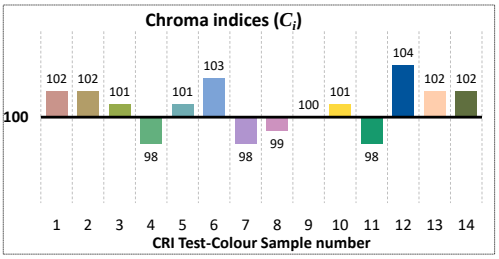

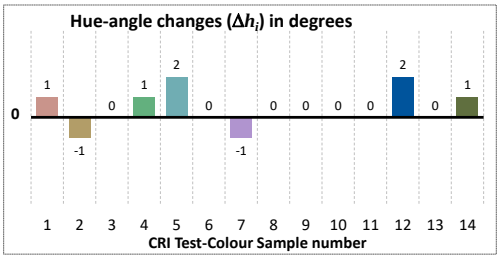

.9 GLA Calculation tool output of CRI-based colour renditions for approximated illuminant C_a (17.9 lux)

Signify Classified - Internal

Output of GLA Calculation Tool for CIE 13.3 CRI and Associated CRI-based Colour Rendition Properties

Test Source:	Recreated Illuminant C	
Notes:	17.9 lux	
Date / Time:	**Wednesday, 26 June 2019**	**14:09:35**

Correlated Colour Temperature (T_{cp}) in K	6684	CIE1931 chromaticity coordinate, x	0.3116
Distance to Blackbody Locus (D_{uv})	-0.0030	CIE1931 chromaticity coordinate, y	0.3160
General Colour Rendering Index (R_a)	**96**	CIE1976 chromaticity coordinate, u'	0.2020
Colour Gamut Index (G_a)	**101**	CIE1976 chromaticity coordinate, v'	0.4610

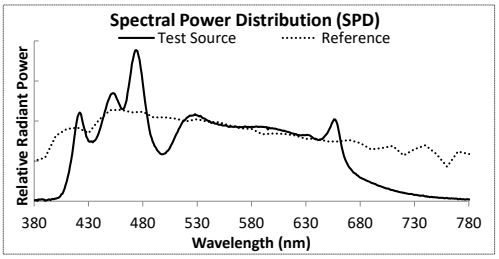

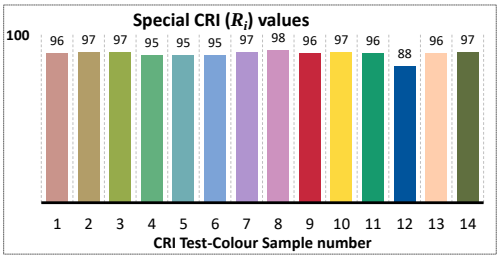

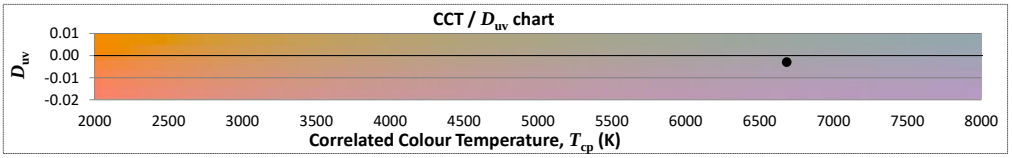

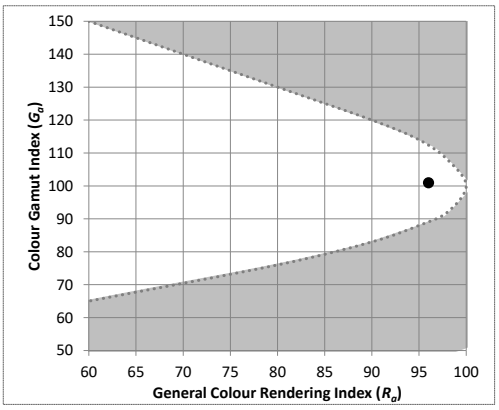

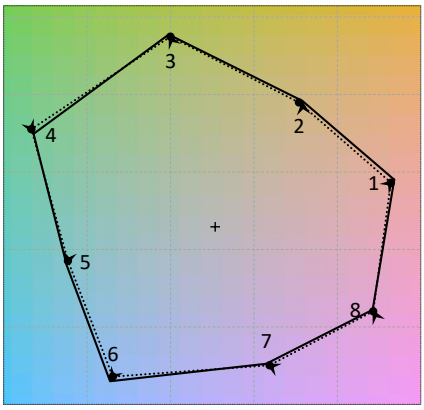

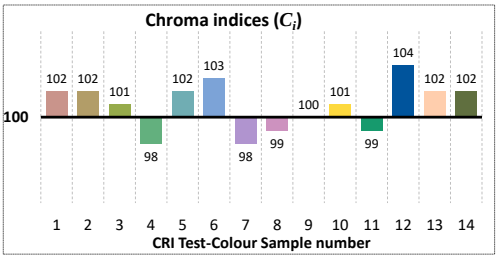

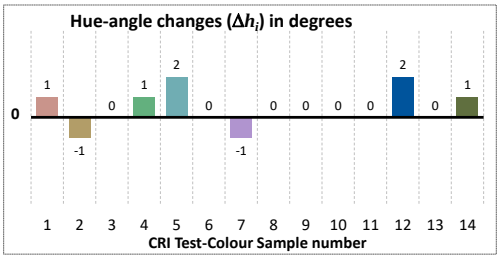

.10 GLA Calculation tool output of CRI-based colour renditions for approximated illuminant C_a (34.9 lux)

Signify Classified - Internal

Output of GLA Calculation Tool for CIE 13.3 CRI and Associated CRI-based Colour Rendition Properties

Test Source:	Recreated Illuminant C	
Notes:	34.9 lux	
Date / Time:	**Wednesday, 26 June 2019**	**14:09:47**

Correlated Colour Temperature (T_{cp}) in K	6634	CIE1931 chromaticity coordinate, x	0.3122
Distance to Blackbody Locus (D_{uv})	-0.0029	CIE1931 chromaticity coordinate, y	0.3169
General Colour Rendering Index (R_a)	**96**	CIE1976 chromaticity coordinate, u'	0.2021
Colour Gamut Index (G_a)	**101**	CIE1976 chromaticity coordinate, v'	0.4616

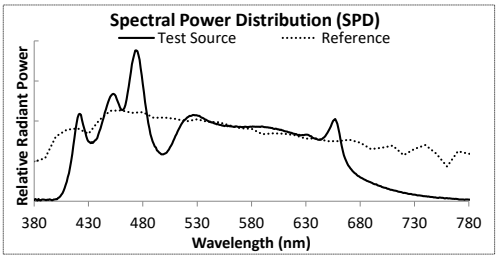

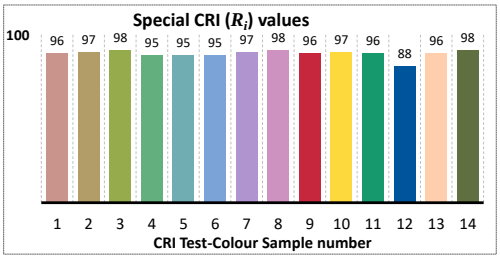

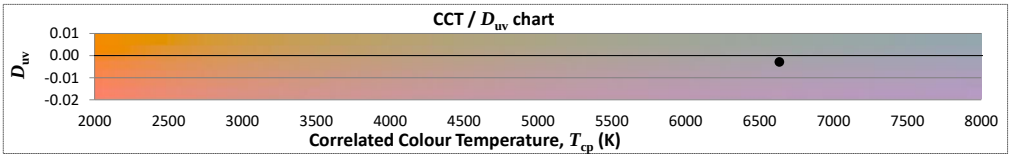

Two-dimensional R_a-G_a Graphic

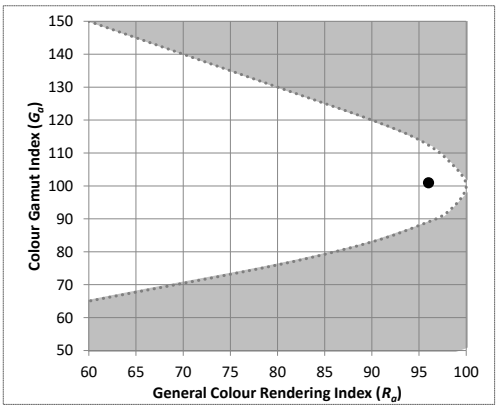

Colour-shift graphic

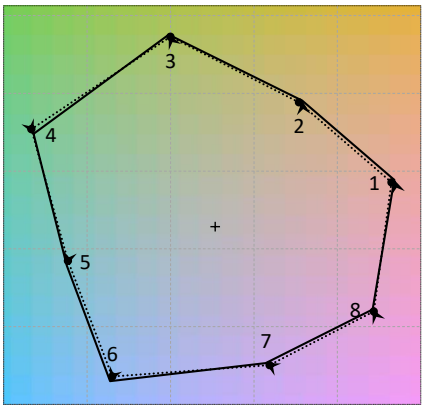

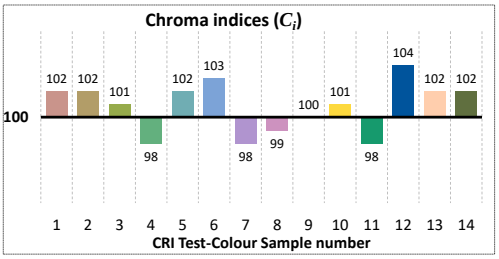

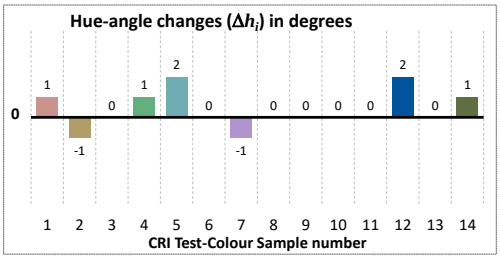

.11 GLA Calculation tool output of CRI-based colour renditions for approximated illuminant C_a (307 lux)

Signify Classified - Internal

Output of GLA Calculation Tool for CIE 13.3 CRI and Associated CRI-based Colour Rendition Properties

Test Source:	Recreated Illuminant C	
Notes:	307 lux	
Date / Time:	**Wednesday, 26 June 2019**	**14:10:11**

Correlated Colour Temperature (T_{cp}) in K	6749	CIE1931 chromaticity coordinate, x	0.3105
Distance to Blackbody Locus (D_{uv})	-0.0023	CIE1931 chromaticity coordinate, y	0.3162
General Colour Rendering Index (R_a)	**97**	CIE1976 chromaticity coordinate, u'	0.2012
Colour Gamut Index (G_a)	**104**	CIE1976 chromaticity coordinate, v'	0.4610

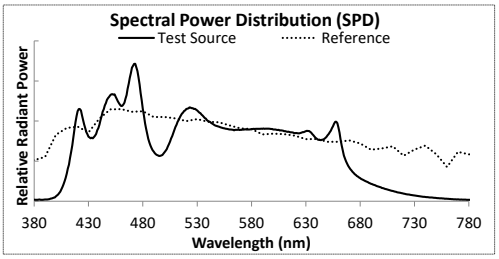

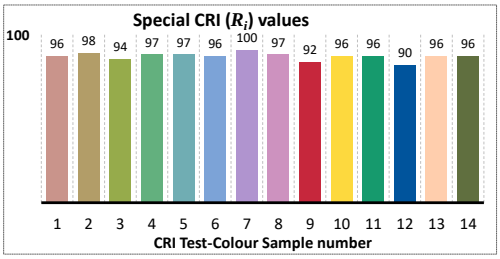

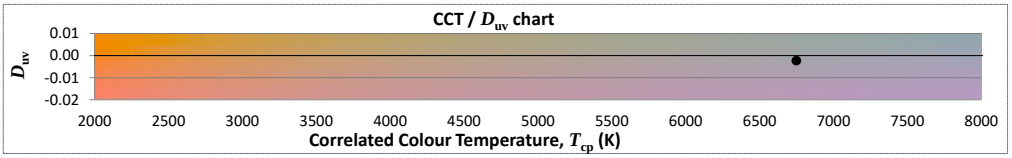

Two-dimensional R_a-G_a Graphic

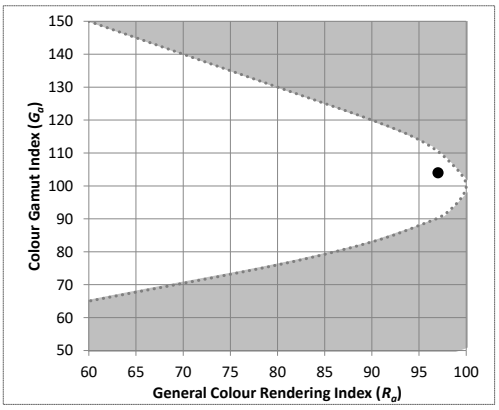

Colour-shift graphic